

3. SITE 548¹

Shipboard Scientific Party²

HOLE 548

Position: 48°54.95'N; 12°09.84'W

Water depth (sea level; corrected m, echo-sounding): 1251

Water depth (rig floor; corrected m, echo-sounding): 1261

Bottom felt (m, drill pipe): 1256

Penetration (m): 211

Number of cores: 35

Total length of cored section (m): 211

Total core recovered (m): 195.4

Core recovery (%): 93

Oldest sediment cored:

Depth sub-bottom (m): 211

Nature: Nannofossil ooze

Age: early Pliocene

Measured velocity (km/s): 1.675

Basement: Not reached

Principal results: See discussion following site data for Hole 548A.

HOLE 548A

Position: 48°54.93'N; 12°09.87'W

Water depth (sea level; corrected m, echo-sounding): 1251

Water depth (rig floor; corrected m, echo-sounding): 1261

Bottom felt (m, drill pipe): 1256

Penetration (m): 551.5

Number of cores: 38

Total length of cored section (m): 345.5

Total core recovered (m): 249.33

Core recovery (%): 72

Oldest sediment cored:

Depth sub-bottom (m): 551.5

Nature: Quartzite

Age: Hercynian (middle to late Devonian)

Measured velocity (km/s): 1.843

Basement:

Depth sub-bottom (m): 551.5

Nature: Quartzite

Principal results: Two holes (548 and 548A) were drilled 30 m apart near the seaward edge of a tilted block of Hercynian basement at the shallowest site on the Goban Spur transect (1256 m water depth) (Fig. 1). Using the variable length hydraulic piston corer (VLHPC) for the first time, we recovered a nearly complete 211 m sequence of Holocene through lower Pliocene nannofossil and marly nannofossil oozes in Hole 548 (Tables 1-3). Rotary coring in Hole 548A penetrated 345.5 m (233 m recovered) of upper Miocene through upper Campanian nannofossil ooze and chalk overlying a sideritic hardground and 21.5 m of quartzitic Hercynian sandstone of middle to late Devonian age (Tables 1-3). A geothermal gradient of 27.2°C/km was documented for this site. Eight lithologic units were identified (Table 3).

Unit 1: 0-72 m below seafloor (BSF), light olive gray or gray, marly, calcareous ooze and olive gray to light gray nannofossil or foraminifer-nannofossil ooze. Rapid input of terrigenous detritus and the alternation of glacial and interglacial sediments and fossil assemblages provide an excellent record of Quaternary paleoclimates. Sediment is late to middle Pleistocene in age and bathyal in nature.

Unit 2: 72-108.5 m BSF, light brown and light gray clay and foraminifer-nannofossil oozes. Sediment is early Pleistocene to late Pliocene in age and bathyal in nature.

Unit 3: 108.5-304.75 m BSF, light greenish gray nannofossil oozes. Sediment is late Pliocene through late Miocene in age. Turbiditic silty muds appear within the lower Pliocene to upper Miocene sediment. The unit lies unconformably above Unit 4; middle Miocene sediment is missing (3 m.y. hiatus). Sediment is bathyal in nature.

Unit 4: 304.75-412.6 m BSF, light greenish gray foraminifer and nannofossil chalks with glauconite. Sediment is early middle Miocene through middle Eocene in age. The lowest sediment accu-

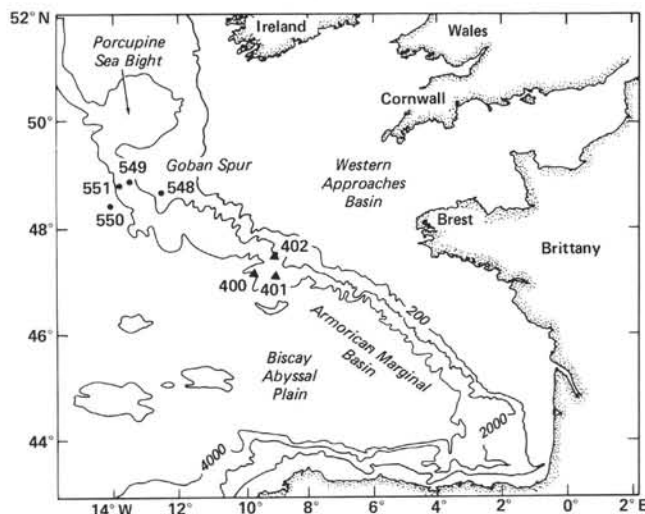


Figure 1. Location of Leg 80 drill sites (548-551). Three Leg 48 drill sites (400-402) are also shown.

¹ Graciansky, P. C. de, Poag, C. W., et al., *Init. Repts. DSDP*, 80: Washington (U.S. Govt. Printing Office).

² Pierre C. de Graciansky (Co-Chief Scientist), École Nationale Supérieure des Mines, Paris, France; C. Wylie Poag (Co-Chief Scientist), U.S. Geological Survey, Woods Hole, Massachusetts; Robert Cunningham, Jr., Exxon Production Research Company, Houston, Texas; Paul Loubere, Oregon State University, Corvallis, Oregon (present address: Northern Illinois University, DeKalb, Illinois); Douglas G. Masson, Institute of Oceanographic Sciences, Wormley, United Kingdom; James M. Mazzullo, Texas A & M University, College Station, Texas; Lucien Montadert, Institut Français du Pétrole, Rueil Malmaison, France; Carla Müller, University of Frankfurt, Frankfurt, Federal Republic of Germany; Kenichi Otsuka, Shizuoka University, Shizuoka, Japan; Leslie Reynolds, U.S. Geological Survey, Woods Hole, Massachusetts (present address: University of South Carolina, Columbia, South Carolina); Jacques Sigal, Vincennes, France; Scott Snyder, East Carolina University, Greenville, North Carolina; Hilary A. Townsend, University of Southampton, Southampton, United Kingdom; Stephanos P. Vaos, Florida State University, Tallahassee, Florida; and Douglas Waples, Mobil Research & Development Corporation, Dallas, Texas.

Table 1. Coring summary, Leg 80.

Hole	Latitude	Longitude	Water depth (m)	Number of cores	Cores with recovery	Percent of cores with recovery ^a	Meters cored	Meters recovered	Percent recovered ^b	Meters drilled	Total penetration (m)	Average penetration rate (m/hr.) ^c	Time on hole or site (hr.)
548	48°54.95'N	12°09.84'W	1256	35	35	100.0	211.0	210.9	99.9	0	211.0		45.2
548A	48°54.93'N	12°09.87'W	1256	38	38	100.0	346.0	246.5	71.2	205.5	551.5	42.4	82.9
Total for site				73	73	100.0	557.0	457.4	82.1	205.5	762.5		128.1
549	49°05.28'N	13°05.88'W	2533	99	93	93.9	812.5	369.7	45.5	189.0	1001.5	7.9	301.2
549A	49°05.29'N	13°05.89'W	2535.5	42	41	77.6	196.0	144.4	73.7	0	198.5		54.2
Total for site				141	134	95.0	1008.5	514.1	51.0	189.0	1200.0		355.4
550	48°30.91'N	13°26.37'W	4432	48	46	95.8	442.5	262.6	59.3	94.0	536.5	36.4	115.3
550A	48°30.91'N	13°26.39'W	4432	0	0	0	0	0	0	95.0	95.0	170.6	19.2
550B	48°30.96'N	13°26.32'W	4432	30	30	100.0	264.5	177.9	67.3	456.0	720.5	14.2	150.3
Total for site				78	76	97.4	707.0	440.5	62.3	645.0	1352.0	34.0 ^d	284.8
551	48°54.64'N	13°30.09'W	3909	14	13	92.9	125.0	81.0	64.8	76.0	201.0	9.1	75.2
Total for leg				306	296	96.7	2397.5	1493.0	62.2	1115.5	3515.5		843.5

Note: Blanks signify that quantities are unknown.

^a Total for site is calculated from total number of cores and total cores with recovery.

^b Total for site is calculated from total meters cored and total meters recovered.

^c Rotary coring only.

^d Total meters penetrated divided by number of rotating hours.

mulation rates at the site occur in this section. Cherts appear in the lowest third of the unit; they are diagenetically more altered than the rest of the section. Middle Oligocene sediment is missing (about 4 m.y. hiatus). Another disconformity (a 1.5 m.y. hiatus) separates Unit 4 (middle Eocene) from Unit 5 (lower Eocene) sediment. Sediment is outer sublittoral-upper bathyal in nature.

Unit 5: 412.6–469.9 m BSF, brownish and greenish gray, marly nanofossil chalk. Sediment is early Eocene in age. Base of unit is an unconformity representing a 10 m.y. hiatus. Sediment is early Eocene in age. Base of unit is an unconformity representing a 10 m.y. hiatus. Sediment is outer sublittoral-upper bathyal in nature.

Unit 6: 469.9–530 m BSF, white foraminifer-nanofossil chalk. Sediment is Danian through late Campanian in age. Base of unit is an unconformity representing a hiatus of unknown duration. Sediment was outer sublittoral-upper bathyal in nature.

Unit 7: 530–535.5 m BSF, sideritic, pyritic hardground. Sediment was deposited in a marine environment.

Unit 8: 535.5–551.5 m BSF, feldspathic quartzitic sandstone. Sediment is middle Devonian in age. There is little evidence of metamorphism. Sediment is underlain by Hercynian basement (which was drilled in the northeast Atlantic for the first time during this leg). Sediment was deposited in a continental(?) environment.

Site chapter results are based chiefly on shipboard analysis and interpretation. The specialty chapters reflect postcruise revisions and additional data. Where discrepancies arise, the specialty chapters should be considered correct.

SITE APPROACH AND OPERATIONS

Glomar Challenger approached Site 548 (Fig. 1) along a northwest heading to shot point (SP) 900 on CEPM seismic line OC 202, 17 naut. mi. (27 km) northeast of the objective (Fig. 2). At 1212 hr. (local time) the vessel turned southwest along a heading of 123° to follow along the control seismic line OC 202 to the site. Adverse weather conditions prevented the ship from maintaining the plotted course precisely, as shown later by satellite positioning. A further navigation problem was caused by damage to the ship's pit (pitot) log, which measures ship speed.

After two good satellite fixes were acquired at 1330 and 1358 hr., a 16 kHz positioning beacon was dropped

at 1410 hr. at 48°54.95'N, 12°09.84'W (as determined from the average of 14 good satellite fixes), where the structure and bathymetry of the seafloor as measured by shipboard instruments were similar to the reference seismic profile. The site is approximately 2 km east of the original target, along the strike of the geologic structure.

The vessel maintained a southwest heading from the beacon before the seismic gear was retrieved. It then returned to a position over the beacon, where the precision depth recorder (PDR) indicated a water depth of 1261 m from the rig floor.

The bottom-hole assembly (BHA) was assembled and the drill pipe was run down far enough to place the bit just above the seafloor. Inasmuch as the drilling at Hole 548 represented a debut for the variable-length hydraulic piston corer, about 2 hr. were spent in deploying the coring assembly and in resolving minor handling problems. The corer was lowered on the sandline to the bit, which was positioned at 1250.5 m below sea level for the first core retrieval attempt. The first 9.5 m core barrel was fired and retrieved; 3.6 m of sediment were recovered. Bottom was thus felt at 1256 m.

Piston coring then proceeded with excellent recovery and minimal handling problems despite adverse weather conditions and swells that reached 3 m. The 9.5 m corer succeeded in penetrating to 108.5 m through soft Pleistocene mud and silt. At this depth the sediments became too stiff to permit the corer to penetrate 9.5 m of sediment in a stroke, and a second unit, prepared for 5 m cores, was deployed. Coring continued in calcareous ooze to 211 m BSF, where the sediment became too stiff for a 5 m stroke. This was judged to be the best time to terminate piston coring operations and to convert to the more rapid rotary coring. The drill string was then recovered; the bit arrived on deck at 1125 hr. on 11 June.

In order to accomplish the deeper coring at Site 548, the rotary coring BHA was assembled and run back to

Table 2. Coring summary, Site 548.

Core	Date (June 1981)	Time (hr.)	Depth from drill floor (m)	Depth below seafloor (m)	Length cored (m)	Length recovered (m)	Recovery (%)
Hole 548							
1	9	2358	1256.0-1260.0	0.0-4.0	4.0	3.60	90
2	10	0135	1260.0-1269.5	4.0-13.5	9.5	9.61	100
3	10	0230	1269.5-1279.0	13.5-23.0	9.5	9.62	100
4	10	0330	1279.0-1288.5	23.0-32.5	9.5	9.67	100
5	10	0452	1288.5-1298.0	32.5-42.0	9.5	9.67	100
6	10	0610	1298.0-1307.5	42.0-51.5	9.5	9.58	100
7	10	0715	1307.5-1317.0	51.5-61.0	9.5	9.66	100
8	10	0815	1317.0-1326.5	61.0-70.5	9.5	9.61	100
9	10	0915	1326.5-1331.0	70.5-75.0	4.5	4.02	89
10	10	1015	1331.0-1336.0	75.0-80.0	5.0	8.66	100
11	10	115	1336.0-1345.5	80.0-89.5	9.5	8.22	87
12	10	1200	1345.5-1348.0	89.5-92.0	2.5	2.48	99
13	10	1315	1348.0-1355.0	92.0-99.0	7.0	8.97	100
14	10	1405	1355.0-1356.5	99.0-100.5	1.5	1.64	100
15	10	1450	1356.5-1364.5	100.5-108.5	8.0	9.51	100
16	10	1535	1364.5-1374.0	108.5-118.0	9.5	8.18	86
17	10	1602	1374.0-1382.0	118.0-126.0	8.0	7.50	94
18	10	1700	1382.0-1387.0	126.0-131.0	5.0	5.04	100
19	10	1755	1387.0-1392.0	131.0-136.0	5.0	5.02	100
20	10	1910	1392.0-1397.0	136.0-141.0	5.0	4.96	99
21	10	2000	1397.0-1402.0	141.0-146.0	5.0	4.25	85
22	10	2045	1402.0-1407.0	146.0-151.0	5.0	4.52	90
23	10	2125	1407.0-1412.0	151.0-156.0	5.0	3.63	73
24	10	2205	1412.0-1417.0	156.0-161.0	5.0	4.18	84
25	10	2255	1417.0-1422.0	161.0-166.0	5.0	3.95	79
26	10	2335	1422.0-1427.0	166.0-171.0	5.0	5.15	100
27	11	0020	1427.0-1432.0	171.0-176.0	5.0	5.17	100
28	11	0115	1432.0-1437.0	176.0-181.0	5.0	5.15	100
29	11	0212	1437.0-1442.0	181.0-186.0	5.0	5.14	100
30	11	0315	1442.0-1447.0	186.0-191.0	5.0	5.14	100
31	11	0410	1447.0-1452.0	191.0-196.0	5.0	4.54	91
32	11	0510	1452.0-1457.0	196.0-201.0	5.0	4.77	95
33	11	0610	1457.0-1462.0	201.0-206.0	5.0	4.85	97
34	11	0640	1462.0-1465.0	206.0-209.0	3.0	3.22	100
35	11	0720	1465.0-1467.0	209.0-211.0	2.0	1.98	99
Hole 548A							
1	12	0625	1461.5-1471.0	205.5-215.0	9.5	Tr	0
2	12	0730	1471.0-1480.5	215.0-224.5	9.5	5.5	58
3	12	0830	1480.5-1490.0	224.5-234.0	9.5	9.13	96
4	12	1000	1490.0-1499.5	234.0-243.5	9.5	8.96	94
5	12	1030	1499.5-1509.0	243.5-253.0	9.5	9.11	96
6	12	1130	1509.0-1518.5	253.0-262.5	9.5	6.27	66
7	12	1230	1518.5-1528.0	262.5-272.0	9.5	4.20	44
8	12	1320	1528.0-1537.5	272.0-281.5	9.5	9.0	95
9	12	1550	1537.5-1547.0	281.5-291.0	9.5	7.6	80
10	12	1655	1547.0-1556.5	291.0-300.5	9.5	9.4	99
11	12	1800	1556.5-1566.0	300.5-310.0	9.5	6.6	69
12	12	1840	1566.0-1575.5	310.0-319.5	9.5	8.8	93
13	12	1935	1575.5-1585.0	319.5-329.0	9.5	9.3	98
14	12	2040	1585.0-1594.5	329.0-338.5	9.5	6.7	71
15	12	2145	1594.5-1604.0	338.5-348.0	9.5	8.12	85
16	12	2235	1604.0-1613.5	348.0-357.5	9.5	7.29	77
17	12	2315	1613.5-1623.0	357.5-367.0	9.5	7.50	79
18	13	0029	1623.0-1632.5	367.0-376.5	9.5	4.69	49
19	13	0130	1632.5-1642.0	376.5-386.0	9.5	8.72	92
20	13	0300	1642.0-1651.5	386.0-395.5	9.5	5.44	57
21	13	0432	1651.5-1661.0	395.5-405.0	9.5	6.19	65
22	13	0543	1661.0-1670.5	405.0-414.5	9.5	9.40	99
23	13	0708	1670.5-1680.0	414.5-424.0	9.5	4.48	47
24	13	0845	1680.0-1689.5	424.0-433.5	9.5	8.70	92
25	13	0941	1689.5-1699.0	433.5-443.0	9.5	8.25	87
26	13	1110	1699.0-1708.5	443.0-452.5	9.5	9.69	100
27	13	1240	1708.5-1718.0	452.5-462.0	9.5	8.03	85
28	13	1400	1718.0-1727.5	462.0-471.5	9.5	9.40	99
29	13	1430	1727.5-1737.0	471.5-481.0	9.5	6.73	71
30	13	1515	1737.0-1746.5	481.0-490.5	9.5	4.45	47
31	13	1630	1746.5-1756.0	490.5-500.0	9.5	3.80	40
31	13	1740	1756.0-1765.5	500.0-509.5	9.5	5.49	58
33	13	1820	1765.5-1775.0	509.5-519.0	9.5	5.03	53
34	13	1903	1775.0-1784.5	519.0-528.5	9.5	9.65	100
35	13	2000	1784.5-1794.0	528.5-538.0	7.0	1.69	24
36	13	2210	1794.0-1803.5	538.0-547.5	2.5	0.05	20
37	14	0205	1803.5-1813.0	547.5-557.0	9.0	0.10	1
38	14	0439	1813.0-1822.5	557.0-566.5	4.5	3.06	68

the seafloor. The vessel was offset 30 m to the west to avoid the area disturbed by the previous drilling, and Hole 548A was spudded at 1800 hr. on 11 June. The hole was drilled to 205.5 m BSF without any attempt to recover sediment. Combination temperature/water sampler probe runs were made at 53.5 and 110.5 m, and a temperature probe was run at 167.5 m. Continuous cor-

ing was then conducted from 205.5 m BSF to total depth. An additional temperature probe was run at 281.5 m.

The sediment section penetrated was soft carbonate ooze and chalk, with the exception of about 50 m of semi-indurated clay. Penetration rate was consequently high, and core recovery was approximately 71%. Basement of quartzitic composition was encountered at 535 m BSF. Only broken rubble and cuttings (no full diameter cores) were recovered from the 16 m of basement drilled. We are not sure why we failed to recover full diameter cores, although hole angle increased from 5.7 to 7.9° from vertical within 10 m of the basement contact, and this may have caused lateral bit movement that partially destroyed the cores.

Mud flushes proved inadequate to keep the hole free of the quartzite cuttings from the basement. We terminated coring operations because of operational difficulties that included torquing and sticking of the drill string, a plugged bit, and difficulty in recovering the inner core barrel. After drilling operations ceased the hole was flushed with a 50-barrel mud flush to prepare the hole for logging. Because fresh water-sensitive clays were encountered, the hole was not filled with fresh water mud, although this type of preparation would have been optimum for running the induction log. A go-devil was then pumped down the pipe to activate the hydraulic bit release. The bit and associated components were left at the bottom of the hole, and the open-ended pipe was pulled to 173 m BSF for logging.

Two open-hole logging runs were made. The first sonde (combination long spaced sonic and dual induction) encountered an obstruction at 210 m, but the heavy tool broke through, and thereafter the hole was clear to 537 m. Neither this tool nor the subsequent compensated neutron density/formation density combination log encountered hole problems. The data from all four logs were of exceptionally high quality, given the physical properties of the very soft sediments.

The drill string was then recovered, and *Glomar Challenger* departed Site 548 at 2220 hr. on 14 June.

SEDIMENT LITHOLOGY

Eight distinct lithologic units were encountered at Site 548 (Table 3). In total, 551.5 m of sediment and sedimentary rocks were cored, ranging in age from middle to late Devonian to Holocene. The Mesozoic and Cenozoic strata consist mainly of calcareous nannofossil oozes and chalks, which can be divided into six major lithologic units on the basis of their visual and microscopic characteristics and logging properties. The middle to late Devonian sequence consists of Hercynian arkoses and black shales.

Unit 1

Unit 1 consists of gray calcareous muds, marly nannofossil oozes, and marly nannofossil-foraminifer oozes. It occurs in Hole 548 from 0 to 72 m BSF³ (Core 1 to Section 548-9-1) and is Holocene to Pleistocene in age.

³ All depths below seafloor are drill string depths, which may not correspond exactly to depths obtained by well-logging techniques.

Table 3. Lithologic summary, Site 548. Water depth: 1256 m.

Unit	Hole-Core-Section (level in cm)	Depth (m BSF) ^a	Main lithologies	Age
1a	548-1 to 548-7-5 (90 cm)	0-59.90	Alternating calcareous mud and marly nannofossil ooze	Holocene and Pleistocene
1b	548-7-5 (90 cm) to 548-9-1	59.90-72		
2	548-9-2 to 548-15-6	72-108.5	Clays and foraminifer-nannofossil oozes	early Pleistocene to late Pliocene
3	548-16 to 548-35 and 548A-1 to 548A-11-3 (125 cm)	Hole 548: 108.5-211.0 Hole 548A: 205.0-304.75	Homogeneous bioturbated nannofossil oozes and chalks interbedded with turbiditic silty mudstones	late Pliocene to late Miocene
4a	548A-11-3 (125 cm) to 548A-18	304.75-376.5	Foraminifer-nannofossil chalks	middle Miocene to middle Eocene
4b	548A-19 to 548A-22-6 (15 cm)	376.5-412.6		middle Eocene
5	548A-22-6 (15 cm) to 548A-28-6 (35 cm)	412.6-469.9	Marly nannofossil chalk	early Eocene to late Paleocene
6	548A-28-6 (35 cm) to 548A-35	469.9-530	Foraminifer-nannofossil chalk	Danian late Maestrichtian to late Campanian
7	548A-35 to 548A-36, CC	530-535.5	Sideritic hardground Quartz sands	Early(?) to pre(?) Cretaceous
8	548A-36 to 548A-38	535.5-551.5	Arkosic sandstone and black shale	middle to late Devonian

Notes: Cross rule denotes change in lithology; wavy line denotes unconformity. Bold wavy line denotes major unconformity.
^a Depths above Unit 3 are for Hole 548; depths below Unit 3 are for Hole 548A.

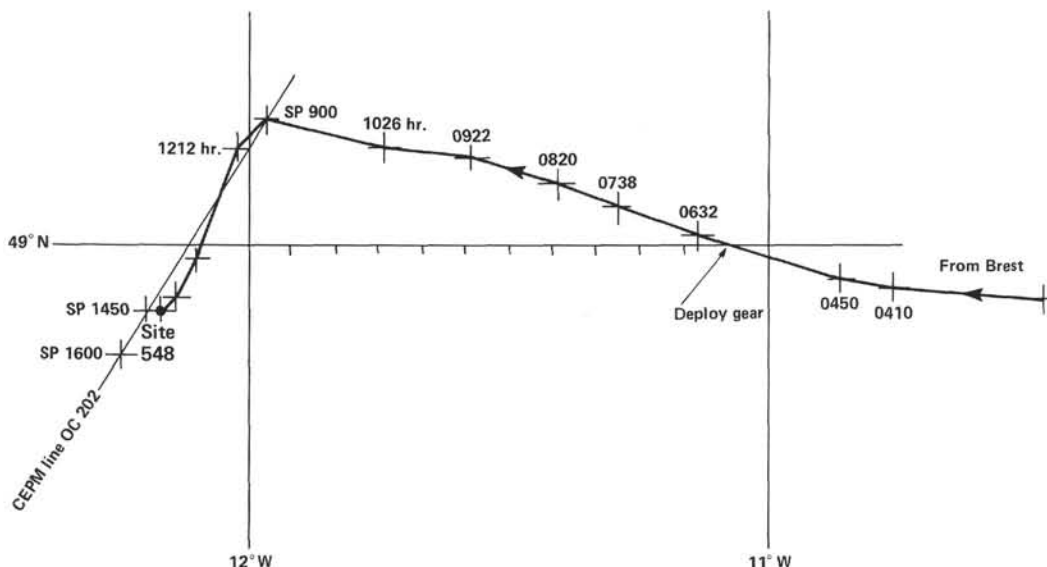


Figure 2. Approach of *Glomar Challenger* to Site 548 (9 June 1981).

Calcium carbonate content, sedimentary structures, and gamma ray intensity data suggest the division of this unit into two subunits.

Subunit 1a

Subunit 1a consists of alternating calcareous muds, marly nannofossil oozes, and marly nannofossil-foraminifer oozes. It occurs from 0 to 59.9 m BSF (Core 1 to 548-7-5, 90 cm) and is Holocene-Pleistocene in age.

Subunit 1a consists of alternating olive gray to gray (5Y 4/1-6/2) calcareous muds and olive gray to light gray (5Y 4/1, 5Y 7/1) marly nannofossil and nannofossil-foraminifer oozes. Smear slide analysis shows that the calcareous muds contain up to 40% quartz, 20 to 60% clay minerals, and 20 to 40% unspecified carbon-

ate (which may be shell debris, because shell fragments are visible in the cores). Nannofossils and foraminifers are rare in the muds, and calcium carbonate values are low (10-25% as measured by carbonate bomb). The marly foraminifer-nannofossil oozes and marly nannofossil oozes contain less than 30% quartz, less than 20% clay minerals, and 40 to 80% calcium carbonate (according to smear slide analysis); however, somewhat lower carbonate values (45-50%) are given by carbonate bomb analysis. The approximate average calcium carbonate value for this subunit is 25%. In Section 548-7-1, the organic carbon values are the highest at the site, averaging about 0.6%.

Shipboard X-ray analysis of Subunit 1a shows a consistent mineralogy of 25% quartz, 20 to 30% calcite,

and small, variable quantities (0–5%) of dolomite, high-magnesium calcite, and anhydrite. The remainder is largely clay minerals (illite, kaolinite, smectite, and chlorite).

The sediments in Subunit 1a are intensely bioturbated, but most contacts between calcareous muds and marly oozes can still be seen. In most cases, the contacts are gradational. However, in some places (Sections 548-3-1 and -2; 548-4-4 and -5; and 548-6-2, -3, -5, and -6), the contacts between the underlying marly oozes and overlying calcareous muds are abrupt. Above such contacts, the muds are graded and often contain shallow water benthic foraminifers. These graded beds vary in thickness from 1 to 80 cm. Lastly, occasional ice-rafted pebbles are often found in this subunit (Chennaux et al., this volume).

The sedimentological and micropaleontological data suggest that the repeated and gradual alternation between marly oozes and calcareous muds reflects sea level fluctuations due to glacial advance and retreat. Terrigenous sediment influx was greatest during glacial periods. The graded muds were presumably deposited by turbidity currents.

All fossil groups indicate a Pleistocene age for this subunit, except for the light brown calcareous ooze in the uppermost 28 cm of Core 1, which is probably Holocene in age.

Subunit 1b

Subunit 1b consists of marly nannofossil oozes and marly foraminifer–nannofossil oozes. It occurs from 59.9 to 72 m BSF (548-7-5, 90 cm to Section 548-9-1) and is Pleistocene in age.

Subunit 1b is distinguished from Subunit 1a by a marked increase in calcium carbonate and a marked decrease in terrigenous debris (especially clay minerals). Because of the smaller amount of terrigenous debris there are fewer interbedded calcareous muds in this subunit, a characteristic reflected in the noticeable reduction in gamma ray intensity at the top of the subunit (see Superlog [back pocket] for Site 548). In addition, there is an abrupt erosional contact between the two subunits. In gross mineralogy and sedimentary structures, the marly oozes of this subunit are similar to those in the subunit above, except that there is evidence of aragonite in 548-8-3 (90–91 cm).

Unit 2

Unit 2 consists of light brown and gray nannofossil foraminifer–nannofossil oozes. It occurs in Hole 548 from 72 to 108.5 m BSF (Sections 548-9-2 to 548-15-6) and is early Pleistocene to late Pliocene in age.

The unit is a complex interbedded sequence of pinkish gray or light brown (7–5Y 6/2) silty clays, olive gray (5Y 6/2), and gray to olive gray (5Y 6/1–5Y 6/2) nannofossil and foraminifer–nannofossil oozes. This unit is generally coarser and composed of more graded layers than Unit 1 (Fig. 3), and it includes olive gray, graded, sandy muds 5 to 50 cm thick. Bioturbation occurs throughout Unit 2, as does disseminated pyrite, which is often found within burrows. Shell fragments and glauconite occur rarely.

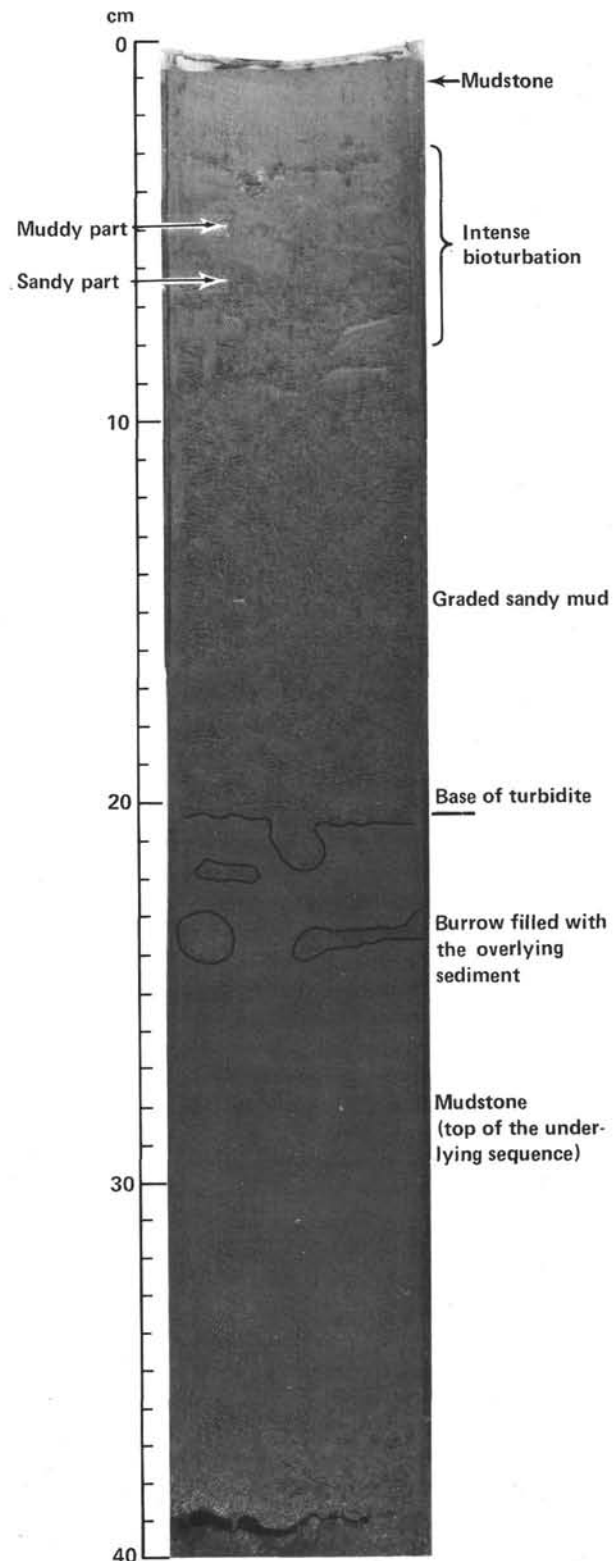


Figure 3. Lithologic Unit 2 turbidite bed (late Pliocene). Base of graded bed occurs at 20 cm; bed grades upward from sandy mud to marly nannofossil ooze. Section 548-15-4.

The biogenic oozes typically consist of 40 to 70% nannofossils, as much as 40% quartz and clay minerals, and as much as 30% foraminifers (according to smear slide analysis). The more terrigenous layers contain up

to 60% clay minerals and 30% quartz (in smear slides). Carbonate bomb analyses give values ranging from 8 to 51% calcium carbonate. As in Unit 1, much of the carbonate in the more marly layers is in the form of unidentified shell fragments. Many sediments intermediate between the ooze described above and the clay lithologies are present.

Shipboard X-ray analysis shows that the concentrations of both quartz (15–40%) and calcite (10–60%) are far more variable in Unit 2 than in Unit 1. Small, variable amounts (0–20%) of Mg calcite, siderite, aragonite, and anhydrite are also present. Within the clay fraction of Units 1 and 2, the relative abundance of clay minerals was also determined by X-ray analysis. Concentrations are generally constant for illite (45–50%), chlorite (10–30%), and kaolinite (10–20%), but the smectite concentrations range cyclically from 5 to 40%. High smectite concentrations may correspond to increases in turbiditic terrigenous debris emplaced during glacial intervals.

Unit 3

Unit 3 consists of nannofossil oozes and chalks and silty mudstones. It occurs in Hole 548 from 108.5 to 211.0 m BSF (Cores 16 to 35) and in Hole 548A from 205 to 304.75 m BSF (Core 1 to 548A-11-3, 125 cm) and is late Pliocene to late Miocene in age.

The part of Unit 3 from 108.5 to 211 m BSF (the part recovered from Hole 548) was cored by using the hydraulic piston corer, and the remainder of the unit (which was recovered from Hole 548A) was sampled by conventional rotary drilling. Unit 3 is a series of intensely bioturbated nannofossil oozes and chalks, with a small but variable terrigenous component. It can be divided into three subunits, although these subunits have not been recognized by the well-logging techniques.

The upper part of Unit 3 (108.5–146 m BSF, Cores 548-16 to -21) is marly nannofossil ooze (quartz 10–25% and clay minerals 5–10%, according to smear slide analysis). The middle part (146–196 m BSF, Cores 548-22 to -31) is nannofossil ooze with less than 10% terrigenous detritus (according to smear slide analysis). The lower part (196–211 m BSF, Cores 548-32 to -35; and 205–304.75 m BSF, Cores 548A-1 to -11) is again more marly (quartz 10–40%, clay minerals 10–30%). Carbonate bomb values are 11 to 60% CaCO₃ in the upper part, 40 to 70% in the middle part, and 30 to 50% in the lower part.

To give a more detailed description, the upper part of Unit 3 is composed of intercalated beds of gray (5Y 5/1) to greenish (5G 6/1) or bluish gray (5B 7/1) nannofossil ooze and greenish gray (5G 6/1–8/1) marly nannofossil ooze. The beds alternate over intervals of 20 cm to 3 or 4 m. Contacts are generally gradational, although some are sharp. Abrupt contacts in the marly ooze are usually accompanied by a slight coarsening of the sediment above the contact. Scattered throughout the upper section, especially in the marly beds, are finely graded sandier intervals. Burrowing is present to a moderate degree, and minute shell fragments and pyrite flecks are disseminated throughout the sediment.

The middle part of Unit 3 is uniform, soft to firm, greenish gray (5G 6/1–7/1) nannofossil ooze containing moderate to extensive burrowing (in shades of gray), scattered minute shell fragments, and pyrite flecks. Color changes (greenish gray, 5GY 4/1, to light bluish gray, 5B 7/1) occur cyclically in this part of the section over intervals of less than a meter. The blue gray material generally grades downward to the green gray material, which has a sharp contact with the next bluish bed. Section 548-29-2 contains a large pebble (1–5 cm); Section 548-23-2 contains an interval of sedimentary clasts. The abundance of foraminifers in this section is variable (5–20%), and the terrigenous component is less than in sediments above and below.

The lower part of Unit 3 is much the same as the upper subunit. Cores 2 to 6 of Hole 548A contain many graded beds of sandy, marly ooze, presumably of turbidity current origin. The sand component is enriched in quartz and glauconite (up to 15%). The sediments are moderately to strongly burrowed in shades of greenish gray. Some of the burrows contain pyrite crystals. Cores 7 to 11 are again nannofossil ooze with only occasional graded, sandy mud intervals. These sediments are heavily burrowed and contain scattered pyrite crystals.

Core 11 contains two sharp contacts that are associated with sediment clasts (several cm across). These contacts, present in Sections 3 (125 cm) and 4 (70 cm), define a transition interval from Unit 3 to 4.

Shipboard X-ray bulk composition analysis of Unit 3 shows quartz and calcite concentrations of about 10 to 30% and 15 to 50%, respectively. X-ray analysis of the clay fraction reveals small concentrations of kaolinite and chlorite (10–20% each), with larger and more variable quantities of smectite and illite (20–50% and 40–60%, respectively). A downward decrease in kaolinite, chlorite, and illite, along with an increase in smectite, takes place in Unit 3.

Unit 4

Unit 4 consists of light gray foraminifer–nannofossil chalks. It occurs in Hole 548A from 304.75 to 412.6 m BSF (Sections 548A-11-3 to 548A-22-6) and is middle Miocene to middle Eocene in age.

Unit 4 consists of a sequence of foraminifer–nannofossil chalks ranging in color from bluish white through light gray to greenish gray. The boundary between Units 3 and 4 is an unconformity, as determined by paleontological data and the visual characteristics of the cores (Fig. 4). Nannofossil Zones NN7 to NN10 and planktonic foraminifer Zones N12 to N15 (upper middle Miocene) are missing. There is a transition interval below the unconformity from 548A-11-3 (125 cm) to 548A-11-4 (70 cm) (Fig. 5). It contains sediment clasts of variable sizes reworked from the underlying Unit 4. We place the boundary between Units 3 and 4 in Section 548A-11-3 at 125 cm, because no nannofossils belonging to Zone NN11 (the oldest zone found in Unit 3) were detected below this depth. The gamma ray log displays a strong drop in intensity across the transition from Units 3 to 4. This is probably due to a reduction in argillaceous com-

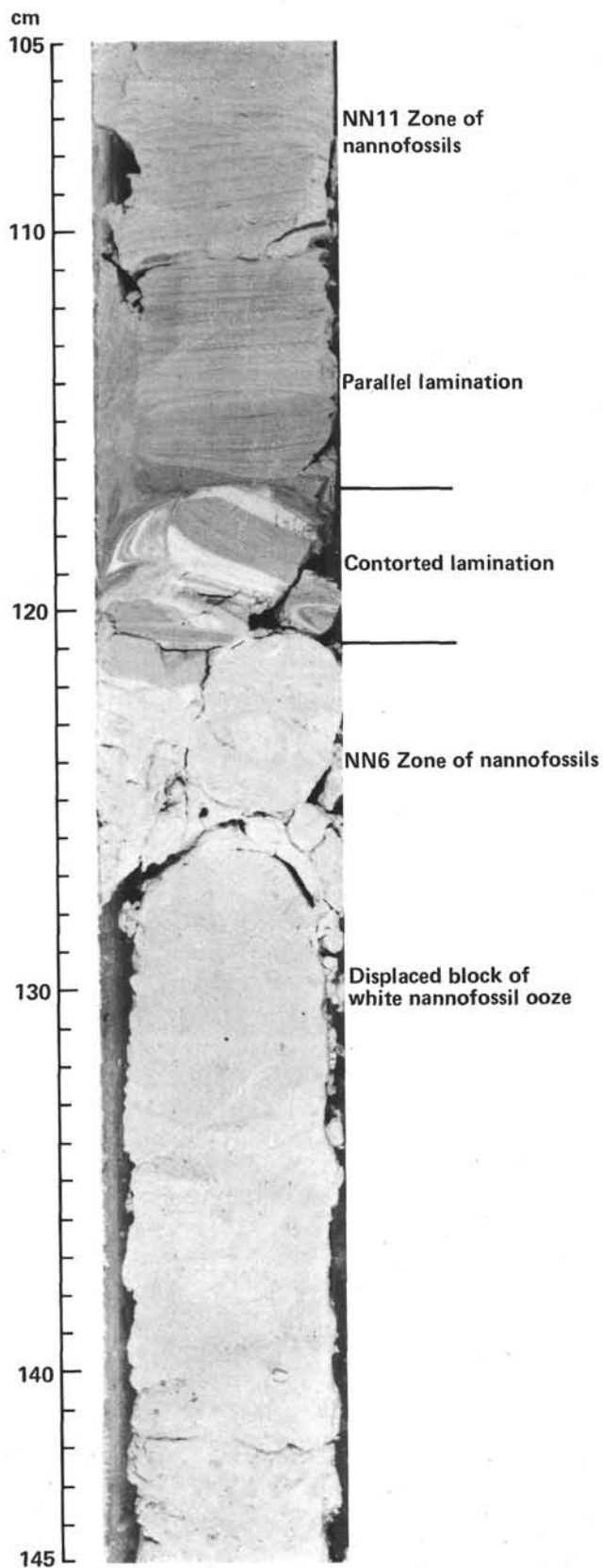


Figure 4. Unconformity between upper and middle Miocene sediments in Section 548A-11-3. Contact is marked by reworked sediment pebbles overlain by laminated nannofossil ooze and a melange of white and greenish gray nannofossil ooze.

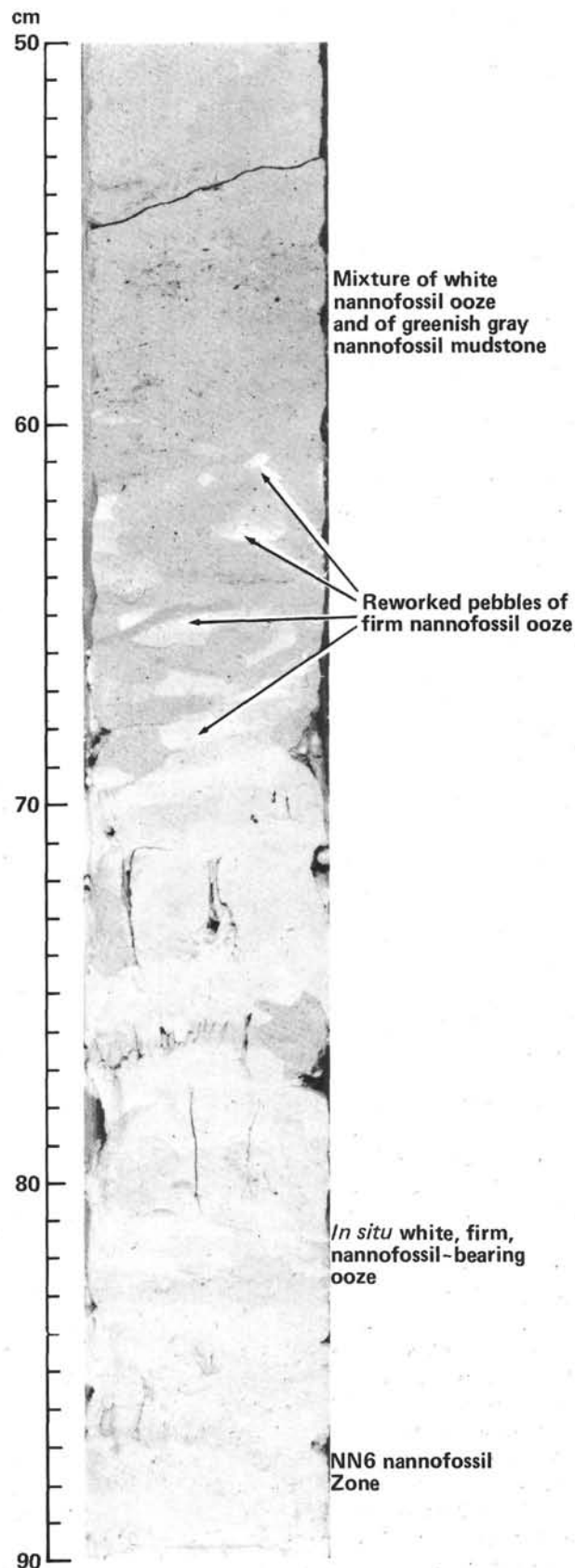


Figure 5. Transition zone below upper to middle Miocene unconformity (Section 548A-11-4). A mixture of white and greenish gray nannofossil ooze appears above white, firm, middle Miocene nannofossil ooze.

ponents across the facies boundary. Unit 4 ranges in age from middle Miocene to middle Eocene. It can be divided into two subunits on the basis of lithologic and well log differences.

Subunit 4a

Subunit 4a occurs from 304.75 to 376.5 m BSF (Section 548A-11-3 to Core 548A-18) and is middle Miocene to middle Eocene in age.

Nannofossil chalks constitute the top and bottom of Subunit 4a, with foraminifer-nannofossil chalks in between. The nannofossil chalks (found in Core 548A-11, Sections 548A-12-1 to 548A-12-4, and Core 548A-15) are firm and moderately to extensively mottled in shades of greenish gray (5GY 7/1-8/1). Core 548A-11 contains a number of silty layers, several of which include fine laminations or a gradual downward increase in grain size. Sand composed of quartz (5-15% of total), foraminifers (5-15%), unspecified carbonate (5-10%), sponge spicules (5-20%), and glauconite (trace to 5%) constitutes 10 to 40% of Core 548A-11. Clay ranges from 40 to 70% and is dominated by nannofossils. Carbonate content ranges from 60 to 90% (according to smear slide and carbonate bomb analysis).

Foraminifer-nannofossil chalks occur in Sections 548A-12-5 and 548A-12-6 and extend to Core 548A-14. The upper contact with the nannofossil chalks is gradational and occurs within Section 548A-12-5. These sediments are similar in appearance to the nannofossil chalk but have a sandier texture. They appear as a peak in intensity on the gamma ray log. Core 14 contains a number of graded siltier layers (30-60 cm thick). This core also contains several thin (less than 1 cm) bands of silica. The sand content of these sediments ranges from 10 to 20%. Foraminifers make up the dominant sand component. Clay content ranges from 50 to 80%; the clay is dominated by nannofossils. The unspecified carbonate content in these sediments ranges from 5 to 20%, and the total carbonate content ranges from 80 to 100% (according to smear slide and carbonate bomb analysis).

The sediments in Core 548A-16 and Sections 548A-17-1 to 548A-17-3, of late Oligocene to late Eocene age, may be separated from the rest on the basis of color and foraminifer preservation (see Biostratigraphy). They are bluish white (5B 7/1) to light greenish gray (5GY 8/1-7/1) and are firm and fairly homogeneous, although contacts between beds of different colors may be sharp and well burrowed. Foraminifer preservation is poor to very poor. These sediments are otherwise similar to, and grade into, those in the lower part of Core 17 (see below). A significant upper Oligocene lithologic discontinuity is present in Section 548A-16-3.

The sediments in Sections 548A-17-4 to 548A-18-1 are firm to very firm and moderately to intensely mottled in light shades of greenish gray (5GY 8/1-7/1). Except for millimeter- to centimeter-sized burrows, the sediments have very little structure. Some sections contain scattered mollusc fragments and glauconite grains. Sand content ranges from 10 to 20% and is composed primarily of foraminifers. Clay and silt content ranges from 80 to 90% and is dominated by nannofossils. Carbonate

bomb analyses show that total carbonate content averages about 70%.

The sediments in Subunit 4a show signs of diagenetic alteration centered on the larger burrows. Certain burrows contain white flecks (millimeters in length) in a green background and are surrounded by one or two very fine blue halos (chert?) (Fig. 6). The entire structure may be several centimeters in diameter.

Shipboard X-ray analysis of the sediments in Subunit 4a shows that quartz concentrations are extremely low (0-5%) and that calcite content is 50 to 70% of the sediment. X-ray analysis of the clay mineral fraction shows a continuous downhole increase in smectite, which comprises up to 70% of the clay fraction. Kaolinite and chlorite are recognizable in small quantities down to Section 548A-15-2. Below Section 548A-15-2, mixed-layer kaolinite-chlorite accounts for 0-5% of the clay composition and illite approximately 20% (Chennaux et al., this volume).

Subunit 4b

Subunit 4b occurs from 376.5 to 412.6 m BSF (Core 548A-19 to Section 548A-22-6) and is middle Eocene in age.

Subunit 4b is separated from Subunit 4a by higher values of formation density (gamma ray), resistivity, sonic velocity, and neutron density (see Downhole Logging). The sediments appear to be harder, and they contain occasional cherty nodules and beds (e.g., Section 19-4, 116-129 cm). Moreover, there is a sharp reduction in CaCO₃ content between Core 17 (average value: about 90%) and Core 18 (average values, Section 2 downward: 70-75%). Although total organic carbon content changes little across the boundary (and is generally very low—0.1%), there is a significant change in the C/N ratio.

X-ray analysis of bulk composition shows that calcite dominates these sediments (50-60%); quartz accounts for only 5 to 10%. The dominant clay minerals are smectite (about 80%) and illite (about 20%).

A thin section from a chert nodule shows a matrix of opal containing scattered clusters of micritic calcite, rare glauconite grains, phosphatic grains, tiny flakes of white mica, and chlorite. Among these are numerous foraminifers, the tests of which have been partly replaced by chalcedony. Opaline sponge spicules are also present, but they are no more numerous than in sediments devoid of cherts. The few radiolarians observed in Unit 4 are not concentrated in the cherty chalks but usually occur in more calcareous strata.

Sedimentation in Unit 4 was dominantly pelagic. Silica enrichment correlates with the generally elevated level of silica production recorded in the Atlantic Ocean for middle to late Eocene time (see the description of Site 400 in, for example, Montadert, Roberts, et al., 1979).

The boundary between Units 4 and 5 is marked by a sharp lithologic change from light-colored chalks to brownish and much more clayey sediment. This lithologic change coincides with a change in paleomagnetic fabric (Hailwood and Folami, this volume). An unconformity is indicated by the absence of the nannofossil Zone NP13, the reduction of Zone NP14 to a few deci-

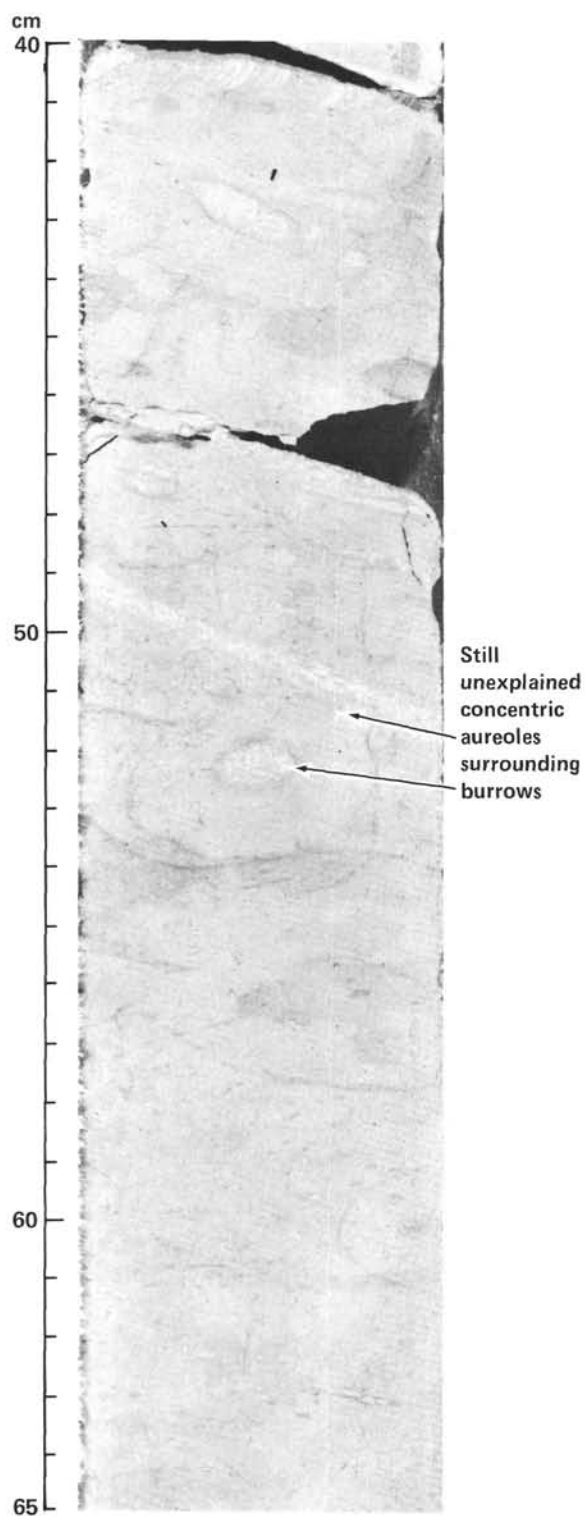


Figure 6. Concretionary aureoles surrounding burrows in greenish gray nanofossil oozes of Section 548A-12-1 (lithologic Subunit 4a).

meters, and the absence of planktonic foraminifer Zones P8 and P9. Inasmuch as these zones correspond to a small part of the Ypresian Stage, the unconformity represents only a short hiatus. Just above the unconformable contact (Fig. 7), reworked nanofossils from the lower Eocene are mixed with species of Zone NP14

(lower middle Eocene) in a 20 cm-thick layer of silty chalk. The short transition is well marked on the gamma ray log, which shows a downward increase in values that corresponds to an increase in the content of terrestrial debris across the unconformity.

Unit 5

Unit 5 consists of brown and gray marly nanofossil chalk. It occurs in Hole 548A from 412.6 to 469.9 m BSF (Sections 548A-22-6 to 548A-28-6) and is early Eocene to late Paleocene in age.

Marly nanofossil chalk first appears in Section 548A-22-6, where it is olive gray (5Y 4/2), firm, and moderately burrowed. In Section 6 the contact with the overlying sediments is sharp. In the upper to middle part of

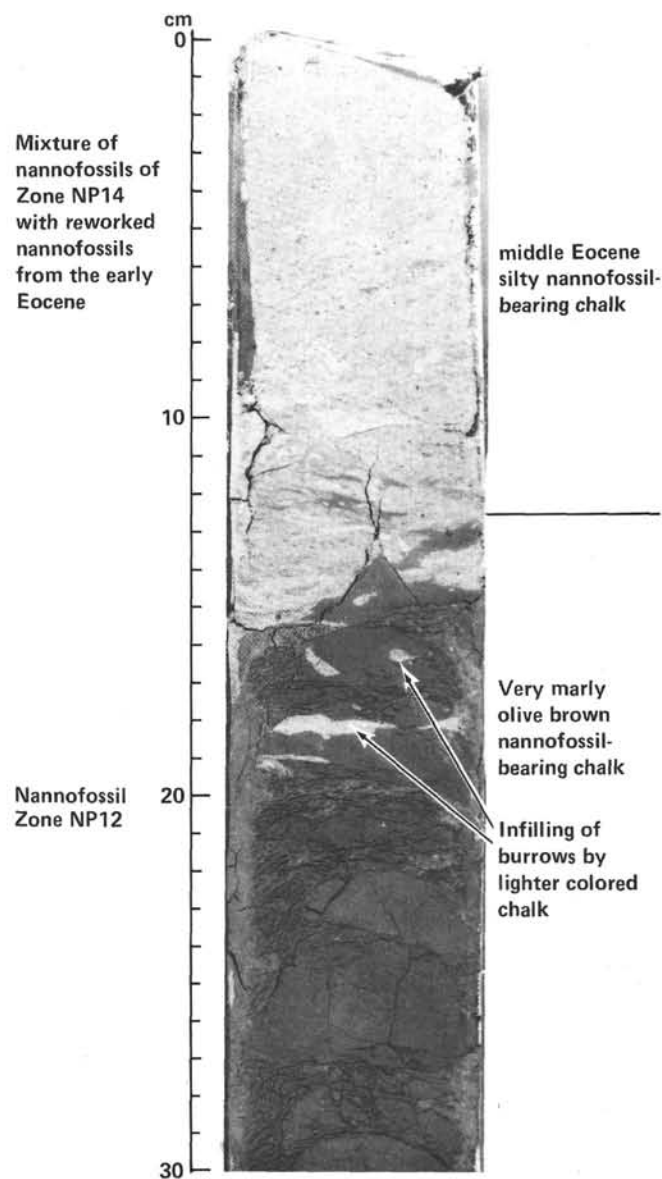


Figure 7. Contact between lithologic Units 4 and 5, which is an unconformity between lower and middle Eocene sediments. Greenish gray nanofossil chalk of Unit 4 overlies very marly olive brown nanofossil-bearing chalk of Unit 5. Section 548A-22-6.

the unit (Section 548A-22-6 to Core 26), brown marly nannofossil chalk dominates; the brown chalk alternates with greenish gray nannofossil chalk at the base (Core 27). Core 28 contains a sharp, unconformable boundary between brown marly nannofossil chalk and the white chalk of Unit 6 (Fig. 8). This lithologic change coincides with a change in the paleomagnetic fabric (Hailwood and Folami, this volume).

X-ray determinations and smear slide data show a marked decrease in calcite (20–40% of the bulk composition) and an increase in quartz (10–20%) in Unit 5. Undifferentiated kaolinite and chlorite make up 10 to 15% of the clay mineral fraction, illite composes 10 to 20%, and smectite dominates (65–85%). The marly chalk of Core 22 contains more quartz (15%) and clay (about 20%) than does the overlying nannofossil chalk, and it is also enriched in sponge spicules (about 10%). In Cores 23 to 26 the marly chalk is gray brown (2.5Y 4/2–5/2) and more homogeneous than the overlying sediments. Here it contains more clay (about 30%) and has a variable content of sand-sized particles (10–20%). The sand is composed largely of quartz and foraminifers (5–10% foraminifers). The clay fraction appears to be 50% clay minerals and 50% nannofossils. Carbonate content is 40 to 50% (according to smear slide analysis) or 20 to 30% (according to carbonate bomb analysis). Diagenesis may be indicated by the occasional filling of burrows by a bright green substance; one smear slide revealed an abundance of glauconite and an amorphous green material.

In Core 27, brown sediments alternate with greenish gray nannofossil chalks in beds centimeters to tens of centimeters thick. All contacts are well defined by contrasting lithologies, although they are extensively burrowed. The brown marly chalk is moderately burrowed in the upper part of the core but becomes more homogeneous toward the base. In Core 28 the sediments are entirely brown marly chalk down to the contact with Danian sediments. These sediments coarsen downhole toward the contact and include several graded beds containing as much as 20% sand (quartz and foraminifers). Basal contacts are sharp in this interval.

Unit 6

Unit 6 is variegated foraminifer–nannofossil chalk. It occurs in Hole 548A from 469.9 to 530 m BSF (Section 548A-28-6 to Core 35) and is Paleocene (Danian) to late Campanian in age.

Unit 6 rests unconformably below Unit 5 (Fig. 8). The sediments of Unit 6 are nannofossil and foraminifer–nannofossil chalks. At the top of the section they are homogeneous and white (10YU 8/2); at the bottom of the section they are more variable in structure and color (Fig. 9). This color variability is present from Core 31 downward and includes moderate orange pink (5YR 8/4), yellow gray (5Y 8/1), grayish orange pink (5YR 7/2), and brown gray (5YR 4/1). The abundance of silt-sized carbonate particles and black pyritic streaks also increases below Core 31. Initial observations suggest that the chalk becomes more indurated toward the base of Unit 6. This correlates with the increase in resistivity (decrease in porosity) recorded by downhole logs.

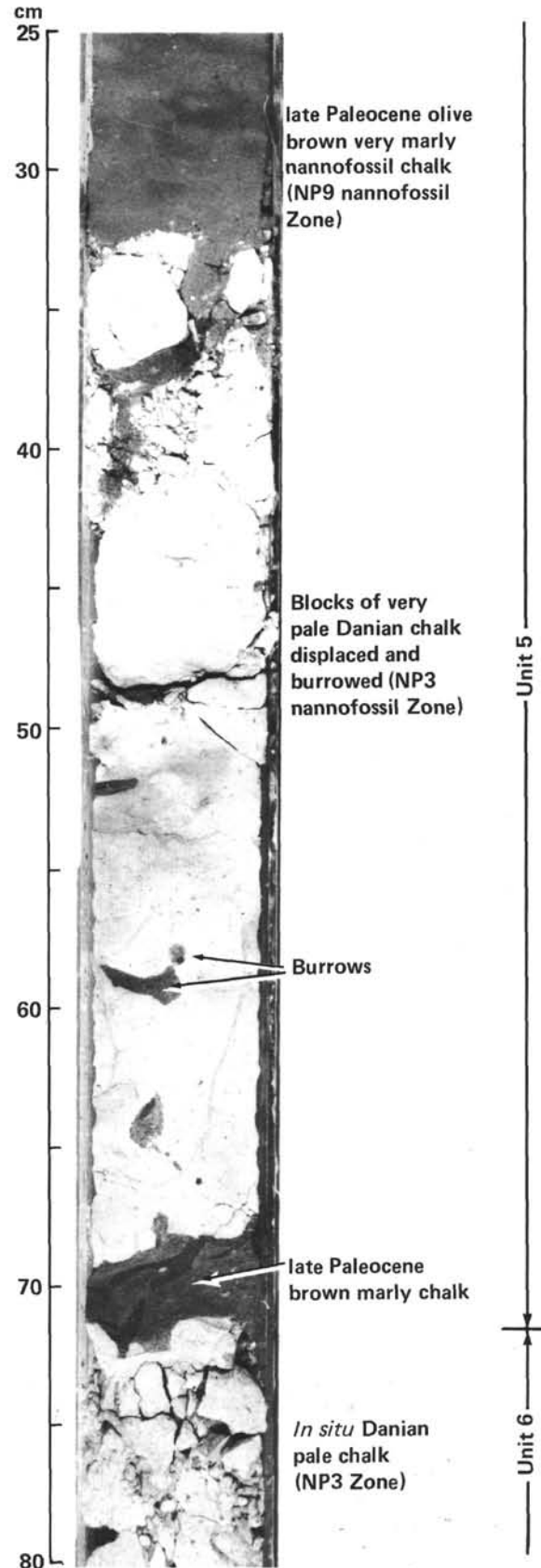


Figure 8. Unconformable contact between lithologic Units 5 and 6: late Paleocene olive brown very marly nannofossil chalk overlying pale Danian chalk. Section 548A-28-6.

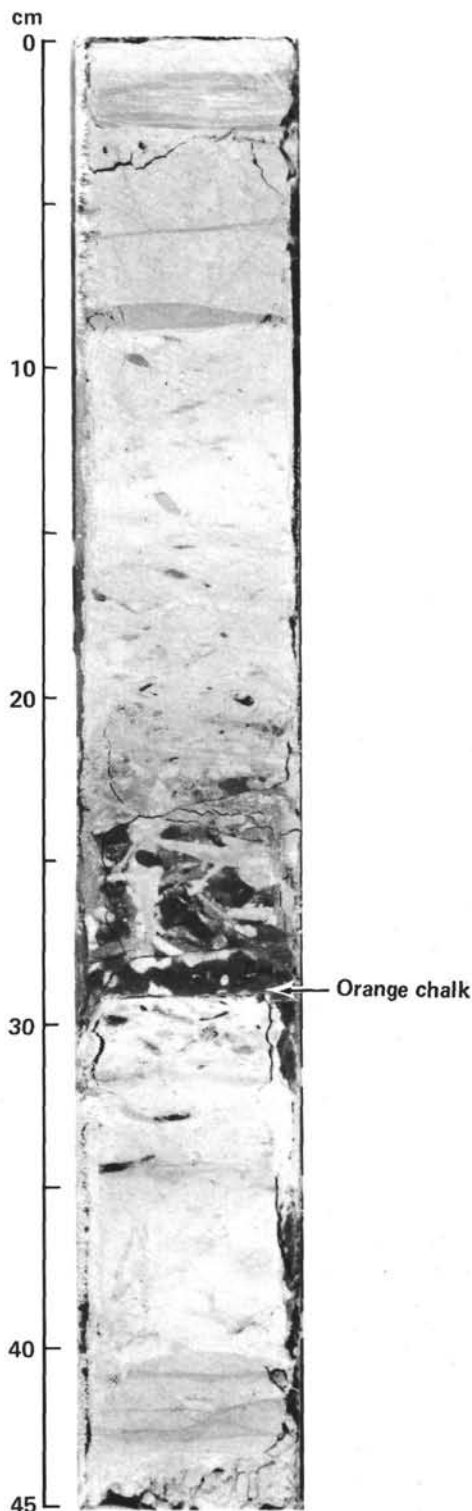


Figure 9. Example of bioturbation in Maestrichtian chalk. Section 548A-33-4.

Unit 6 sediments are composed of unspecified carbonate particles (5–15%), foraminifers (5–15%), and nannofossils (60–85%) (according to smear slide analysis). Mollusc fragments are recorded in Sections 548A-32-2 and 548A-32-3. Carbonate bomb analyses show almost

100% CaCO_3 . Mineralogical analysis shows that the sediments consist mainly of biogenic and diagenetic calcite, as supported by this high value. Terrigenous influx is recorded as a diversified clay–mineral association, with smectite, mixed-layer clay minerals, illite, kaolinite, and minor chlorite (Granansky and Bourbon, this volume).

Nannofossil Zones NP4 to NP8 are absent at Site 548. Cores 28 and 29 contain Zones NP3 and NP9, respectively; thus, the contact between Danian and late Maestrichtian beds is unconformable. However, no lithologic change occurs between these strata, so the Danian and Cretaceous are included in a single lithologic unit.

Unit 7

Unit 7 consists of sideritic hardground and coarse quartzose sands and muds. It occurs in Hole 548A from 530 to 535.5 m BSF (Cores 35 to 36) and may be Early or perhaps pre-Cretaceous in age.

The core catcher of Core 35 contained a small (3–5 cm) rock fragment (Fig. 10) consisting of two parts. The upper part is white limestone containing one fragment of quartz (reworked from the Hercynian basement) together with abundant glauconite. The lower part is composed of wavy laminations of a dark material comprising mainly concretions of siderite, pyrite, and calcite (X-ray diffraction). Geochemical analysis reveals the dominant elements to be calcium, phosphorus, and manganese (Karpoff et al., this volume). The lower part also contains burrows filled with foraminifer-bearing chalk. There is no difference between the foraminiferal assemblages of the concretions and of the burrow-filling chalk. The foraminifer tests within the concretions are partly covered by the concretionary material, a condition that suggests a diagenetic origin for the concretions.

In Core 36, quartz sands of unknown age (535.5 m BSF) were recovered along with a soft argillaceous mass (500 cc) and many millimeter-sized rounded grains of quartz. It is possible that the quartz represents an otherwise unsampled interval of Early or pre-Cretaceous sedimentary rocks.

Unit 8

Unit 8 (basement rocks) consists of arkosic sandstones and black shales. It occurs in Hole 548A from 535.5 to 551.5 m BSF (Cores 36 to 38) and is middle to late Devonian in age.

The basement rocks at Hole 548A are well indurated and probably very brittle, causing slow coring rates (8 hr. for 23 m of penetration) and poor recovery. Cores 36, 37, and 38 contain sand-sized to 5- to 10-cm blocks and fragments of arkosic sandstone and lustrous black shale.

A thin section from the sandstone contains mainly quartz, highly altered feldspars, argillaceous material, a few white micas, chlorite, and zircons. The micas seem to be of detrital origin. The tectonic fabric of the rock is not pronounced. Analysis of the shale by palynological

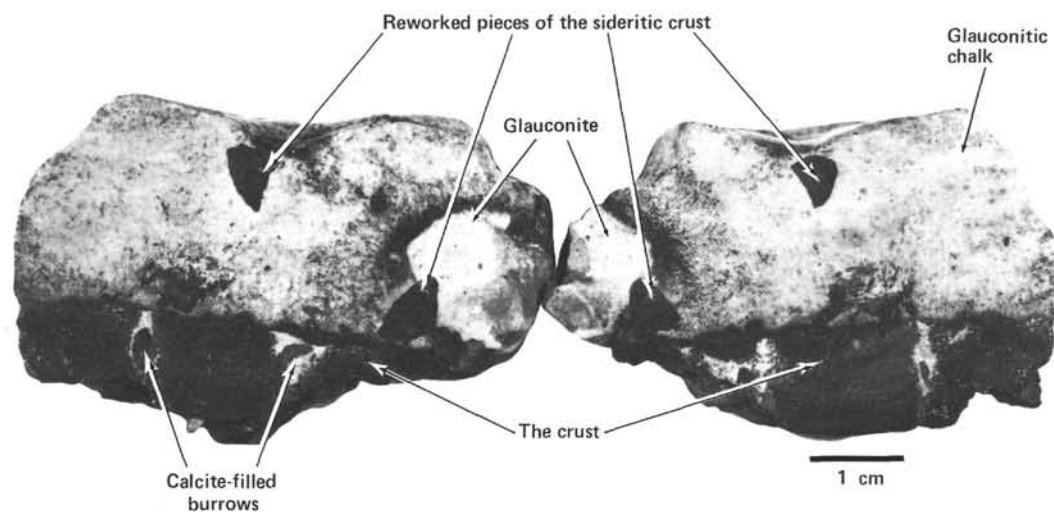


Figure 10. Hardground fragments of siderite and pyrite (Section 548A-35,CC) at base of Cretaceous chinks. These fragments represent Unit 7.

techniques revealed carbonized, highly fragmented debris; spores; and acritarchs of middle to late Devonian age (Lefort et al., this volume).

BIOSTRATIGRAPHY

Summary

Approximately 528 m of sediments, ranging in age from Late Cretaceous to Holocene, were cored above middle to late Devonian basement at Site 548 (Superlog and Fig. 11). The Pleistocene section, which is approximately 102 m thick, can be subdivided into glacial and interglacial deposits on the basis of microfaunal and nannofloral changes. Low diversity assemblages dominated by cold water species and associated with marly sediments represent intervals of glaciation. Higher diversity assemblages containing temperate and a few warmer water species are associated with the more calcareous deposits and characterize interglacial periods. Climate-associated fluctuations in assemblage are most pronounced in the upper Pleistocene section. Nannofossils and foraminifers are abundant and well preserved throughout the sequence.

The subdivision of the Pliocene section (which is 108 m thick) is difficult; both the paleontology and lithology are hard to interpret. Specimens of foraminifers and nannofossils are abundant and well preserved, but reliable index species are generally absent. However, the faunal and floral evidence suggests a transition from warmer conditions in the early Pliocene to cooler conditions in the late Pliocene.

The upper Miocene sequence in Hole 548A is a thick (95 m) accumulation of chinks interbedded with turbiditic sandy mudstones. Microfaunal and nannofloral specimens in these deposits are abundant and well preserved. As in the Pliocene, the fossils suggest that warmer conditions prevailed in the early portion of the late Miocene and were followed by a cooling trend. Sponge spicules are a minor but conspicuous component of the samples from the Miocene and Pliocene. They were not observed with any degree of regularity in sediments older than

Miocene. Sedimentation rates were high in the upper Miocene, in contrast to the lower rates and more compressed section (37 m) of the lower middle and lower Miocene. In fact, from the lower upper Miocene downward, there are numerous stratigraphic gaps and condensed intervals in the sediment sections.

Beneath the Miocene section there is a highly condensed (14 m-thick) but nearly complete Oligocene sequence. A short hiatus is present between nannofossil Zones NP24 and NP23.

Biotic deposition was apparently continuous across the Oligocene/Eocene boundary, and there is no marked change in lithology across it. Eocene microfaunal and nannofloral specimens are abundant, but preservation through the upper and middle Eocene varies from poor to moderate as a result of recrystallization and secondary encrustation. An unconformity separates the light, greenish gray nannofossil chinks of the middle Eocene from the brown, very marly nannofossil chinks of the lower Eocene. The lower Eocene section contains assemblages with fewer individuals, but they are much better preserved. The faunal changes coincide with the change in lithology across the unconformable lower/middle Eocene boundary. The combined lower Oligocene through middle Eocene section is only 60 m thick. The lower Eocene, which is characterized by higher sedimentation rates, is 55 m thick.

A thin (less than 2 m) wedge of upper Paleocene sediments lies conformably below the Eocene. A major unconformity separates this unit from a thin (1.5 m) layer of lower Paleocene (lower Danian) sediments. The Paleocene foraminifer assemblages are dominated by small globigerinids. Nannofossils are common, but many have recrystallized.

The Cretaceous deposits, which are separated from overlying Danian sediments by an unconformity, are approximately 60 m thick. Nannofossils are abundant, but breakage presents some identification problems. Foraminifers are abundant and moderately well preserved, and the assemblage is similar to that described from DSDP Site 402 (an outer shelf environment). In total, 57 m of

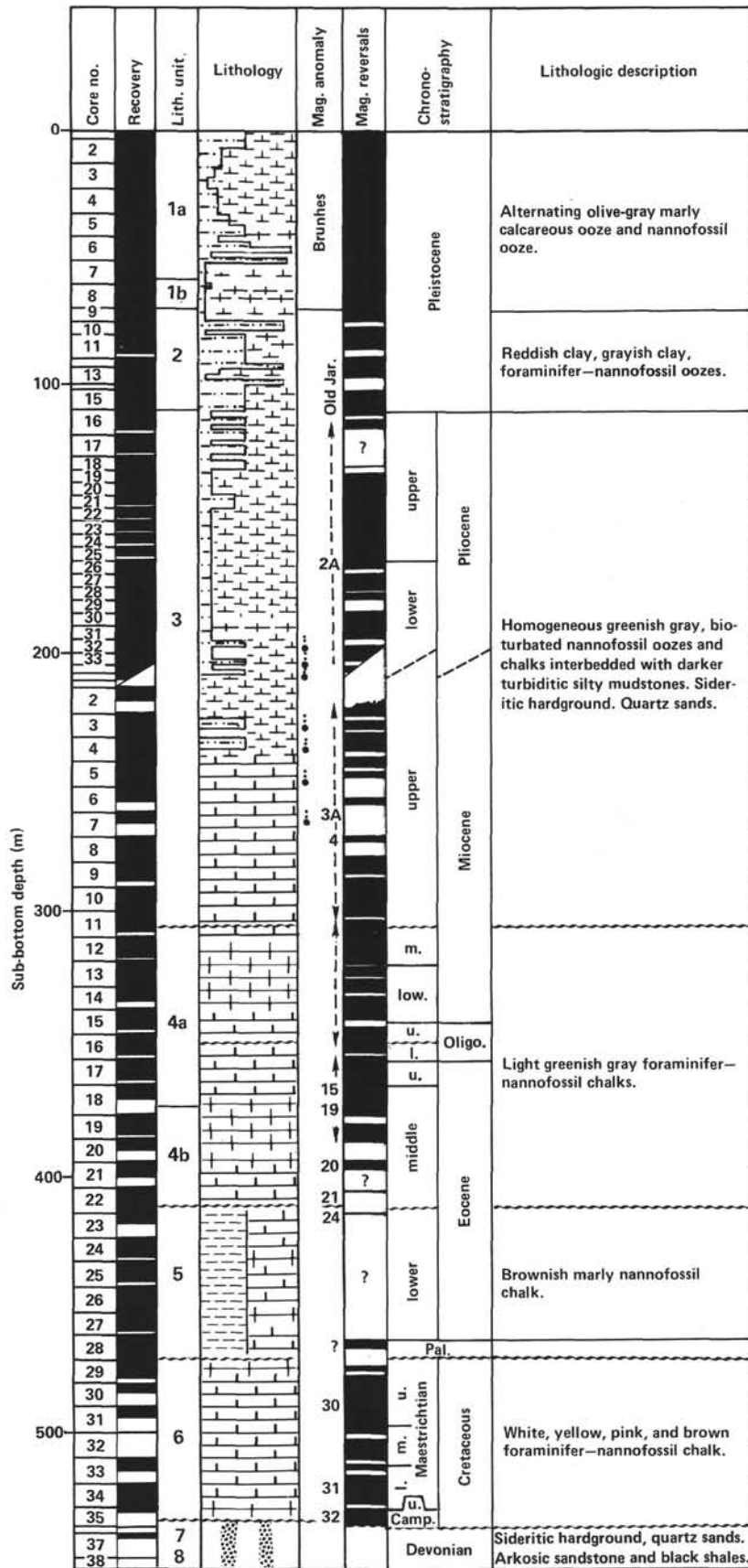


Figure 11. Stratigraphic column for Site 548. Pleistocene and Pliocene sediments were recovered from Hole 548; Miocene and older sediments were recovered from Hole 548A. Legend as explained in Explanatory Notes.

Maestrichtian and Campanian foraminifer-nannofossil chalks overlie undated sideritic hardgrounds, which lie above Devonian sandstones of the Hercynian basement.

The depths (and sample numbers) specified in the following discussion for the biostratigraphic boundaries were identified on board ship. In the course of subsequent work on shore the boundaries between the top of the Oligocene and the bottom of the Eocene shifted slightly. The revised boundaries are shown in the Superlog and supersede those in the text.

Foraminifers

Hole 548

Hole 548 penetrated approximately 210 m of Cenozoic (Holocene, Pleistocene, and Pliocene) sediments (Fig. 11). Planktonic foraminifers are abundant and generally well preserved throughout the sequence. Changes in species diversity (which varied from low to moderate) generally correspond to marked changes in the species composition of the faunas.

Below a thin surficial layer of Holocene sediment lies a sequence of Pleistocene sediments approximately 102 m thick (Core 1 to Section 548A-15-2). The Pleistocene is characterized by the alternation of distinctly different assemblages that reflect major fluctuations in climate. The interglacial assemblages are characterized by moderate diversity and the presence of very few benthic foraminifers, and they are numerically dominated by *Globigerina bulloides* and *Globorotalia inflata*. The intervening glacial assemblages are dominated by *Neogloboquadrina pachyderma* and *N. "du/pac"*, the latter considered to be a form intergradational between *N. dutertrei* and *N. pachyderma* (Poore, 1979, p. 472). The glacial assemblages are less diverse and usually contain a slightly higher percentage of benthic foraminifers than the interglacial assemblages. Some samples (e.g., 548-4-3, 90–93 cm and 548-5-3, 60–63 cm) contain sublittoral benthic species that belong to such genera as *Quinqueloculina*, *Elphidium*, and *Buccella*. Their presence indicates faunal mixing caused by downslope transport. Faunal changes throughout the Pleistocene section correlate with variations in sediment type. Glacial assemblages are associated with influxes of detrital sediment, mostly quartz. Interglacial assemblages are associated with sediments that lack detrital components. Preservation is excellent in samples that contain interglacial assemblages, but moderate breakage and recrystallization characterize the glacial assemblages.

The Pliocene/Pleistocene boundary, if defined by the *Globorotalia tosaensis*–*G. truncatulinoides* transition, is present between Samples 548-13-6, 51–54 cm and 548-14-1, 33–36 cm. This does not coincide with the nannofossil-indicated Pleistocene base. Both of these *Globorotalia* species are rare at this latitude, and they occur only sporadically through their respective stratigraphic ranges. Thus, the true first appearance datum (FAD) of *G. truncatulinoides* may not have been observed, and the Pliocene/Pleistocene boundary may lie lower within the section. The nannofossil-based boundary is lower and correlates more closely with paleomagnetic evidence.

An alternative to using the FAD of *G. truncatulinoides* in this high latitude region is to base the boundary on the last appearance datum (LAD) of *Neogloboquadrina atlantica* (Berggren, 1972). Use of this datum at Site 548 brings the planktonic foraminiferal base of the Pleistocene into agreement with both nannofossil and paleomagnetic evidence. The LAD of *N. atlantica* occurs between Samples 548-15-2, 76–79 cm and 548-15-3, 76–79 cm.

The identification of the Pleistocene/Pliocene boundary exemplifies the difficulty of interpreting high latitude biostratigraphy. Because standard planktonic foraminiferal zonations are based on tropical faunas, the species used to define such zones are usually absent at higher latitudes. Therefore, the identification of many of the zones discussed here is based on the presence of those few stratigraphically significant species that have been recovered. Positions of the zonal boundaries should, therefore, be considered tentative.

The Pliocene section is approximately 108 m thick, extending downhole from Sample 548-15-3, 76–79 cm through 548-35-1, 90–93 cm. *Globigerina bulloides*, *Neogloboquadrina atlantica*, and *N. acostaensis* are common throughout the Pliocene. The upper part of Zone N19 contains many specimens of *Globorotalia inflata*. The FAD of *G. inflata* corresponds roughly to the LAD of *G. puncticulata*, a faunal transition that marks the middle of Zone N19. The lower portion of N19 is characterized by the simultaneous occurrence of *G. puncticulata* and *G. margaritae*. The boundary between Zones N19 and N18, based on the FAD of *G. puncticulata* and the LAD of *G. janaei*, lies between Samples 548-33-2, 90–93 cm and 548-33-3, 90–93 cm. The planktonic foraminiferal assemblages indicate that climatic fluctuations, although more difficult to detect than those in the Pleistocene, also occurred during the Pliocene. The species composition and faunal diversity of the lower Pliocene assemblages (Zones N18 and lower N19) suggest temperate conditions. The warmer water indicator species include the keeled *G. margaritae* and *G. janaei* and rare but consistently present specimens of *Globigerinoides obliquus*, *G. extremus*, *G. quadrilobatus*, and *G. sacculifer*. The upper Pliocene assemblages suggest cooler water, because the warm water indicators are absent and *Globigerina bulloides* and *Globorotalia inflata* are more abundant. Hole 548 did not penetrate below the base of the Pliocene.

Hole 548A

Tertiary

Hole 548A penetrated approximately 325 m of Miocene through Danian sediments. The planktonic foraminiferal assemblages in the uppermost part of Hole 548A indicate an age of late Miocene. The Pliocene/Miocene contact evidently lies at the juncture between the two holes; the boundary was recovered from neither.

The upper Miocene section (Zones N17 and N16) is a sequence of turbidites approximately 95 m thick. Planktonic foraminifers are generally abundant and well preserved, but species diversity is moderate to low, and

relatively few reliable index species are present. *Neogloboquadrina acostaensis* and *Globigerina bulloides* predominate throughout the upper Miocene section. Species of secondary abundance include *Globorotalia continua*, *Globigerina decoraperta*, and *Neogloboquadrina atlantica*. The Zone N17/N16 boundary, based primarily on the LAD of *Globorotalia linguaensis*, occurs between Samples 548A-6-2, 47–51 cm and 548A-6-3, 114–117 cm. Immediately below, in Sample 548A-7-1, 133–137 cm, there is an abrupt change in the coiling direction of *Neogloboquadrina acostaensis*. Specimens below this point coil sinistrally, while those above coil dextrally. Because of the abundance of *N. acostaensis*, this abrupt change in coiling direction is an excellent stratigraphic marker. The base of Zone N16 is marked by the FAD of such numerically important forms as *Globigerina bulloides*, *G. decoraperta*, and *Neogloboquadrina acostaensis*.

Faunal changes at the base of the turbidite sequence (lithologic Unit 3) indicate a significant hiatus. Sediments containing the previously described upper Miocene assemblages occur in Sample 548A-11-3, 130–132 cm, whereas Sample 548A-11-4, 9–11 cm contains a lower middle Miocene assemblage. Important marker species that occur immediately below the unconformity include *Globorotalia fohsi fohsi*, *G. fohsi peripheroronda*, *G. siakensis*, and *Globigerinoides sicanus*. Sediments from Sample 548A-11-4, 9–11 cm downward through Sample 548A-12-6, 66–68 cm lie within the middle Miocene. Low sedimentation rates produced a condensed section that is only about 13 m thick, and some of the planktonic foraminiferal zones (such as Zones N10 to N12) cannot be reliably differentiated. Zone N9 is differentiated on the basis of the FAD of *Globorotalia fohsi fohsi* and on the last common appearance of *Praeorbulina glomerosa*. Zone N8 is distinguished from Zone N9 on the basis of the FAD of *Orbulina*.

The lower Miocene sequence is approximately 28 m thick. Zone N7, which lies immediately below the FAD of *Praeorbulina glomerosa*, extends from Sample 548A-13-1, 80–82 cm through Sample 548A-14-1, 90–92 cm. The N7/N6 zonal boundary is based on the LAD of *Catapsydrax dissimilis* and *C. unicavus*. The boundary between Zones N6 and N5 is tentatively placed between Samples 548A-14-4, 90–92 cm and 548A-14-5, 90–92 cm because of the FAD of *Globigerinoides subquadratus*. Zones N4 to P21 extend from Sample 548A-15-3, 58–60 cm downward through Sample 548A-16-2, 39–41 cm. These zones cannot be reliably separated on the basis of the planktonic foraminifers; thus, the location of the Oligocene/Miocene boundary cannot be precisely determined. The Oligocene section, although nearly complete, is condensed, extending downward only through Sample 548A-16-5, 39–41 cm. An unconformity is present within Zone P21. Thus, the entire Oligocene sequence is only about 12 m thick. *Catapsydrax unicavus* and *C. dissimilis* occur throughout the Oligocene. The upper and lower portions of the Oligocene are easily distinguished, because only the latter contains *Globigerina ampliaper-tura*, *G. angiporoides*, and *Globorotalia increbescens*.

The Eocene/Oligocene boundary lies between Samples 548A-17-1, 66–69 cm and 548A-16-5, 39–41 cm. Its location is based on the LAD of *Globorotalia cerroazulensis cerroazulensis* and *G. cerroazulensis cocoazulensis*. The upper Eocene section is complete but moderately compressed, extending downward through Sample 548A-18-1, 67–69 cm (a thickness of about 10 m). The upper Eocene sediments are characterized by species of *Catapsydrax*, the *Globorotalia cerroazulensis* complex, *Globigerinatheka index*, and several species of *Globigerina* (*G. angiporoides*, *G. corpulenta*, and *G. gortanii*). The middle Eocene, which is also complete, is less compressed (about 46 m thick). The upper/middle Eocene (P15/P14) boundary is based on the LAD of *Truncorotaloides rohri* and *T. collactea*, and on the FAD of *Globorotalia cerroazulensis cerroazulensis*. Middle Eocene assemblages are characterized by abundant specimens of *Acarinina* (most notably *A. bullbrookii*), *Globigerina frontosa*, several species of *Globigerinatheka* (particularly *G. barri* and *G. index*), and several species of *Truncorotaloides* (*T. collactea*, *T. rohri*, and *T. topilensis*). Between Sample 548A-22-5, 87–89 cm, which is lowermost middle Eocene, and Sample 548A-22-6, 87–89 cm lies an unconformity (Zones P9 and P8 are absent). The portion of the lower Eocene that is present (Zones P7 and P6) is approximately 55 m thick. The fauna consists of a diverse assemblage of *Acarinina* spp., most importantly *A. nitida*, *A. broedermanni*, *A. pseudotopilensis*, *A. soldadoensis soldadoensis*, and *A. soldadoensis angulosa*. Several species of *Morozovella*, namely *M. formosa gracilis*, *M. lensiformis*, *M. quetra*, *M. subbotinae*, and *M. aequa*, are useful in identifying and subdividing this interval. *Planorotalites chapmani* occurs consistently throughout Zone P6. A single sample (548A-28-5, 62–65 cm) is assigned to Zone P5 (upper Paleocene) because it contains many specimens of *Acarinina mckannai*.

An unconformity below the sediments of Zone P5 represents a hiatus that spans most of the Thanetian and late Danian (Zones P4–P2). Sample 548A-28-7, 28–30 cm, which lies immediately below the unconformity, contains an assemblage that is assigned to Zone P1d. Characteristic species are *Subbotina triloculinoides*, *S. trinidadensis*, *S. pseudobulloides*, and *Eoglobigerina daubjergensis*. This interval is, in turn, separated from underlying Cretaceous sediments by an unconformity (between Core 28 and 29), because of which the early Danian is missing (Zones P1a–P1c).

Cretaceous

The Cretaceous/Danian boundary is placed between Cores 28 and 29, because the first late Maestrichtian foraminifers occur 3 cm below the top of Core 29 (Fig. 11). Cores 29 to 34 belong to the Maestrichtian stage, and Core 35 may reach the Campanian stage. All of the Cretaceous strata accumulated in pelagic outer shelf or upper slope environments. Although preservation is usually moderate to bad, with frequently recrystallized, partly dissolved, and fragmented tests, the core-catcher samples examined on board ship have shown that successive foraminiferal zones are recognizable, as follows.

Upper part of Maestrichtian (MC11 or *mayaroensis* Zone): Cores 29 and 30. Diagnostic species include the key species and the *Globotruncana arca*, *G. caliciformis*, *G. citae*, *G. contusa*, *G. wiewickae* group, as well as *Globigerinelloides messinae subcarinata*, *Racemiguembelina fructicosa*, and *Bolivinoidea peterssoni*.

Middle part of Maestrichtian (more or less equivalent to the lower part of MC10 or *gansseri* Zone): Core 31. Diagnostic species include the key species and *Globotruncana contusa*, *G. stuartiformis*, *Pseudotextularia varians*, and *Planoglobulina acervulinoides*.

Core 32 occupies an intermediary zonal position between MC10 and MC9. Core 33 does not provide precise biostratigraphic data because of poor specimen preservation.

Lower part of Maestrichtian (MC9 or *stuarti-falso-stuarti* Zone): Core 34. Diagnostic species include the key species and *Globotruncana contusa*, *G. elevata*, *G. fornicata*, *G. cf. pembergeri*, *Globigerinelloides bollii*, *Stensioeina* spp., and *Reussella szajnochae* var.

Core 35 (Samples 548A-35-1, 45–46 cm and 548A-35-1, 135–136 cm) belongs either to the lower Maestrichtian (MC9) or the upper Campanian (MC8 or MC7 Zones). The foraminiferal assemblage (including *Globotruncana arca*, *G. fornicata*, *Reussella szajnochae* var., and *Bolivinoidea laevigata*) is not diagnostic, because key fossils are missing.

Nannoplankton

Hole 548

Quaternary

The Quaternary was encountered from the top of the section to a depth of 101 m (Core 1 to 548-15-1, 30 cm) (Fig. 11). The *Emiliania huxleyi* Zone (NN21), present from Cores 1 to 5, is underlain by the *Gephyrocapsa oceanica* Zone (NN20) in Core 6 to Sample 548-7-2, 40–43 cm and the *Pseudoemiliania lacunosa* Zone (NN19) from Sample 548-7-4, 40–43 cm to 548-15-1, 30 cm. The thinness of the *G. oceanica* Zone suggests that part of it was eroded or not deposited. The uppermost part of Zone NN19 is present, as indicated by the occurrence of the typical “small *Gephyrocapsa*” layer (see Pujos; and Caralp et al., this volume).

The Quaternary sequence is characterized by the alternation of layers that contain abundant well preserved nannoplankton and layers that contain only a few indigenous species, a great number of reworked nannoplankton (mainly from Cretaceous and Eocene rocks), and an abundance of ice-rafted detritus. The layers with abundant nannoplankton are interpreted as having been deposited during interglacials, when warmer water masses penetrated farther to the north. The nannoplankton-poor sediments were deposited during glacials, when cold water masses drifted to the south as far as 42°N. The alternation of nannoplankton-rich and nannoplankton-poor layers is less pronounced within the lower Pleistocene (NN19), indicating that the early Pleistocene climate may have been more stable in this region.

On the whole, the Pleistocene nannoplankton assemblages are of low diversity. Dominant species are *Coccolithus pelagicus*, *Gephyrocapsa ericsonii*, and *Emiliania huxleyi*. There were no signs of dissolution in the Quaternary sequence. The presence of diatoms, fragments of radiolarians, and sponge spicules in Zone NN19 (from Samples 548-7-6, 40–43 cm to 548-8-6, 69–70 cm) might indicate a change in oceanographic conditions. The Pliocene/Pleistocene boundary is identified by the extinction of *Cyclococcolithus macintyreii*, because discoasters are not present within the upper Pliocene in this area. The paleomagnetic results from both this leg and Leg 48 show that the *C. macintyreii* extinction lies within the upper part of the Olduvai Event, which is also the extinction level for discoasters in other areas.

Tertiary

The upper Pliocene (nannoplankton Zones NN18–NN16) extends from 548-15-2, 30 cm to Sample 548-19-1, 70–73 cm; the extinction of *Reticulofenestra pseudoumbilica* marks the base of Zone NN16. The location of this boundary is somewhat questionable in Hole 548, because *R. pseudoumbilica* occurs only very rarely within the upper part of Zone NN15. A subdivision of the upper Pliocene is not possible because of the absence of discoasters. The nannoplankton assemblages of the upper Pliocene consist mainly of *Coccolithus pelagicus*, *Cyclococcolithus macintyreii*, *Pseudoemiliania lacunosa*, *Helicosphaera sellii*, *Syracosphaera pulchra*, *Pontosphaera pacifica*, and *Discolithina japonica*. Layers that are poor in nannoplankton and contain terrigenous detritus and reworked specimens appear in Sample 548-16-2, 20–23 cm; Section 548-16,CC; and Sample 548-19-2, 45–48 cm. These constituents may indicate climatic fluctuations during late Pliocene time.

The lower Pliocene (nannoplankton Zones NN15–NN12) is encountered from Sample 548-19-2, 45–48 cm to Section 548-35,CC. Only a rough subdivision is possible because of the scarcity of discoasters. Zones NN15 to NN14 extend from 548-19-2, 45 cm to Sample 548-30-1, 60–63 cm (first *Discoaster asymmetricus*). Zones NN13 to NN12 extend from Sample 548-30-2, 80–81 cm to Section 548-35,CC.

The interval from 548-19-3, 45 cm to 548-19-3, 70 cm is characterized by the almost complete dissolution of the nannoplankton. This level is believed to correspond to the onset of glaciation in the Northern Hemisphere about 3.0 m.y. ago (during the uppermost part of Zone NN15).

Discoasters are generally rare, but together with some scyphospheres and *Amaurolithus delicatus*, they become more frequent in a few layers within the lower part of the lower Pliocene sequence. This observation suggests a slight increase of water temperature at the base of the Pliocene, in accord with results from Leg 48.

Nannoplankton are common and well preserved throughout the Pliocene. However, within the interval from Zone NN15 to NN14, there are some layers in which the abundance of nannoplankton decreases at the same time that the amount of terrigenous detritus in-

creases (Sample 548-20-3, 10–13 cm and 548-24-2, 57–60 cm). Sponge spicules are common within the lower Pliocene, and in some layers there are fragments of diatoms and radiolarians.

Hole 548A

Tertiary

A thick upper Miocene sequence is encountered from Section 548A-1, CC to 548A-11-3, 102 cm (Fig. 11 and Superlog). The entire sequence probably belongs to the *Discoaster quinqueramus* Zone (NN11), and this zonal assignment is certain down to the base of Core 8. However, below this level, *D. quinqueramus* is missing, probably as a result of unfavorable environmental conditions; this species is more sensitive to low water temperature than *D. calcaris*. The latter species, together with *D. variabilis*, is still well represented within the upper Miocene sediments of this region.

The nannoplankton are abundant and well preserved within the upper Miocene sequence. However, a slight fragmentation can be observed in some samples, indicating slight fluctuations in calcite dissolution. Climatic fluctuations are indicated by variations in the abundances of discoasters. The nannoplankton assemblages are relatively low in diversity, containing chiefly *Coccolithus pelagicus*, *Reticulofenestra pseudoumbilica*, *Cyclococcolithus leptoporus*, *C. macintyreii*, and *Helicosphaera carteri*. *Discoaster variabilis* and *D. calcaris* are common in several layers: *D. quinqueramus* and *Amaurolithus delicatus* are always rare.

Radiolarian and diatom fragments are present throughout the sequence but are often strongly dissolved. Fine-grained pyrite is common in several layers (Samples 548A-2-3, 18–20 cm; 548A-3-4, 86–92 cm; and 548A-4-6, 108–109 cm). Some reworked Eocene specimens and glauconite grains were observed in almost all samples.

The upper Miocene sequence (probably Zone NN11) is underlain by middle Miocene rocks of nannoplankton Zone NN6 (*Discoaster exilis* Zone). The unconformity between the two biostratigraphic units represents a hiatus of at least 5 m.y.

The interval from 548A-11-3, 140 cm to Sample 548A-12-1, 63–65 cm belongs to the lower part of the *D. exilis* Zone (NN6), as shown by the presence of *Cyclicargolithus abisectus*, *C. floridanus*, *D. exilis*, *Coronocyclus nitescens*, *Helicosphaera perch-nielseniae*, and the abundance of large specimens of *Coccolithus pelagicus*. Siliceous microfossils are absent. The nannoplankton are very abundant, having varying degrees of overgrowth and fragmentation due to diagenesis.

The *Sphenolithus heteromorphus* Zone (NN5) is present from Sample 548A-12-1, 110–112 cm to Section 548A-12, CC as determined by the presence of *S. heteromorphus*. The nannoplankton are abundant and are of better preservation than in the preceding section.

A complete lower Miocene sequence (nannoplankton Zones NN4–NN1) is encountered from Samples 548A-13-1, 61–64 cm to 548A-15-4, 25–27 cm. Zone NN4 includes Sample 548A-13-1, 61–63 cm to Section 548A-13, CC, as indicated by the presence of *S. heteromorphus*

and *Helicosphaera ampliaperta*. Zone NN3 includes Sample 548A-14-1, 52–54 cm to 548A-14-3, 100 cm; Zone NN2 includes Samples 548A-14-4, 52–54 cm to 548A-15-2, 101–102 cm; and Zone NN1 includes Samples 548A-15-2, 25–27 cm to 548A-15-4, 25–27 cm. The sediments are very rich in nannoplankton; the coccoliths are well preserved, whereas the discoasters display overgrowths.

A nearly complete but extremely condensed Oligocene section is present from Sample 548A-15-4, 100–102 cm to 548A-17-1, 27 cm. The *Sphenolithus ciproensis* Zone (NP25) of the upper Oligocene is present from Sample 548A-15-4, 100–102 cm to 548A-16-1, 100 cm; it contains *S. ciproensis*, *Helicosphaera recta*, *Cyclicargolithus abisectus*, *H. bramlettei*, and *Discoaster* cf. *enormis*. The interval from Sample 548A-16-2, 43–45 cm to 548A-16-3, 66 cm belongs to Zone NP24 (*Sphenolithus distentus* Zone), as indicated by the presence of *S. distentus*, *S. predistentus*, and *Chiasmolithus altus*. The interval from 548A-16-3, 74 cm to Sample 548A-16-3, 106–108 cm belongs to the *Sphenolithus predistentus* Zone (NP23). This very condensed sequence is the result of both a significant change in accumulation rate during the middle Oligocene and an unconformity between biozones NP23 and NP24, which was recognized on the basis of a lithologic discontinuity (Poag et al., this volume).

The lower Oligocene is represented from Sample 548A-16-4, 24–26 cm to 548A-17-1, 21 cm. Zone NP22 is recognized in Sample 548A-16-4, 24–26 cm and 548A-16-4, 90 cm by the occurrence of *Cyclococcolithus formosus* and *Reticulofenestra umbilica*. The interval from Sample 548A-16-5, 33–35 cm to 548A-17-1, 27 cm belongs to Zone NP21.

The Eocene/Oligocene boundary is placed between 548A-17-1, 27 cm and Sample 548A-17-1, 64–66 cm by the extinction of *Discoaster saipanensis* and *D. barbadiensis*. The upper Eocene (Zones NP20 to NP18) was encountered in the interval from Samples 548A-17-1, 64–66 cm to 548A-18-1, 38–40 cm. The nannoplankton are very abundant and contain thin calcite overgrowths. Zones NP19 and NP20 (Sample 548A-17-1, 64–66 cm to 548A-17-5, 30 cm) cannot be subdivided. Zone NP18 is present from 548A-17-6, 100 cm to Sample 548A-18-1, 38–40 cm, as determined by the occurrence of *Chiasmolithus oamaruensis* without *Isthmolithus recurvus*.

The middle Eocene sequence is complete. It is encountered from Sample 548A-18-2, 38–40 cm to 548A-22-6, 13 cm. It is separated from the lower Eocene by an unconformity representing nannoplankton Zone NP13 (lower Eocene), a hiatus of 1.0 m.y.

The *Discoaster saipanensis* Zone (NP17) is present from Sample 548A-18-2, 38–40 cm to Section 548A-18, CC; the *D. tani nodifer* Zone (NP16) from Sample 548A-19-1, 40–42 cm to 548A-19-4, 57–60 cm; the *Chiphragmalithus alatus* Zone (NP15) from Samples 548A-19-6, 53–54 cm to 548A-22-1, 51–54 cm; and the *Discoaster subloadoensis* Zone (NP14) from Samples 548A-22-3, 54–56 cm to 548A-22-6, 13 cm.

Nannoplankton are very abundant in the middle Eocene sediments. Calcite overgrowths and slight fragmentation are caused by diagenesis. The abundance of *Braa-*

rudosphaera bigelowi, *Zyghabliithus bijugatus*, *Pemma rotundum*, and species of *Micrantholithus*, as well as the scarcity of the discoasters, indicates that this sequence was deposited in an outer sublittoral to upper bathyal environment.

An important lithologic change (from nannofossil chalk to marly mudstone) coincides with the middle/lower Eocene boundary. The uppermost lower Eocene nannoplankton zone (NP13) is missing. The *Marthasterites tribrachiatus* Zone (NP12) is encountered from 548A-22-6, 22 cm to Sample 548A-25-3, 80–81 cm and is underlain by the *Discoaster binodosus* Zone (NP11) from Samples 548A-25-4, 50–54 cm to 548A-28-1, 60–61 cm and the *Marthasterites contortus* Zone (NP10) from Sample 548A-28-3, 60–61 cm to 548A-28-4, 40–41 cm.

Nannoplankton are common throughout the lower Eocene sequence, but they are somewhat diluted by the high amount of terrigenous material. Preservation is very good because of the clay content in the sediments. The abundance of *Zyghabliithus bijugatus*, *Transversopontis pulcher*, *Braarudosphaera bigelowi*, *Lophodolihus nascentis*, and species of *Rhabdosphaera* indicate deposition of these sediments in an outer sublittoral to upper bathyal environment.

The Paleocene/Eocene boundary lies between Samples 548A-28-5, 60–61 cm and 548A-28-6, 6–7 cm, as determined by the extinction of *Fasciculithus tympaniformis*. The greatest part of the Paleocene sequence is missing. The *Discoaster multiradiatus* Zone (NP9), which is represented by only a few centimeters (Samples 548A-28-6, 6–7 cm to 548A-28-6, 27–28 cm), is underlain by nannoplankton Zone NP3 (Danian), which is encountered from Sample 548A-28-6, 41–42 cm to Section 548A-28,CC. These sediments have abundant nannoplankton that display strong signs of diagenesis. The assemblages consist predominantly of *Braarudosphaera bigelowi*. *Thoracosphaera deflandrei* becomes common in several layers (Sample 548A-28-6, 115–116 cm; Sample 548A-28-6, 140–141 cm; Section 548A-28,CC).

Cretaceous

The Cretaceous/Tertiary boundary was not recovered in Hole 548A. Zone NP3 is underlain by the late Maestrichtian *Micula mura* Zone from Sample 548A-29-1, 1–2 cm to Section 548A-30,CC. The *Lithraphidites quadratus* Zone of middle Maestrichtian age is present from Samples 548A-31-1, 70–72 cm to 548A-33-1, 6–7 cm, and the *Tetralithus trifidus* Zone of the lower Maestrichtian is present from Sample 548A-33-3, 6–7 cm to Section 548A-34,CC.

The upper Campanian (*T. trifidus* Zone) is identified in Core 35 by the occurrence of *Broinsonia parca*, *Eiffellithus eximius*, and *Tetralithus gothicus*.

All of the Cretaceous sediments have abundant nannoplankton, which show increasing effects of diagenesis (fragmentation) with increasing depth. The abundance of *Lucianorhabdus cayeuxi* shows that these sediments were deposited in an outer sublittoral to bathyal environment.

Palynomorphs

Palynological analyses (J. Deunff, pers. comm., 1982) revealed Paleozoic spores and acritarchs in Core 38 within a bulk of carbonized, fragmented plant tissues (Lefort et al., this volume). These constituents suggest a subcontinental to shallow water environment.

Because of their state of preservation (a few of them are transparent), the spores cannot be easily identified specifically. Nevertheless, some large specimens are similar to species known in the late middle Devonian from the Sahara and Libya in North Africa. The genera identified include *Calyptosporites*, *Hystrichosporites*, *?An-cyrospora*, *Calamospora*, *Apiculatisporites*, and *Retusotriletes*.

The acritarchs are also difficult to identify. Several genera have been identified (*Ammonidium*, *Micrhystridium*, *Multiplicisphaeridium*, *?Staplinium*, *Polyedryxium*, *?Palacanthus*, *Veryhachium*, *Buedingiisphaeridium*, *Villosacapsula*, and *Cymatosphaera*), but a true characteristic association cannot be established. Nevertheless, some of these forms suggest a middle to late Devonian age.

SEDIMENT ACCUMULATION RATES

The oldest section for which sediment accumulation rates could be calculated at Site 548 is lithologic Unit 6, of Campanian to Danian age (Fig. 12). These strata accumulated at a rate of 7.9 m/m.y. Above an unconformity representing a hiatus of about 6 m.y., the late Paleocene/early Eocene Unit 5 accumulated nearly three times as rapidly (21.8 m/m.y.) as Unit 6. This accelerated rate is due in part to the introduction of terrigenous clays and fine-grained sands.

Above another unconformity (a hiatus of about 1.5 m.y.), the marly nannofossil chalk of Subunit 4b accumulated at a markedly reduced rate of 8 m/m.y. during the early middle Eocene. Accumulation continued to diminish during the late middle Eocene and Oligocene, reaching a minimum for this site of 2.2 m/m.y. An unconformity is present within the Oligocene interval (between nannoplankton Zones NP23 and NP24), but the hiatus represented (about 2 m.y.) is too small to account for the low accumulation rate. It is clear that the deposition rate was also quite low during this interval.

Accumulation doubled (to an average rate of 4.2 m/m.y.) over the early and middle Miocene. Following erosion that produced a 6 m.y. hiatus, upper Miocene strata accumulated at a dramatically accelerated rate of 20.6 m/m.y. The rate increased steadily to 32.3 m/m.y. during the Pliocene and culminated in a maximum rate for this site of 55.5 m/m.y. as continental detritus built a thick Pleistocene sequence.

ORGANIC GEOCHEMISTRY

The total organic carbon (TOC), carbonate, and total nitrogen contents of approximately 170 samples from Holes 548 and 548A were measured by standard shipboard procedures (Waples and Cunningham, this vol-

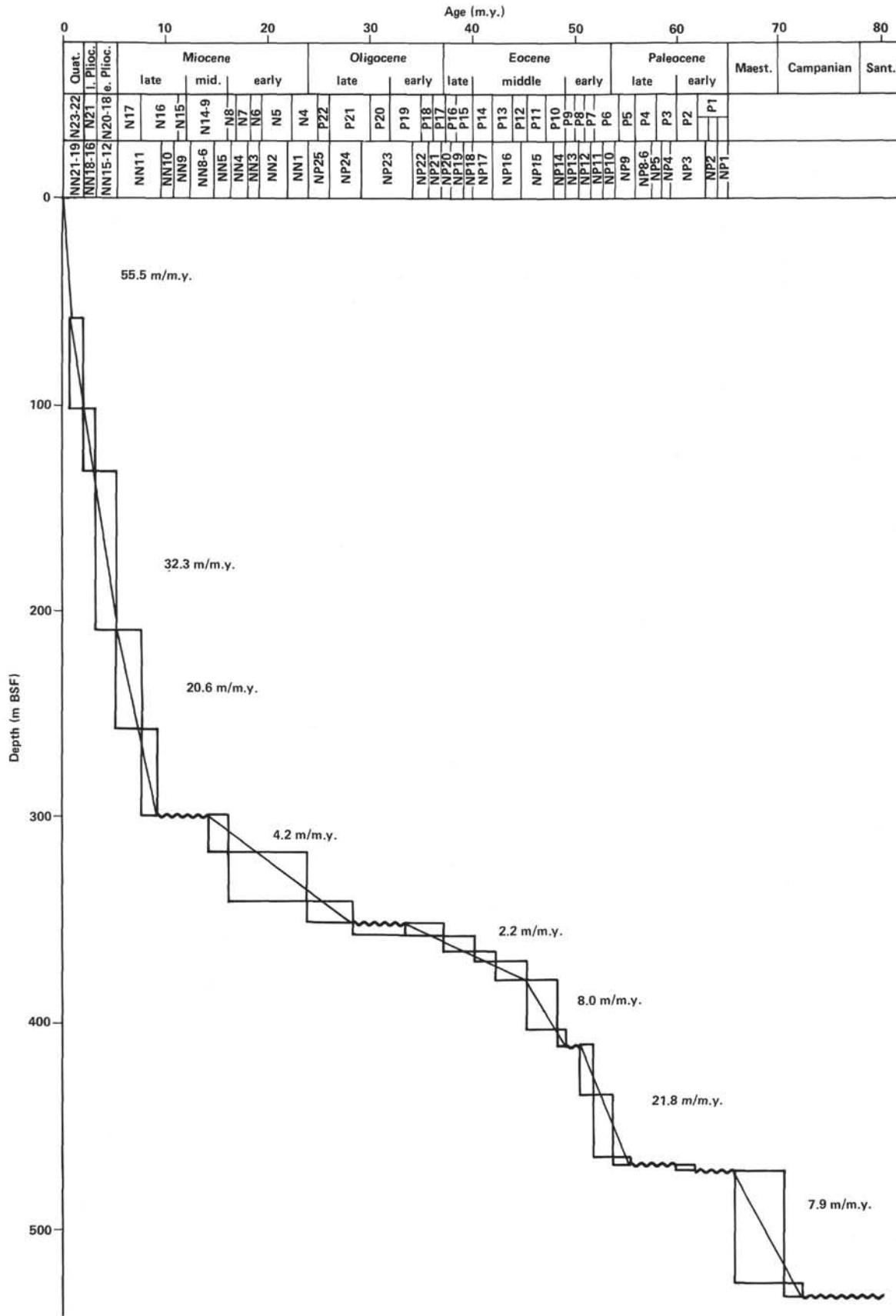


Figure 12. Sediment accumulation rate curve for Site 548. Wavy line denotes hiatus.

ume). In addition, Rock-Eval pyrolysis was carried out on 41 samples. The results of these analyses are tabulated in Waples and Cunningham (this volume).

Total Organic Carbon and Carbonate

All samples analyzed were organically lean, the maximum TOC value being less than 0.8%. Plots of TOC versus burial depth (Fig. 13) show a pronounced decrease in TOC with increasing depth of burial. Several factors that may contribute to this trend include sediment type, sediment accumulation rate, differential input of organic material, and microbial diagenesis. The influences of each are discussed in more detail by Waples and Cunningham (this volume).

Carbonate contents (expressed as wt.% CaCO₃ of whole rock) range from 8 to 100%. There is an inverse relationship between TOC and carbonate content (Waples and Cunningham, this volume).

Rock-Eval Pyrolysis

Rock-Eval analyses of samples from all lithologic units indicated low to moderate hydrogen indices (5–370 mg HC/g TOC) (Table 4). The samples with the highest hydrogen indices are from the more calcareous layers. Oxygen indices sometimes exceed 400 mg CO₂/g TOC in the upper 120 m of sediment but are generally less than 200 mg CO₂/g TOC below this depth. Hydrogen indices for these samples were plotted versus their oxygen indices on a Van Krevelen diagram (Fig. 14). Most samples plot in the Type III region, suggesting that they contain kerogen of terrestrial origin. The immaturity of these samples is indicated by the low temperatures ($T_{max} = 378\text{--}423^\circ\text{C}$) at which maximum pyrolysis yield occurred.

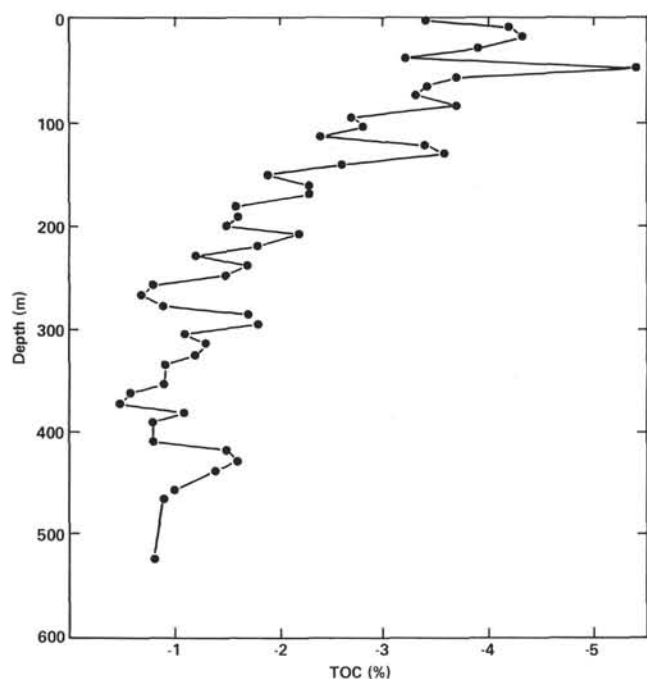


Figure 13. Total organic carbon versus burial depth at Site 548. Values are averaged over 9.5 m intervals.

Table 4. Rock-Eval data from Site 548.

Core-Section (interval in cm)	T_{max}	H index	O index	$S_1/(S_1 + S_2)$
Hole 548				
1-2, 100-102	423	30	282	0.24
2-2, 43-44	416	15	164	0.40
3-1, 57-58	410	97	91	
3-5, 57-58	420	26	130	0.21
4-2, 77-78	387	26	432	0.33
4-5, 77-78	422	81	104	
5-1, 75-76	388	72	120	
5-2, 51-52	401	23	482	0.29
6-2, 32-33	408	22	108	
6-3, 30-31	413	124	54	
6-5, 30-31	417	16	0	
6-6, 30-31	420	80	33	
7-4, 86-87	405	76	124	
7-6, 51-52	410	370	145	
8-1, 91-92	410	221	82	
8-2, 91-92	407	213	66	
8-5, 91-92	404	27	147	
9-2, 45-46	394	5	0	
10-2, 45-46	403	73	245	0.22
10-4, 45-46	384	56	89	
10-5, 45-46	383	62	143	
11-2, 75-76	396	27	272	0.23
11-5, 75-76	416	218	44	
12-2, 37-38	397	33	361	0.29
13-2, 8-9	376	40	526	0.32
13-3, 8-9	385	81	163	
14-2, 19-20	393	20	501	0.50
15-2, 65-66	395	50	396	0.20
15-4, 65-66	381	70	79	
16-2, 46-47	3	38	490	0.33
16-3, 46-47	390	58	92	
17-2, 63-64	386	167	119	
20-3, 49-50	378	44	61	
24-2, 66-67	382	124	129	
Hole 548A				
5-2, 30-31	388	95	105	
10-2, 75-76	390	128	127	
12-2, 68-69	388	150	280	
13-2, 72-73	387	300	160	
14-2, 22-24	396	27	191	
19-2, 50-51	421	73	218	
24-5, 58-59	410	0	150	

Organic Facies

The Rock-Eval pyrolysis results suggest that the particulate organic matter in the sediments at Site 548 is largely of terrestrial origin. There is also a minor component of marine organic matter in the upper part of the section (lithologic Units 1 and 2), a conclusion supported by visual kerogen analyses (Cunningham and Gilbert, this volume). The organic matter was deposited as finely divided, highly oxidized particles that were transported to this location by bottom currents, turbidity flows, or as suspended particulate matter. The water column remained oxidizing throughout the deposition of these sediments, so virtually all the marine-derived organic matter was destroyed before it was deeply buried. Microbial decomposition apparently has not yet removed all of the marine organic matter from the Quaternary section, however.

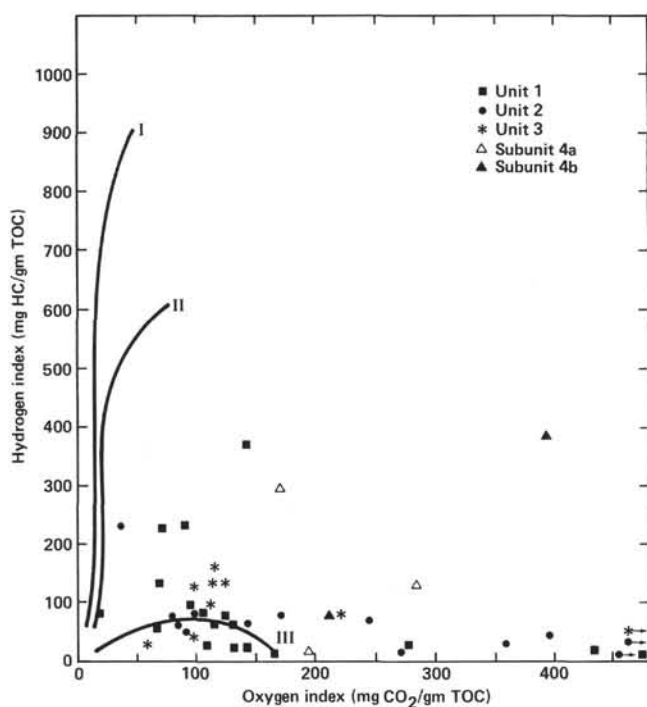


Figure 14. Van Krevelen diagram for hydrogen and oxygen indices at Site 548.

Finely divided pyrite was ubiquitous throughout the section at Site 548. Such pyrite originates from the breakdown of organic matter by anaerobic sulfate-reducing bacteria. Reducing conditions therefore probably existed in microenvironments among these sediments, although they were deposited within a consistently oxidizing paleoenvironment.

PALEOMAGNETISM

As part of the Leg 80 sampling program, one or two oriented samples per section were taken for paleomagnetic studies. The principal objective of this work was to construct a magnetostratigraphy and to produce a correlation between the paleomagnetic and biostratigraphic studies (Fig. 11). A detailed discussion of all the paleomagnetic results is presented by Townsend (this volume). The magnetic remanence measurements also provided a method of orienting the samples for the magnetic anisotropy studies (Hailwood and Folami, this volume).

The sequence of Pleistocene and Pliocene sediments recovered from Hole 548 yielded relatively good paleomagnetic data that enabled the Jaramillo and Olduvai Events to be clearly defined. The identification of the Olduvai Event, which spans nannofossil Zones NN18 and NN19, is of value in positioning the Pliocene/Pleistocene boundary.

The results from the upper part of Hole 548A (Cores 1-17) were difficult to interpret because the sediments are very weakly magnetized. In addition, the sequence is very condensed in parts and is interrupted by several unconformities. However, it was possible to identify the series of magnetic polarity reversals from Anomalies 20 to

24 and 30 to 32), which appeared in the lower part of this hole (Cores 17-35).

PHYSICAL PROPERTIES

The physical properties of the Site 548 section are discussed in Appendix I.

DOWNHOLE LOGGING

Operations

Wireline logging operations were performed using Schlumberger equipment (Table 5). The first log was run with a combination tool that provided dual induction and spherically focused resistivities, a long spacing sonic velocity log, and caliper and gamma ray logs. Because the uncompacted formation caused the sonic transit time to skip, an attempt was made to use the backup sonic tool to try to improve the velocity data. The sonic tools were exchanged, but a surface equipment failure aborted the run.

A second logging run was then made with porosity tools, which provided a record of formation density, neutron porosity, natural gamma ray, and hole caliper. The gamma ray curve from the nuclear tool had an abnormally high (constant) background, but shifting the data by an increment based on the first gamma ray record proved to be a satisfactory correction.

Hole conditions were acceptable, and both tools went down (without pumping) to within a few meters of the original total drilling depth. However, it should be noted that because of the nature of the formations (soft sediments) and fluid in the hole (salt water), a large borehole correction to the measurements was necessary. The logs obtained at this site are probably among the best recorded in DSDP holes (Fig. 15; and see also the Superlog [back pocket]).

Interpretation

Unit 1 (0-72 m BSF)

Subunit 1a (0-59.90 m BSF)

The gamma ray curve recorded through the drill pipe was the only log recorded over Subunit 1a. Pronounced variations in gamma ray intensity were observed; they are probably related to fluctuations in the carbonate and detrital clay contents of the alternating more calcareous (56% CaCO_3) interglacial sediments and more argillaceous (15% CaCO_3) glacial sediments. Five peaks in the gamma ray curve that correspond to the more argillaceous sediments are visible in Cores 3 (18 m BSF), 4 (30 m BSF), 5 (37 m BSF), 6 (52 m BSF), and 7 (55 m BSF). The shapes of the cyclic log signatures are symmetrical, with smooth transitions between the two end-member lithologies, except in Cores 3, 4, and 5, where more abrupt or sharp changes may be inferred from the gamma ray signature.

At the boundary between Subunits 1a and 1b (58 m BSF from the log, 59.90 m from the drill pipe measurements), the gamma ray log suggests that terrigenous con-

Table 5. Logging summary, Leg 80.

Hole	Total depth (m)	Water depth (m)	Depth of open-ended pipe (m)	Fluid in hole	Total time for logging (hr.)	Run	Logs recorded ^a	Interval logged (m sub-bottom)	Observations
548	1467	1256	—	—	—	—	—	—	No logs requested—HPC (hydraulic piston corer) hole.
548A	1807.5	1256	1429	Seawater	3.2	1	SLS-DIT-GR-CAL	1788–1428.5	Good logs—sonic velocities seem high. Wave form and variable density presentations included.
			1429	Seawater	2.5	1	FGT-CNL-GR-CAL	1783.5–1428.0	Caliper shifted (1 in. too big); otherwise good log. GR and CNL logged to above seafloor.
					6.2	—	—	—	Release bit, flush hole, rig up, troubleshoot, rig down.
					11.9	—	—	—	—
549	3534.5	2533	2642	Gel mud	25.4	1	SLS-DIT-GR-CAL	3532–2642	Sonic log poor—inadequate centralization; GR logged to above seafloor.
549A	2731.5	2535.5	—	—	—	—	—	—	No logs requested—HPC hole.
550	4968.5	4432	—	—	—	—	—	—	Hole aborted by weather—unable to log.
550A	4527.0	4432	—	—	—	—	—	—	Struck boulder at 95 m—no logs.
550B	5152.5	4432	4523	Seawater	6.4	1	SLS-GR-CAL	5123–4523	Caliper shifted; GR run to 4518 m.
			4523	Seawater	5.2	1	DLT-GR	5123–4523	Good log.
			4551	Seawater	5.7	1	FGT-CNL-CAL-GR	5123.5–4551	Caliper dead; GR run to 4528 m.
					2.3	—	—	—	Release bit; rig up and down.
					19.6	—	—	—	—
551	4110.0	3909	—	—	—	—	—	—	No logs requested. Shallow penetration and time limitation.

Note: Bit size was 9 7/8 in.

^a SLS = sonic long spacing, DIT = dual induction, GR = gamma ray, CAL = hole caliper, FGT = formation density, CNL = compensated neutron log, DLT = dual laterolog.

tent increases briefly at the top of Core 7 and then decreases progressively uphole (within Core 6) just before the development of the more symmetrical cycles of Subunit 1a.

Subunit 1b (59.9–72 m BSF)

The flat gamma ray curve through Subunit 1b suggests a relatively constant and high calcareous content (about 50% CaCO₃) except near the top of the subunit, where argillaceous content progressively increases upward.

Unit 2 (72–108.5 m BSF)

Unit 2 is characterized by a smooth gamma ray record corresponding to an average 50% CaCO₃ content. The presence of beds of argillaceous and calcareous sediments (18–50% CaCO₃) in Cores 9 to 14 is not marked by gamma ray fluctuations. However, clear peaks in the gamma ray curve within Cores 12 (92 m BSF), 13 (97 m BSF), and 14 (100 m BSF), the last of which was incompletely recovered, suggest the presence of marly beds 1 to 2 m thick.

Unit 3 (108.5–304.75 m BSF)

In Unit 3, all logs show a regular and smooth record that corresponds to rather constant CaCO₃ contents (50–68%). The boundary between the Miocene and the Pliocene at approximately 210 m is marked by a peak in the gamma ray, caliper, resistivity, density, neutron, and sonic velocity logs, probably as the result of a concentration of clay minerals along the boundary.

Oscillations of the gamma ray and sonic velocity logs at 241 and 245 m BSF and between 250 and 275 m BSF can be interpreted as indications of more argillaceous beds in the upper Miocene section. Those at 241 and 245 m BSF might correspond to argillaceous beds observed in Sections 548A-4-6 and 548A-5-1, which were interpreted as turbiditic silty mudstones.

Unit 4 (304.75–412.6 m BSF)

Subunit 4a (304.75–376.5 m BSF)

A sudden deflection in all log curves at 305 m BSF corresponds precisely to the boundary between Units 3 and 4, to a downhole increase in CaCO₃ content (from 50 to 90%), and to an unconformity within the Miocene. Peaks in radioactivity and density mark the unconformity. The sediment in Core 12 (310–320 m BSF) is more radioactive (i.e., more clayey) than in the overlying and underlying beds. No major deflection in the log records corresponds to the erosional unconformity observed in Core 16 at 348 m BSF near the middle of Subunit 4a (mid-Oligocene).

Subunit 4b (376.5–412.6 m BSF)

The subdivision of Unit 4 into Subunits 4a and 4b is documented by both increases in the values in the logging records (gamma ray, induction, density, neutron, resistivity, and sonic velocity) and a decrease in CaCO₃ content, which declines downhole across the subunit boundary at 376 m BSF from 90 to 65.70%. Just below this boundary, an argillaceous bed 2 to 3 m thick is re-

corded in the gamma ray, caliper, density, and sonic velocity curves, although it was not recovered by drilling (bottom part of Core 18; 375 m BSF).

Unit 5 (412.6–469.9 m BSF)

The Eocene–Paleocene marly nannofossil chalk of Unit 5 is bounded by unconformities and has distinctive logging characteristics. The logs show higher gamma ray values, lower sonic velocity, and lower porosity than the overlying unit. The logs also show large fluctuations that correspond to the alternation of beds that are either more calcareous (74% CaCO₃) or more argillaceous (30% CaCO₃) in composition. The fluctuation is especially pronounced in the lower part of the unit (443–469.9 m BSF).

The increase in carbonate in Unit 5 from 17% at the top to 32% at the bottom is reflected in decreasing gamma ray values. A highly radioactive level at 459 m BSF (near the boundary between Cores 548A-27 and 548A-28) has no clear counterpart in the other logging curves, and we can offer no obvious explanation for it.

Unit 6 (469.9–530 m BSF)

The Upper Cretaceous foraminifer–nannofossil chalk of Unit 6 contains more than 90% CaCO₃ and has uniform logging and lithologic characteristics. The unit has low gamma ray intensity, low resistivity, and high sonic velocity. The low density might correspond to both the relative undercompaction of the sediment and the high porosity. The slumped chalk beds observed in Cores 31 to 35 (490–530 m BSF) show more variable resistivity, density, and neutron (porosity) curves than the regularly bedded strata.

CORRELATION OF SEISMIC PROFILES WITH DRILLING RESULTS

The correlation of the Site 548 seismic profiles with the drilling results is discussed in Appendix I.

SUMMARY AND CONCLUSIONS

A complex of rift-phase listric normal faults trends northwest–southeast across the Goban Spur, breaking the Hercynian basement rocks into a series of tilted blocks and half-grabens and forming the framework for Mesozoic–Cenozoic sedimentation (Montadert, Roberts, et al., 1979). At the termination of continental rifting in this area, the half-grabens had essentially filled with Mesozoic synrift sediments, and erosion had truncated many of the higher fault blocks.

As seafloor spreading west of the Goban Spur began and thermal subsidence replaced stretching and faulting as the chief tectonic movement, the sediment supply on the Goban Spur dwindled. It remained relatively poor, and the sediments over the postrift unconformity are thin. As a result, conditions are unusually suitable for open-hole coring to basement. It was realized that a transect of relatively shallow sections might permit the development of a passive continental margin to be traced and its relationship with the adjoining oceanic plate to be documented.

Site 548 was the most landward point in just such a transect along the Goban Spur. It was located on the upper slope (1256 m water depth) over the truncated tip of a high basement block. The chief objectives of drilling at the site were (1) to determine the nature, age, and subsidence history of the basement; the nature and age of the postrift sediments; the paleoenvironments during postrift deposition; and (2) to sample the strata surrounding a series of unconformities that were clearly visible in our seismic reflection profiles (Fig. 16). These goals were achieved through the recovery of 454.9 m of Upper Cretaceous through Holocene sedimentary strata and 3.21 m of basement rocks from two holes. The postrift sediments are chiefly outer sublittoral and bathyal and contain rich microfaunal and nannofossil assemblages that provide excellent biochronology. The abundant fossils and variable lithic components have clearly recorded the paleoclimatic and paleoceanographic history of the Goban Spur. Five distinct unconformities were documented, and the contacts of four were recovered; four correlate well with the seismic reflection profiles. Basement recovery was sparse.

Hercynian Basement

A few chunks and some gravel-sized rubble of quartzite and lustrous black shale were recovered from 16 m of penetration into basement rocks (their depth coincides with that of the basement seismic reflector). Quartz, altered plagioclase, clay minerals, detrital micas, and traces of calcite were identified in the quartzite. The rocks contain middle to late Devonian palynomorphs and are therefore interpreted as a facies of the Hercynian basement sequence. Isolated millimeter-sized quartz grains were recovered from a sample of drilling mud and may represent a basal sand deposit that formed directly on the basement.

Campanian Hardground

A hard crust a few centimeters thick that was dated as pre- to late Campanian was recovered just below Upper Cretaceous chalk (Fig. 10). Shipboard X-ray diffraction analysis revealed siderite, goethite(?), pyrite, psilomelane, and calcite. Onshore chemical analysis showed the predominant major elements to be Ca, P, Mn, and Fe and the predominant trace elements to be Ti, Sr, Ba, Ni, Co, Zn, and Cu. The presence of distinct borings and the geochemical composition of the rock indicate that it formed in a marine environment and at relatively shallow depths—depths estimated by other methods to be 500 to 700 m (Karpoff et al., this volume).

Upper Cretaceous–Lower Paleocene Chalks

White bioturbated chalks that were 60 m thick and greater than 95% carbonate were found to contain diagnostic Danian, Maestrichtian, and upper Campanian micro- and nannofossils. The chalks coincide with magnetic Anomalies 30, 31, and 32. They accumulated in outer sublittoral to upper bathyal environments (200–500 m deep) in well oxygenated waters (organic carbon is negligible) at an average rate of about 7.9 m/m.y. The

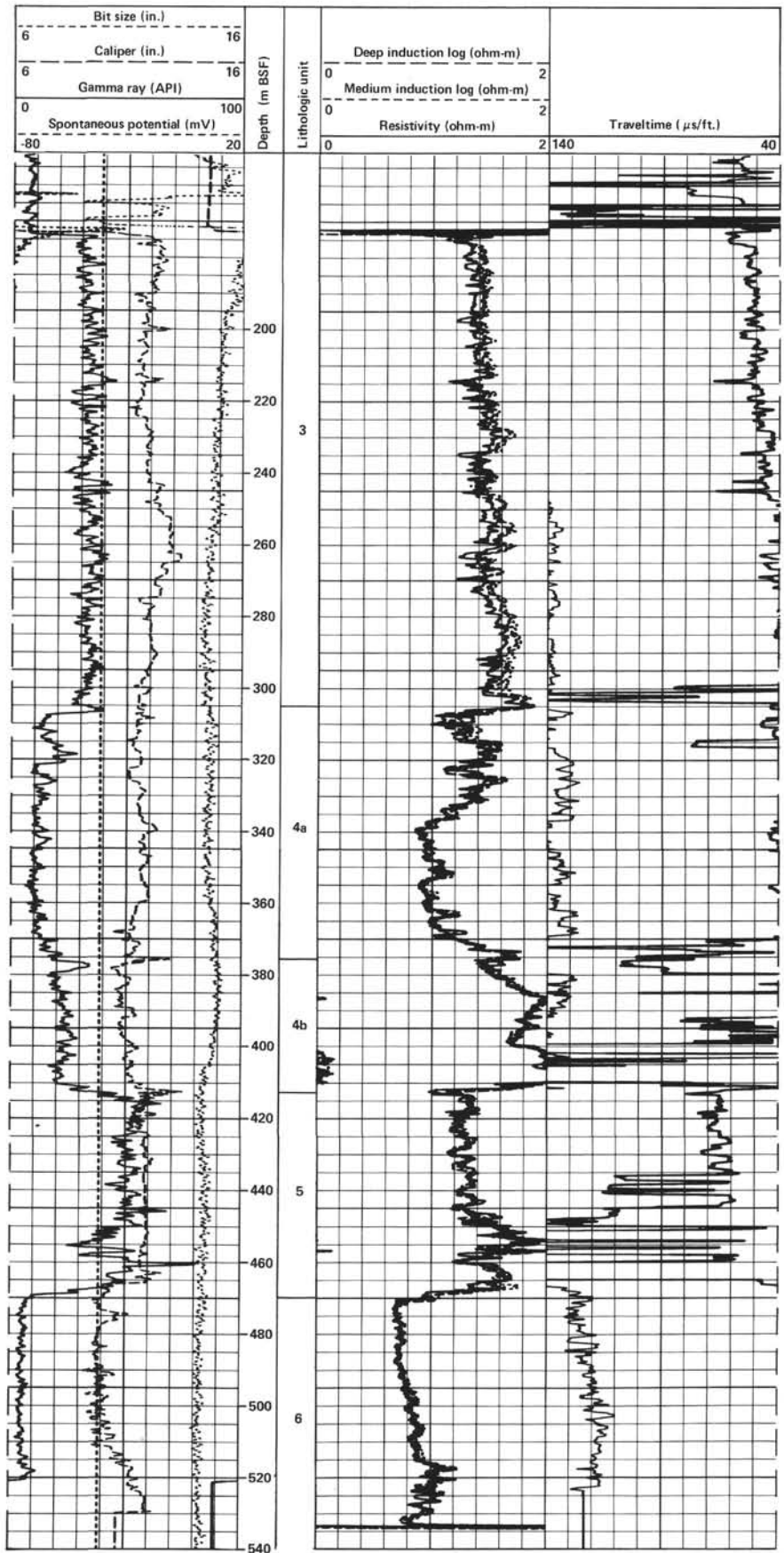


Figure 15. Downhole log obtained at Site 548.

upper chalks are soft, contain significant quantities of interstitial water, and exhibit low electrical resistivity and sonic velocity (1680 m/s).

Paleocene Hiatus

A chronostratigraphic gap of approximately 4 m.y. separates Danian chalk from upper Paleocene clays and marls. The northwestern European continent emerged during the corresponding interval. There, conglomerates, sands, and clays accumulated widely in fluvial, lacustrine, and paludal environments, which often preserved primitive mammal faunas. At Site 548, a distinct erosional disconformity represents the hiatus (Fig. 8). A conglomerate 40 m thick contains reworked and bored blocks of Danian chalk in a matrix of olive brown upper Paleocene clay. The marked change in acoustic impedance across the contact (Fig. 16) produces a high amplitude reflector that is easy to trace as an unconformity on the seismic profile. The changes in the magnetic fabric across the contact, which suggest a sharp change in the pattern of oceanic circulation, may be related to the incursion of Arctic waters in this part of the Atlantic (Hailwood and Folami, this volume). The Paleocene unit appears to be relatively thick and more complete not far updip, but it thins rapidly beneath Site 548 and may pinch out just downdip.

Lower Eocene

The initial lower Eocene deposition consisted of olive brown and light greenish gray marly nannofossil chalks. The fossil assemblages suggest continued deposition in outer sublittoral to upper bathyal environments in well oxygenated bottom waters (organic carbon content is low). The color of the chalks and their noticeably high remanent magnetization, relatively high rate of deposition (Fig. 12), cyclically distributed detrital minerals, and relatively high clay content reflect a significant clastic contribution from terrestrial sources. An alternative source for the magnetic minerals has been proposed by Hailwood (1979), who studied coeval strata at Site 400 (Montadert, Roberts, et al., 1979). He suggested that magnetite grains might be derived from volcanic sources associated with seafloor spreading. Abundant tuffaceous horizons on Rockall Bank, the widespread intercalation of ash beds in North Sea strata, and a volcanic ash bed at Site 549 (site chapter, this volume), all of early Eocene age, lend support to Hailwood's proposal. The identification of specific polarity reversals in the lower Eocene through middle Miocene interval is difficult because the sediment column is so condensed, but the association of Anomaly 24 with the top of the lower Eocene section appears to be valid.

The compacted, argillaceous nature of these chalks renders them impermeable, a condition that may have sealed the interstitial fluids of the underlying Danian and Upper Cretaceous chalks, preventing their upward migration during compaction.

Middle Eocene through Lower Oligocene

A sharp uphole decrease in terrigenous detritus marks the disconformity that separates the lower from the middle

Eocene sediments (1.5 m.y. hiatus). The resulting increase in carbonate content is accompanied by a decrease in accumulation rate (from 21.8 m/m.y. below to 8.0 m/m.y. above, Fig. 12). Light greenish gray to bluish white nannofossil chalks and foraminifer-nannofossil chalks predominate. Molluscan debris and glauconite grains are scattered throughout, and chert nodules are conspicuous in the lower beds. Outer sublittoral to upper bathyal conditions still prevailed, and the abundance of burrows attests to well oxygenated substrates and bottom waters.

Of particular interest here is the presence of chert nodules and opal-CT (the latter revealed in bulk mineralogy analysis). A concentration of biogenic silica and a significant shoaling of the calcite compensation depth (CCD) during the middle Eocene were observed at Site 400 (Roberts and Montadert, 1979), which is considerably deeper than Site 548, and the presence of biogenic silica and shoaling of the CCD have also been noted at abyssal sites elsewhere (van Andel, 1975). Among the factors that may have contributed to the silica enrichment at Site 548 are the warming of the North Atlantic Ocean (Roberts and Montadert, 1979), a global rise in sea level (Vail et al., 1977), an increase in volcanism (Montadert, Roberts, et al., 1979), and local upwelling.

The disconformity between the lower and middle Eocene strata is one of the most visually striking at Site 548; it is clearly shown by the mixture of the dark and light lithologies across the erosional contact (Fig. 7). This zone corresponds to a widely traceable unconformable reflector on the seismic profiles. Strong reflectors are also apparent on seismic profiles within the middle Eocene; they can be associated with fluctuations in acoustic impedance measurements for Hole 548A.

Middle Oligocene Hiatus

A 4 m.y. hiatus that may have worldwide implications has been recognized within the late Oligocene strata at Site 548. The irregular unconformable contact is marked by a distinct diagonal color change (darker above) and an uphole increase in dark mineral grains. Above the erosional contact there is a short zone of mixed lithologies and reworking that contains several fairly large mollusc shells. This unconformity is precisely correlated with the global sea level drop postulated by Vail et al. (1977). The proximity of the dramatic middle Miocene unconformity (Fig. 16) makes the middle Oligocene unconformity difficult to recognize in the seismic profiles for the vicinity of Site 548.

Upper Oligocene through Lower Middle Miocene

Nannofossil chalks resumed relatively slow (4.2 m/m.y.) deposition in warm, sublittoral to upper bathyal environments following the mid-Oligocene erosion. Sonic velocities of 1700 m/s increase to 1960 m/s uphole, creating the potential for a good seismic reflector within the section.

Middle Miocene Hiatus

A sharp lithologic change, an uphole increase in sediment accumulation rate, a paleoclimatic shift, and a

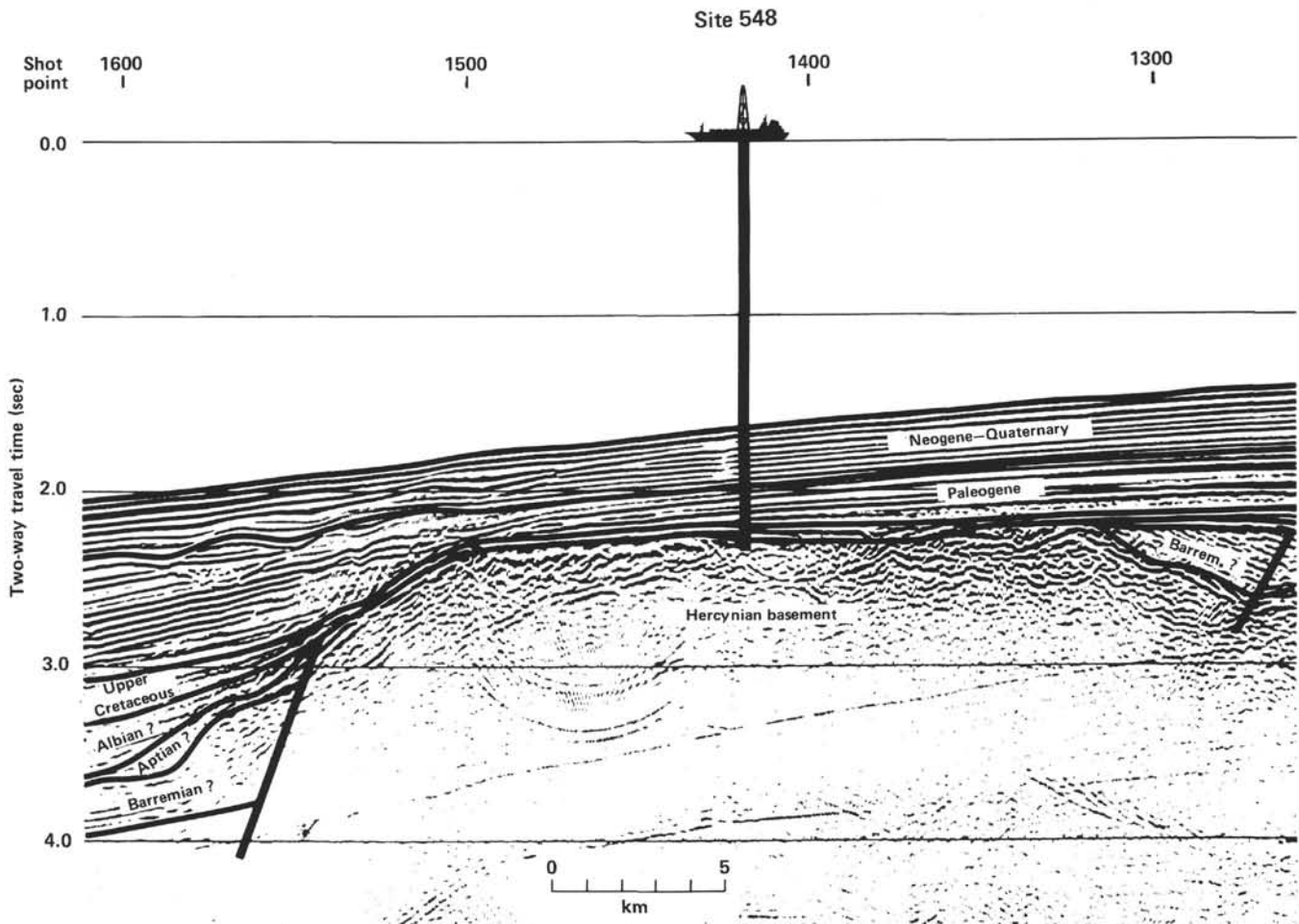


Figure 16. Segment of multichannel seismic reflection profile OC 202 across Site 548 (see Fig. 2).

prominent unconformity are evidence of a 6 m.y. hiatus that separates lower middle Miocene sediments from upper Miocene sediments (Fig. 4). This contact can be correlated with the most prominent of the seismic unconformities in the vicinity of Site 548 and corresponds to a significant peak in the gamma ray and density logs. The unconformity can be traced widely over this fault block (on seismic profiles) as it truncates the thick middle Miocene section that is present updip from the core site. A coeval unconformity has been observed at several other North Atlantic core sites. Its origin may be related to vigorous bottom currents that developed as the Norwegian Sea became a source of North Atlantic bottom waters (Jones et al., 1971; Roberts and Montadert, 1979).

Late Miocene to Pleistocene

Major changes in fossil assemblages, depositional style, and sediment source accompanied the cooler paleoclimates and increasing paleodepths (chiefly bathyal) that followed the middle Miocene erosion. Muddy turbidity flows began to spread terrigenous layers cyclically among the greenish gray nannofossil oozes. The terrigenous cycles are especially marked in the Pleistocene strata, where the natural remanent magnetization increases in proportion to the supply of land-derived(?) magnetic

particles. The 211 m of nearly continuous recovery by the piston corer in this stratigraphic interval should permit unusually fine scale paleoclimatic, biochronological, and paleomagnetic studies.

Conclusion

The success of our investigations at Site 548 can be attributed in large part to its particular location and to three technological improvements. The site is well above the present CCD, and our work shows that it has generally remained so since the first incursion of marine waters into the area. As a result, the calcareous fossil specimens are generally well preserved and abundant, conditions essential for refined biostratigraphic and paleoenvironmental studies. The proximity of the European landmass has caused the repeated enrichment of the marine sediments with terrestrial magnetic particles, which has enhanced the paleomagnetic studies. The introduction of land-derived detritus has also helped produce clearly defined depositional sequences. The moderate sediment accumulation rates at this upper slope site have resulted in thick deposits between the major unconformities, enhancing the identification of lithic and faunal changes across the contacts. Yet the total accumulation is thin enough to allow open-hole drilling to basement.

First among the technical improvements is the availability of exceptionally good multichannel seismic profiles, which allowed careful site selection during pre-cruise planning and later permitted the extrapolation of the core hole data to seismic sequences across the entire fault block.

Second, the variable length hydraulic piston corer (VLHPC) was an outstanding success; we achieved nearly 100% recovery in the upper 211 m.

Third, the prototype logging tool configurations we used gave us a reliable series of downhole geophysical measurements that correlate well with the shipboard physical measurements, the seismic data, and the results of sedimentological analyses.

The results of shore-based studies of the Site 548 cores have, in particular, advanced our ability to accurately interpret paleoenvironments and paleoclimates, and they have provided detailed documentation as to the causes of major unconformities and their processes of formation on passive margins (see Snyder, Müller, et al.; Poag and Low; Poag et al.; Miller et al.; Loubere and Jakiel; Caralp; Pujol et al.; and Vergnaud Grazzini and Saliège, all this volume).

REFERENCES

Berggren, W. A., 1972. Cenozoic biostratigraphy and paleobiogeography of the North Atlantic. In Laughton, A. S., Berggren, W.

- A., et al., *Init. Repts. DSDP*, 12: Washington (U.S. Govt. Printing Office), 965-1001.
- Hailwood, E. A., 1979. Paleomagnetism of late Mesozoic to Holocene sediments from the Bay of Biscay and Rockall Plateau, drilled on IPOD Leg 48. In Montadert, L., Roberts, D. G., et al., *Init. Repts. DSDP*, 48: Washington (U.S. Govt. Printing Office), 305-340.
- Jones, E. J. W., Ewing, M., Ewing, J. I., and Eittreim, S., 1971. Influences of Norwegian Sea overflow water on sedimentation in the northern North Atlantic and Labrador Sea. *J. Geophys. Res.*, 75: 1655-1680.
- Montadert, L., Roberts, D. G., et al., 1979. *Init. Repts. DSDP*, 48: Washington (U.S. Govt. Printing Office).
- Poore, R. Z., 1979. Oligocene through Quaternary planktonic foraminiferal biostratigraphy of the North Atlantic: DSDP Leg 49. In Luyendyk, B. P., Cann, J. R., et al., *Init. Repts. DSDP*, 49: Washington (U.S. Govt. Printing Office), 447-476.
- Roberts, D. G., and Montadert, L., 1979. Evolution of passive rifted margins—perspective and retrospective of DSDP Leg 48. In Montadert, L., Roberts, D. G., et al., *Init. Repts. DSDP*, 48: Washington (U.S. Govt. Printing Office), 1143-1153.
- Vail, P. R., Mitchum, R. M., Jr., Todd, R. G., Widmier, J. M., Thompson, S. III, et al., 1977. Seismic stratigraphy and global changes of sea level. In Payton, C. E. (Ed.), *Seismic Stratigraphy—Applications to Hydrocarbon Exploration*. Mem. Am. Assoc. Pet. Geol., 26:49-212.
- van Andel, T. H., 1975. Mesozoic-Cenozoic calcite compensation depth and global distribution of calcareous sediments. *Earth Planet. Sci. Lett.*, 26:187-194.

Date of Initial Receipt: September 6, 1983

Date of Acceptance: November 9, 1983

SITE 548		HOLE			CORE 1		CORED INTERVAL 0.0-4.0 m	
TIME - ROCK UNIT	BIOSTRATIGRAPHIC ZONE	FOSSIL CHARACTER			SECTION METERS	GRAPHIC LITHOLOGY	DISTURBANCE	LITHOLOGIC DESCRIPTION
		FORAMINIFERS	NANNOFOSSILS	RADIOLARIANS				
Quaternary	Emiliana hualeiyi (NN21) (N)	AG	AG		1		*	2.5Y 5/2
		AG	AG	RG				5Y 5/3
		CG						5Y 5/1
	N22(N23) (F)				2		*	5Y 5/2
		RG		5Y 5/2				
	CG	AG	RG		3		*	5Y 5/2
		CC						

LITHOLOGIC DESCRIPTION

Olive gray to gray marly calcareous, nannofossil or foram-nannofossil ooze. Sparse black organic; or pyritic spots throughout.

SMEAR SLIDE SUMMARY (%):

	1, 12	1, 77	2, 28	2, 120	3, 22
D	D	D	D	D	D

Texture:

Sand	-	-	-	10	-
Silt	20	50	20	40	40
Clay	80	50	80	50	60

Composition:

Quartz	10	20	-	40	-
Feldspar	-	-	-	5	-
Mica	-	-	-	-	-
Clay	65	40	40	20	50
Carbonate unspec.	10	10	50	10	50
Foraminifers	5	-	-	-	-
Calc. nannofossils	10	30	10	30	-

ORGANIC CARBON AND CARBONATE (%):

	1, 9	1, 100	2, 100
Organic carbon	0.24	0.37	0.42
Carbonate	48	22	17

SITE 548		HOLE			CORE 2		CORED INTERVAL 4.0-13.5 m			
TIME - ROCK UNIT	BIOSTRATIGRAPHIC ZONE	FOSSIL CHARACTER			SECTION METERS	GRAPHIC LITHOLOGY	DISTURBANCE	LITHOLOGIC DESCRIPTION		
		FORAMINIFERS	NANNOFOSSILS	RADIOLARIANS					DIATOMS	
Quaternary	Emiliana hualeiyi (NN21) (N)	AG	AG		1		*	5Y 4/3		
		AG	AG	RG				5Y 5/2		
			N22 (F)			2		*	5Y 5/2	
				FG					5Y 5/2	
				RG					5Y 5/2	
				AG	AG		3		*	5Y 4/1
				AG		5Y 5/2				
	N22 (F)				4		*	5Y 5/2		
		CG		5Y 4/2						
		CG		5Y 5/2						
					5		*	5Y 5/2		
				VOID						
		AG	AG		6		*	5Y 4/2		
		CG		5Y 5/2						
		AG	AG		7		*	5Y 5/2		
		AG	AG	CC				5Y 5/2		

LITHOLOGIC DESCRIPTION

Olive gray to gray marly calcareous, nanno or foram-nannofossil ooze in upper part. Calcareous ooze in lower part. Sparse black spots of pyrite? or organic material? throughout. Occasional mollusc shells, scaphopods, clay balls and pebbles.

SMEAR SLIDE SUMMARY (%):

	1, 64	3, 22	5, 30	5, 99
D	D	D	D	D

Texture:

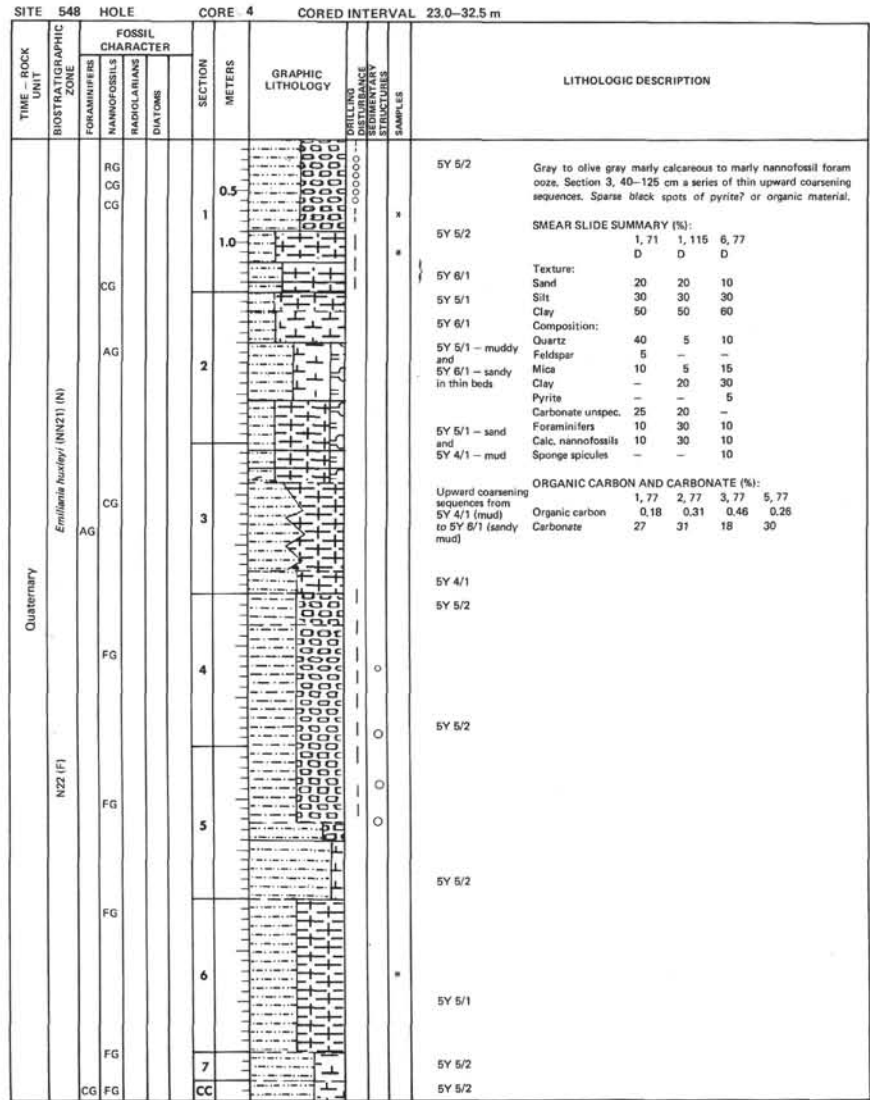
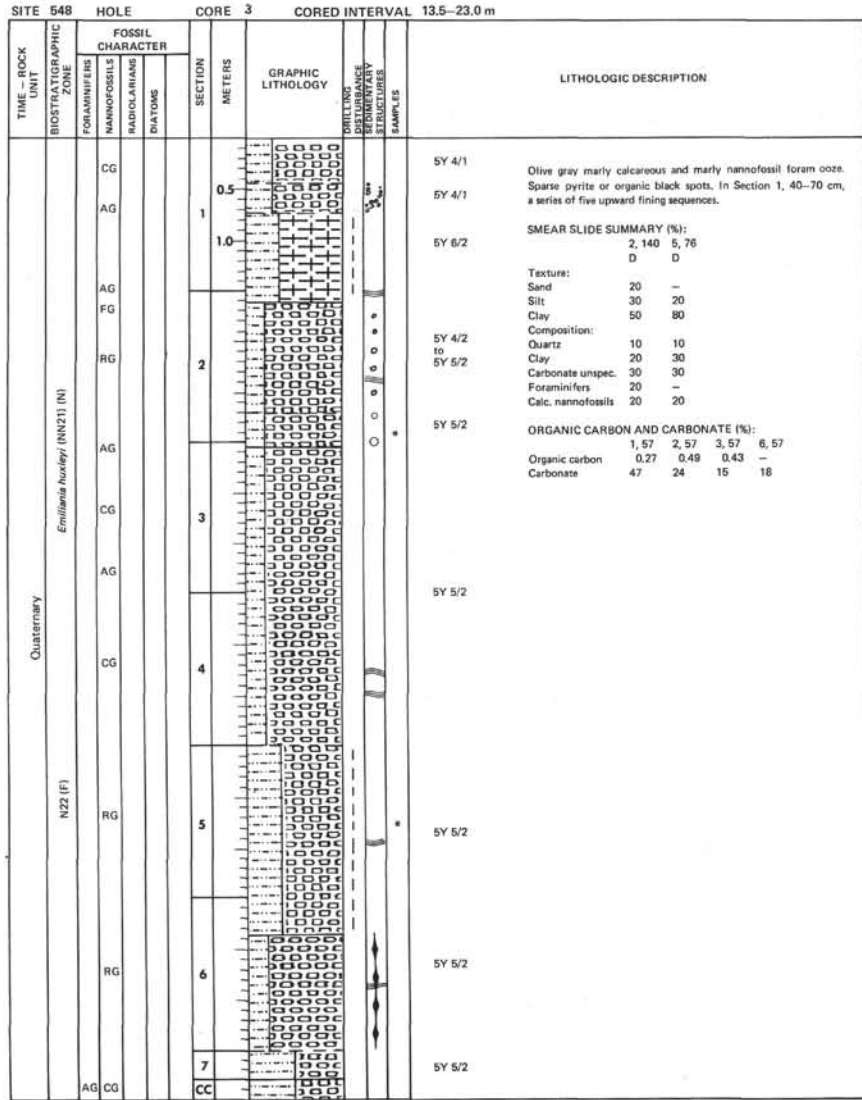
Silt	10	20	25	25
Clay	90	80	75	75

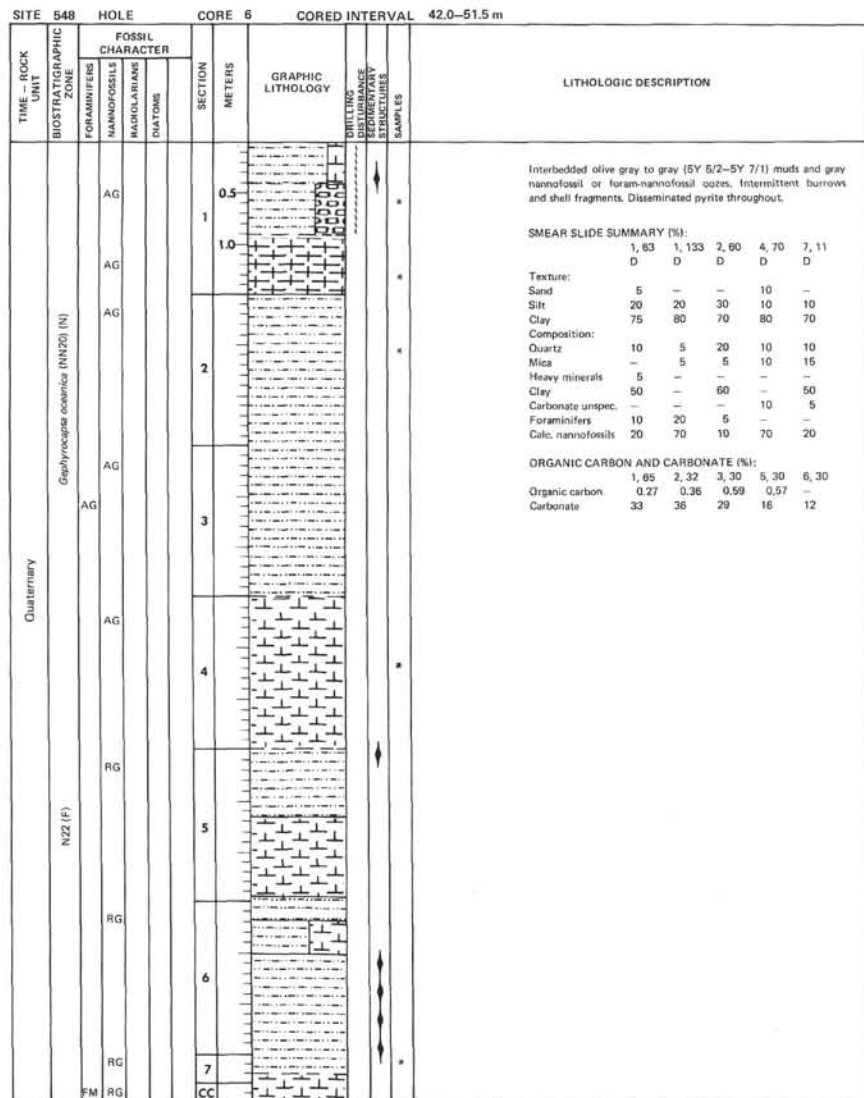
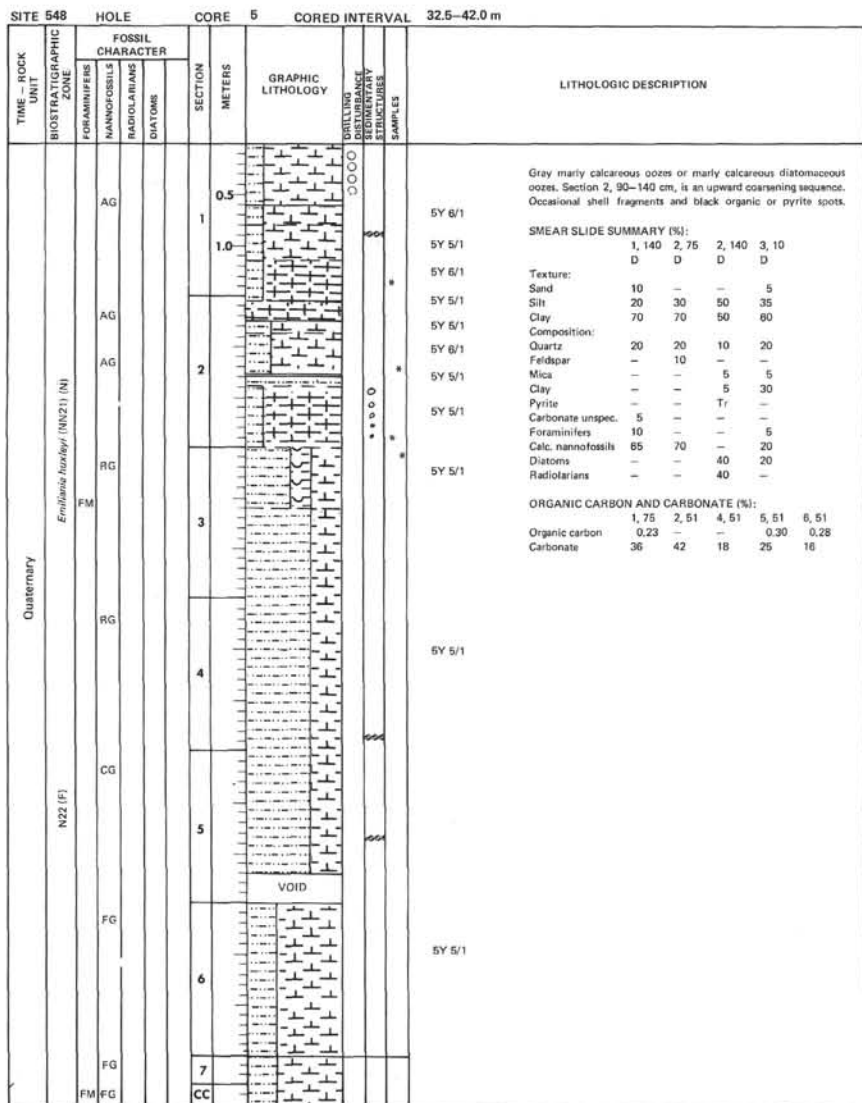
Composition:

Quartz	-	20	40	10
Mica	10	-	5	10
Heavy minerals	-	5	-	-
Clay	45	-	-	-
Carbonate unspec.	45	30	25	60
Foraminifers	-	5	5	10
Calc. nannofossils	-	50	30	10
Fish remains	-	-	Tr	-

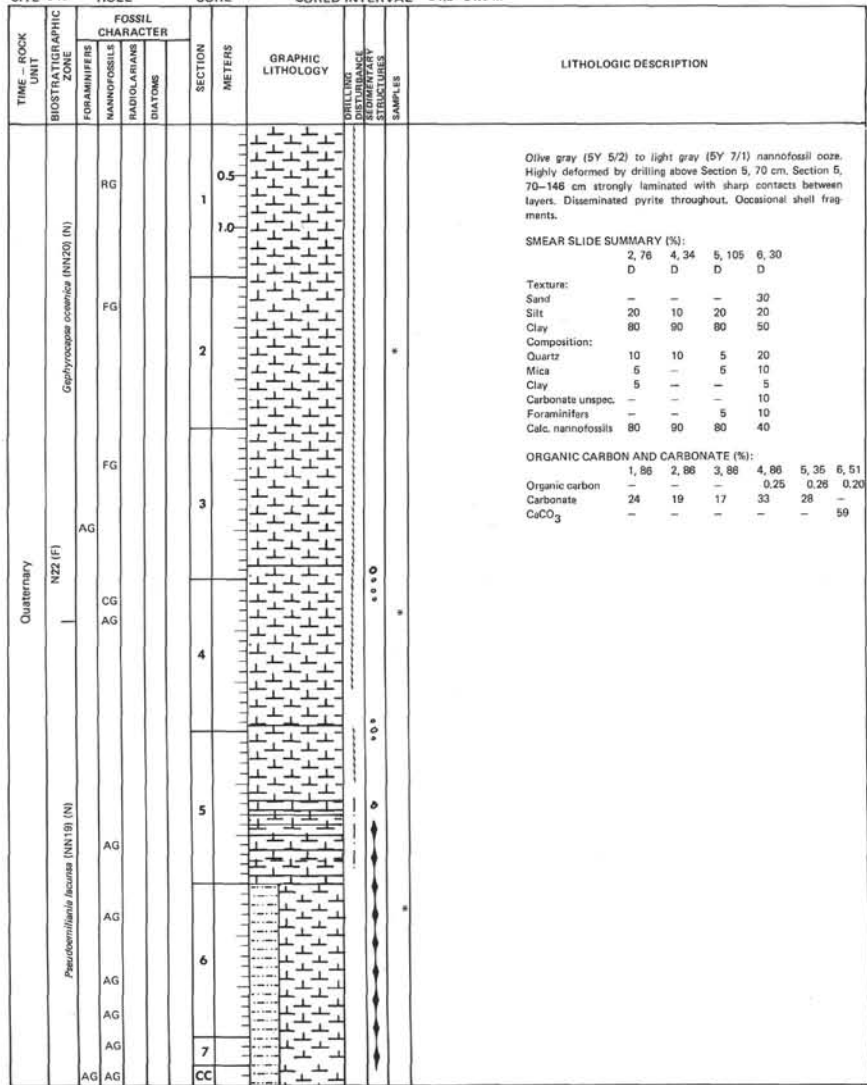
ORGANIC CARBON AND CARBONATE (%):

	2, 43	4, 35	5, 35
Organic carbon	0.41	0.32	0.31
Carbonate	19	23	19

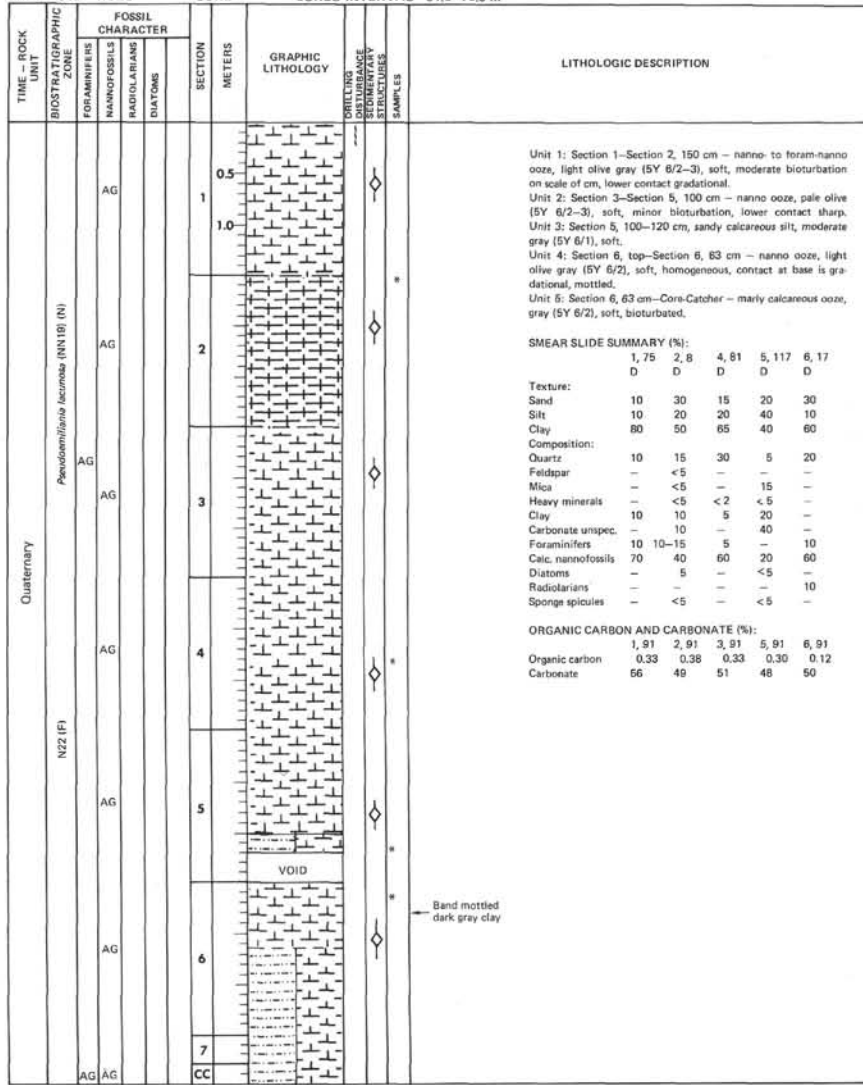




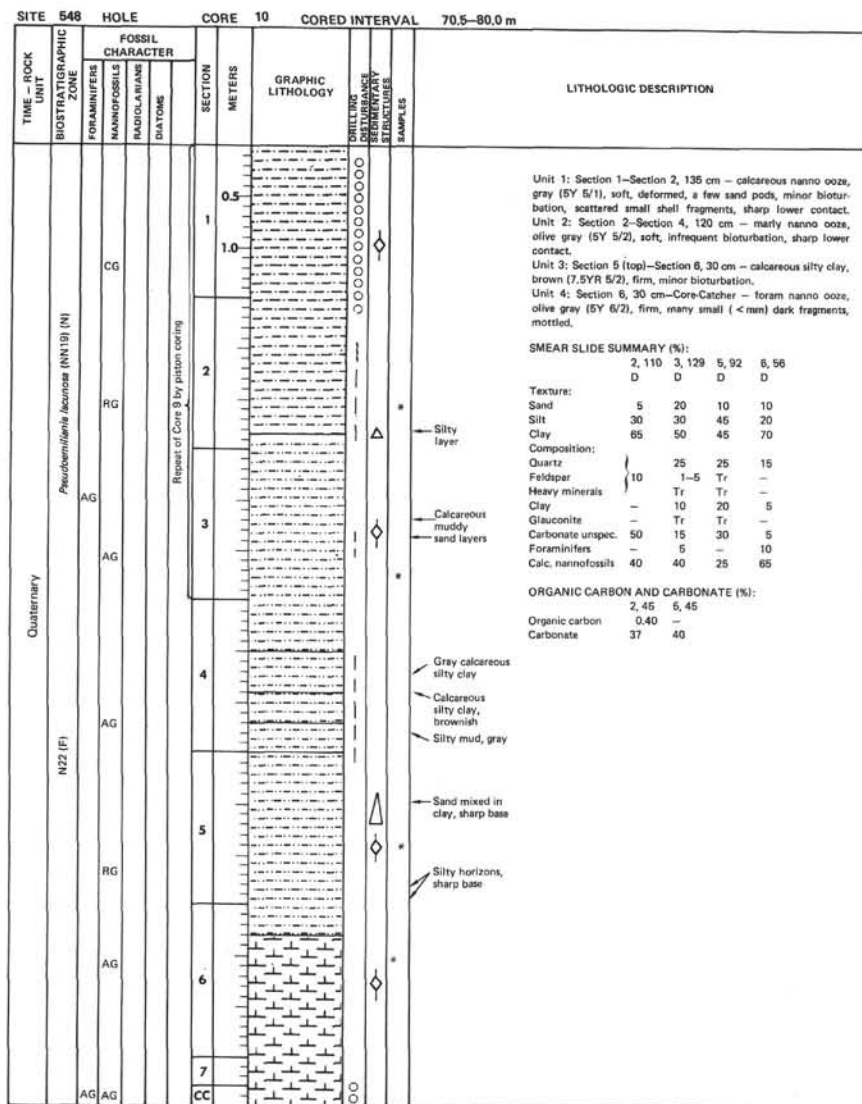
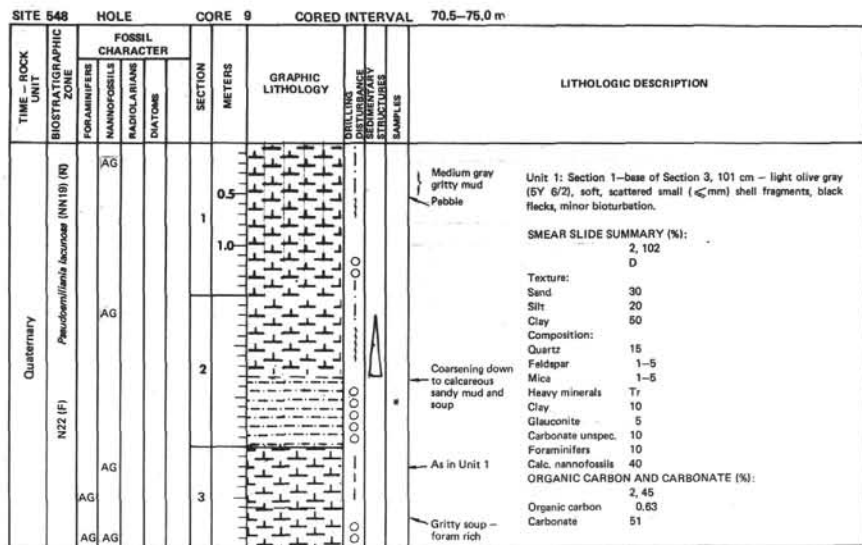
SITE 548 HOLE CORE 7 CORED INTERVAL 51.5-61.0 m

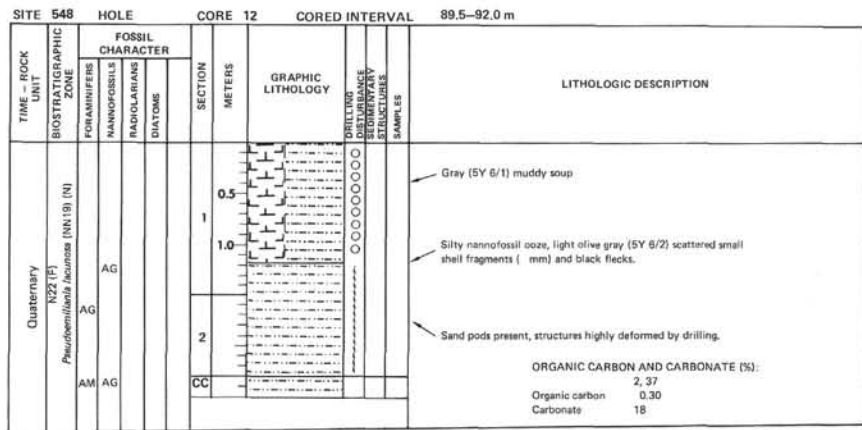
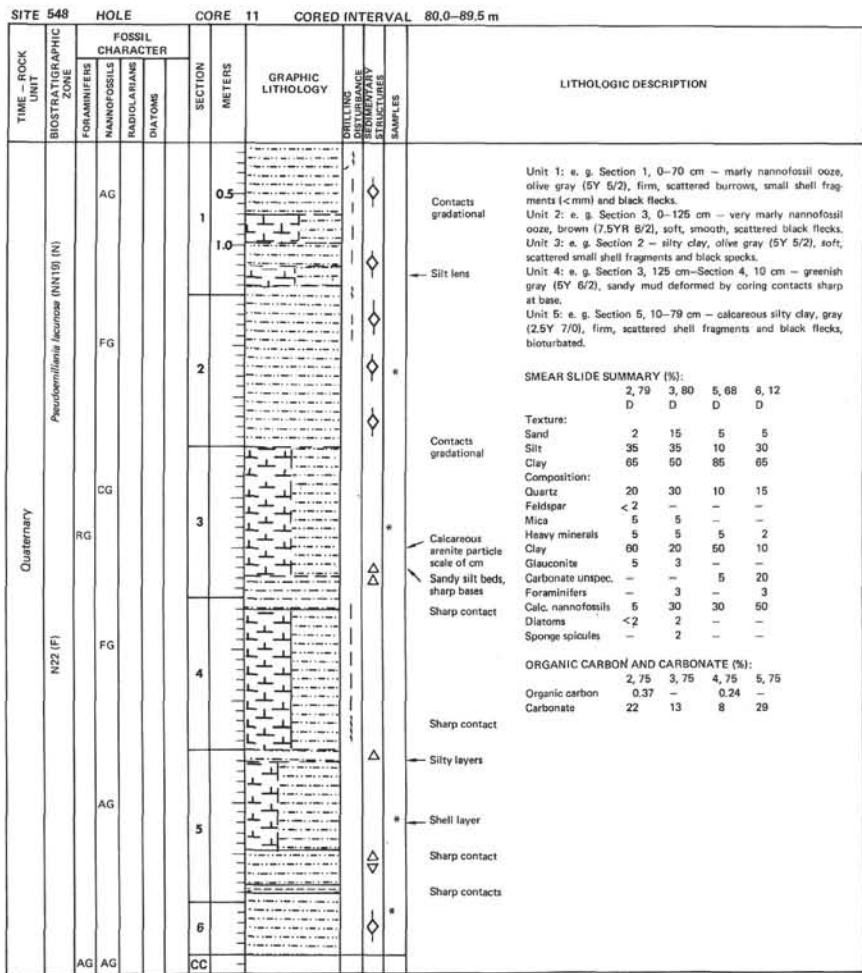


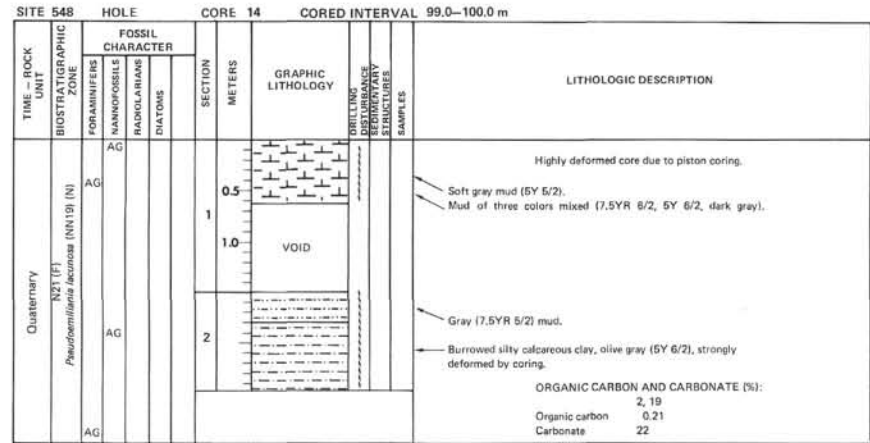
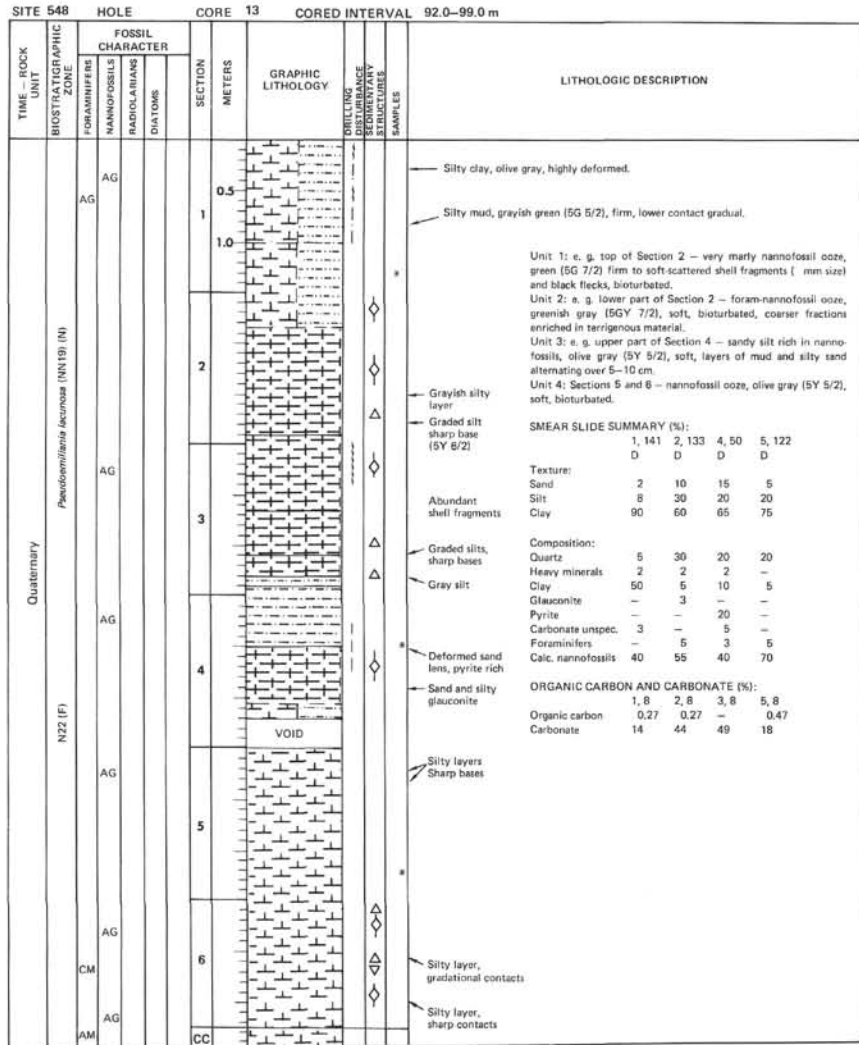
SITE 548 HOLE CORE 8 CORED INTERVAL 61.0-70.5 m

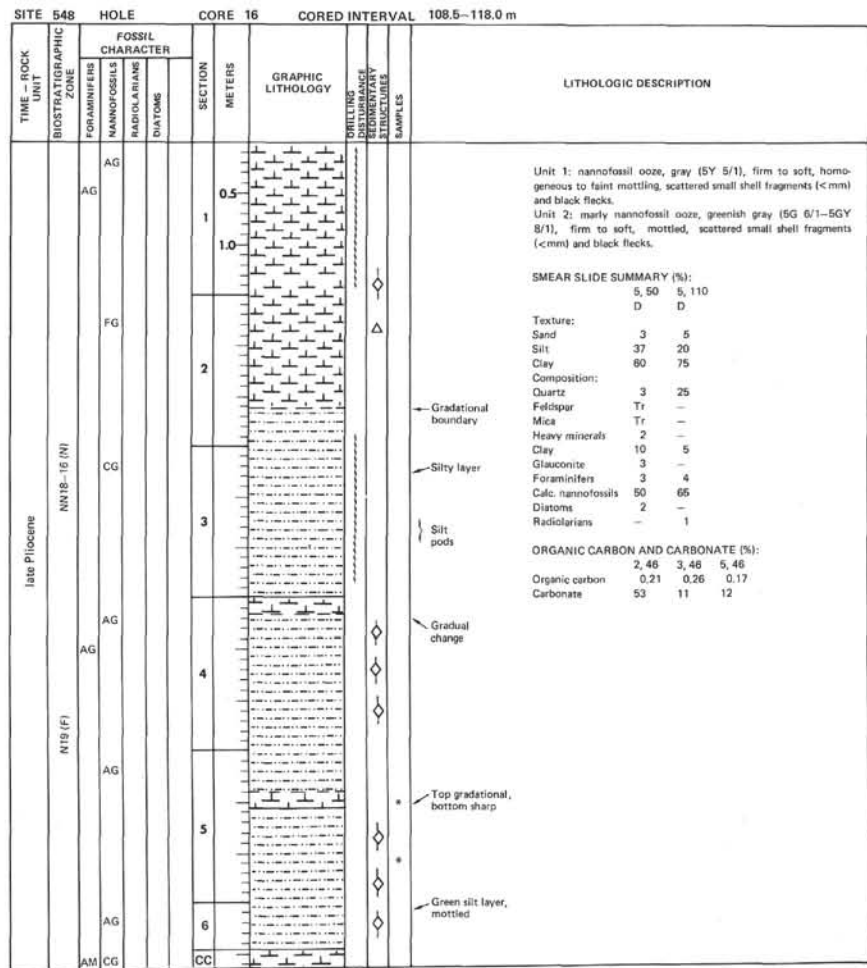
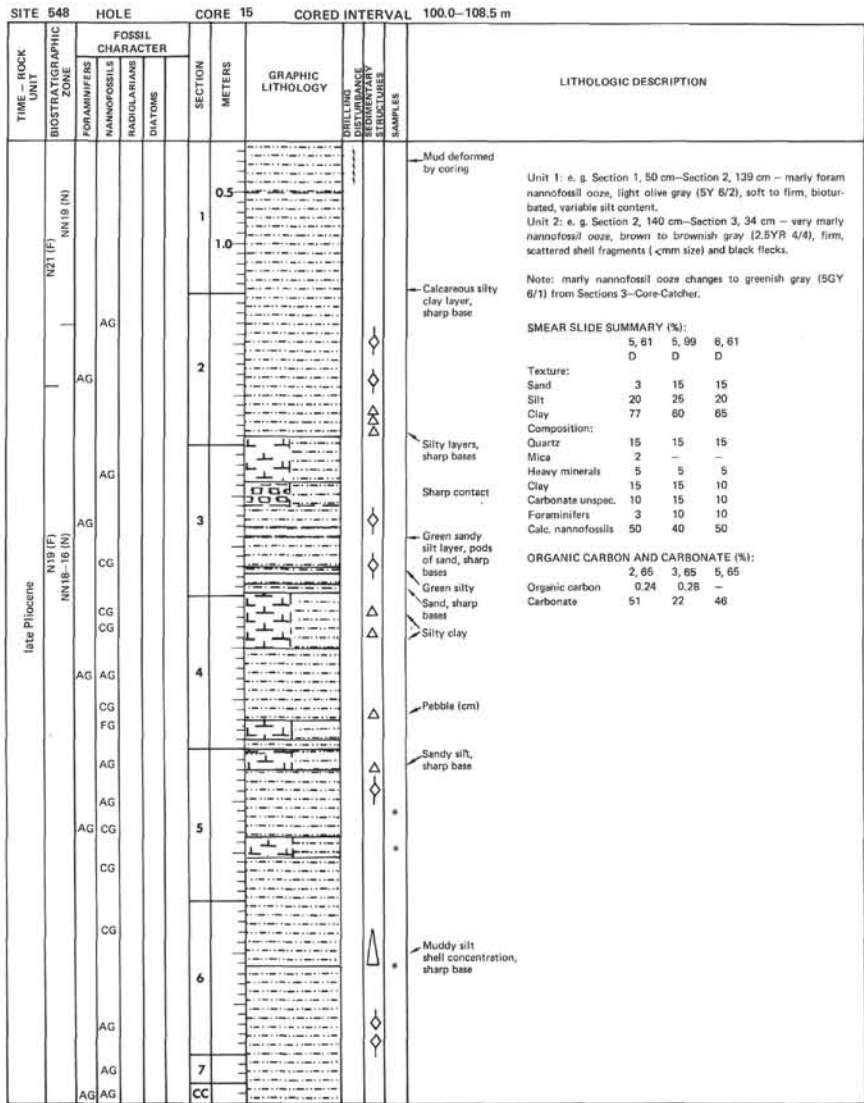


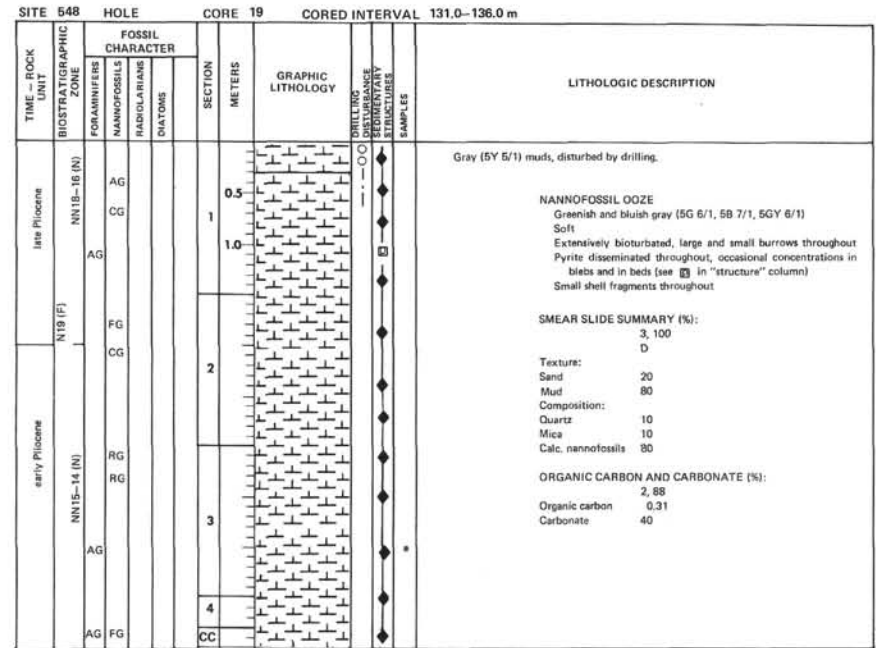
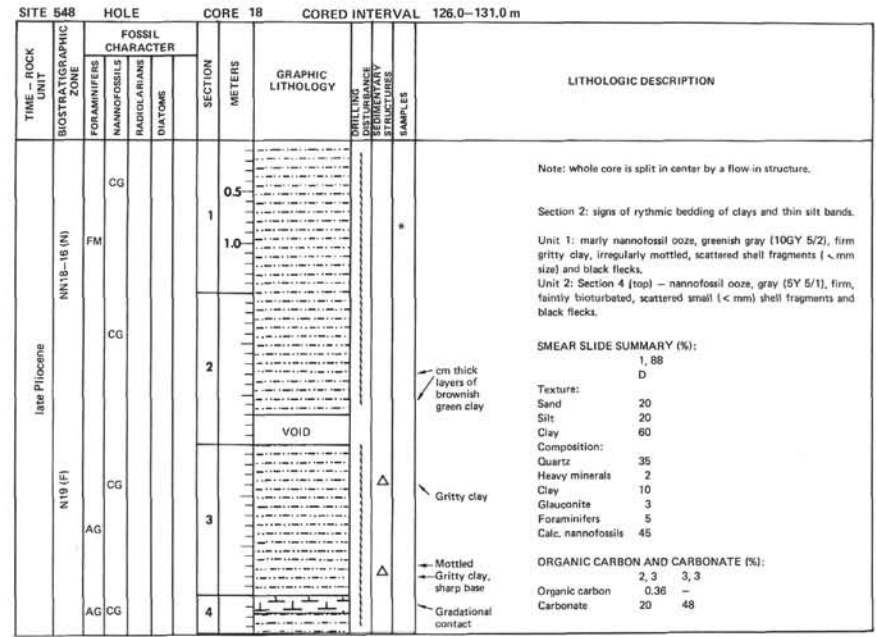
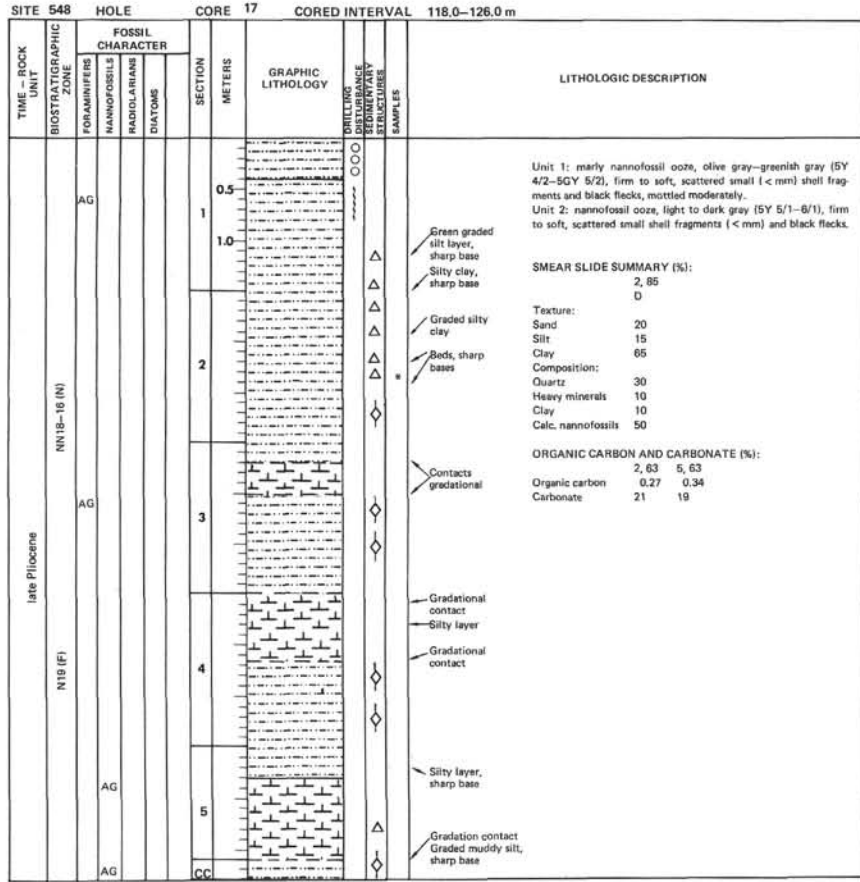
Band mottled dark gray clay

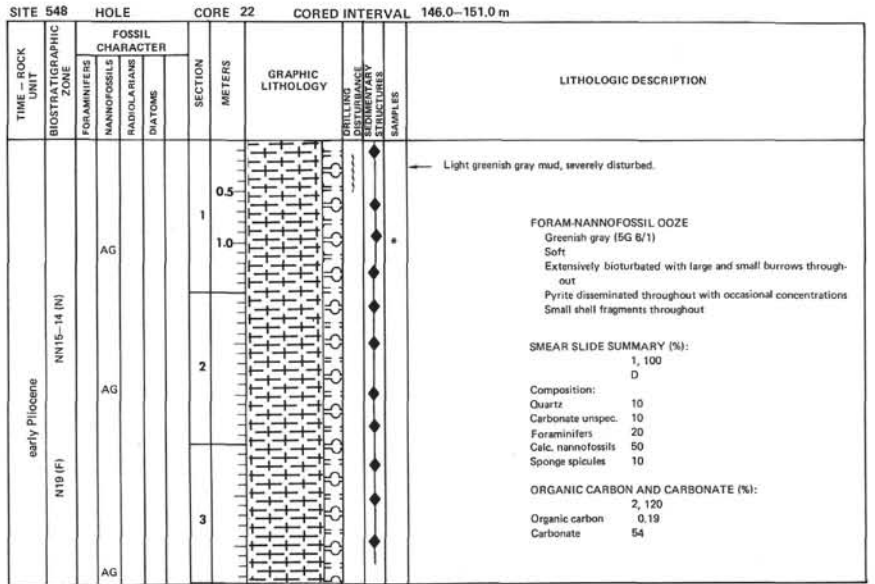
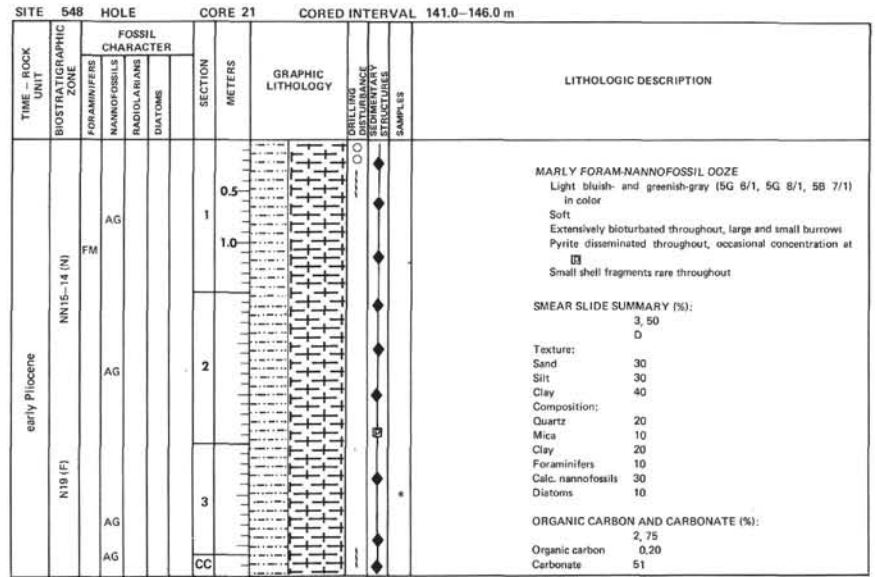
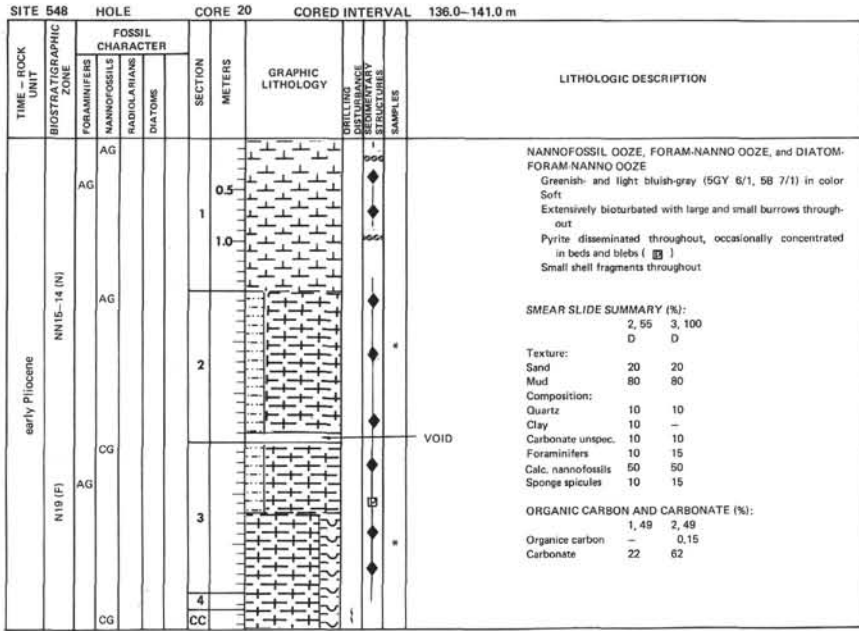


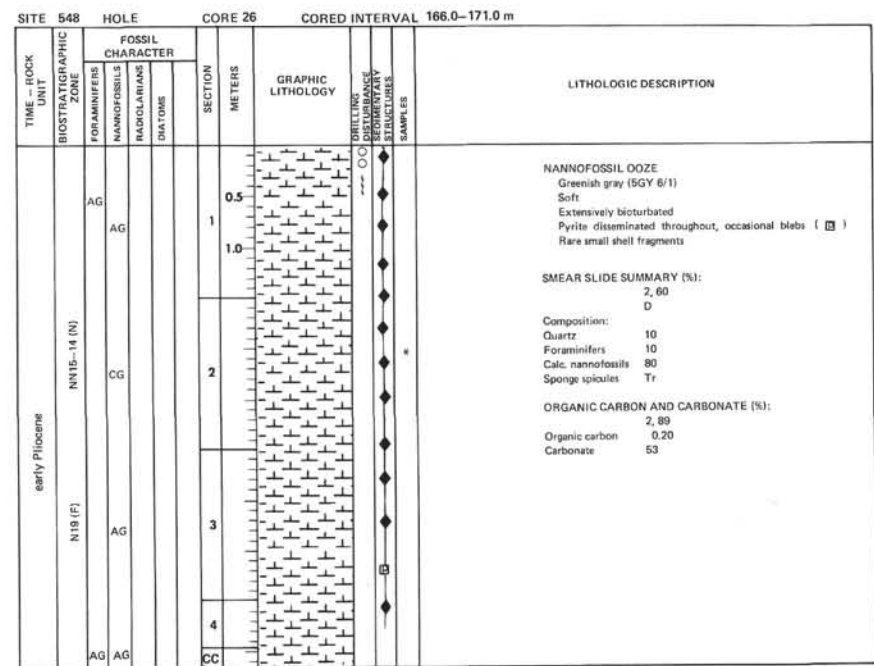
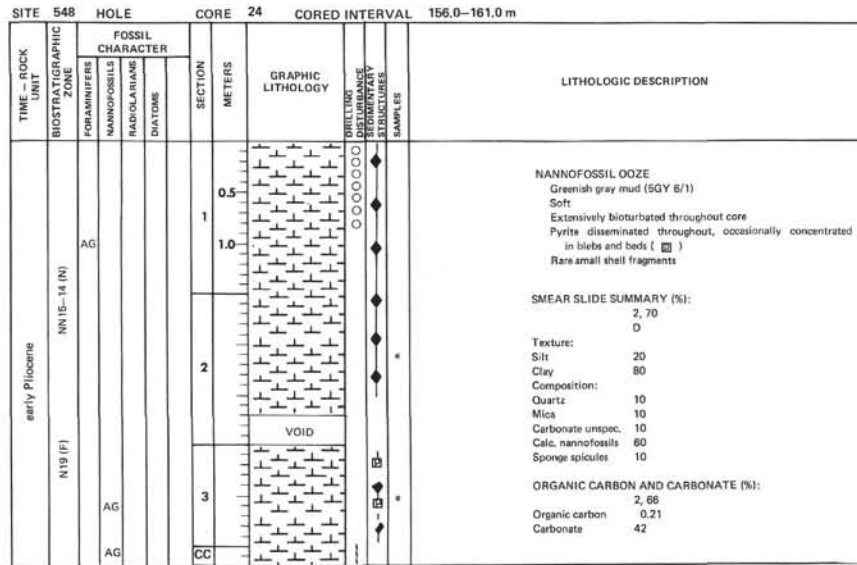
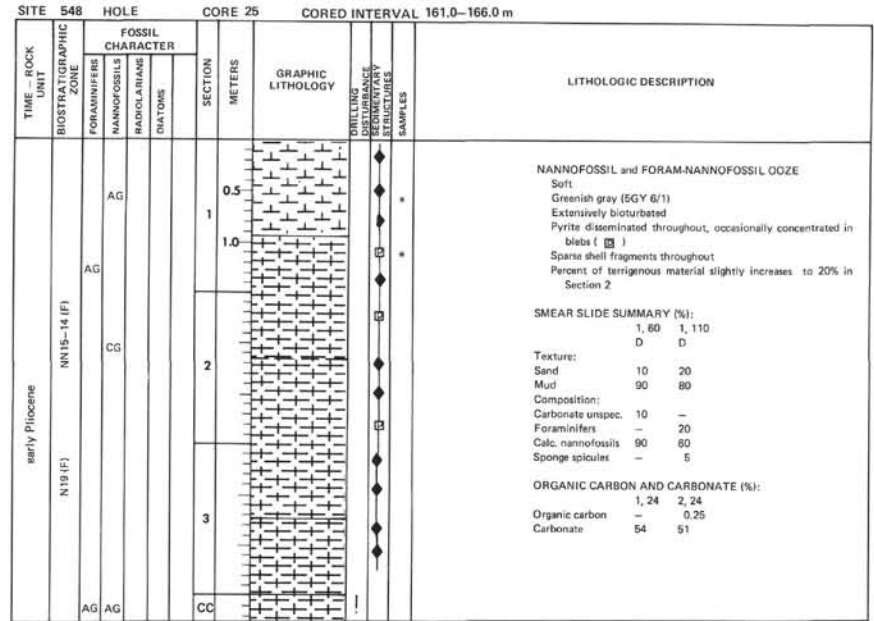
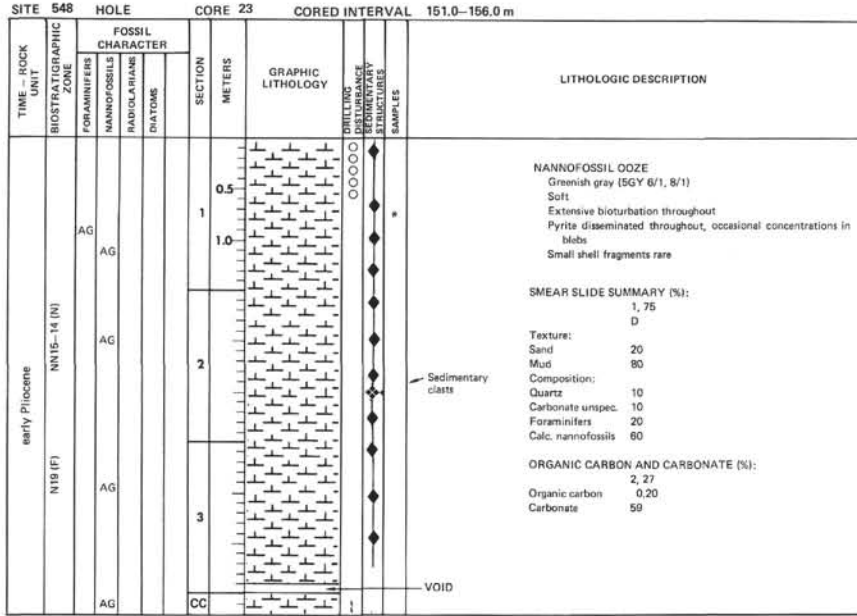












SITE 548 HOLE CORE 27 CORED INTERVAL 171.0-176.0 m		FOSSIL CHARACTER		SECTION METERS	GRAPHIC LITHOLOGY	DRELLING DISTURBANCE STRUCTURES	SAMPLES	LITHOLOGIC DESCRIPTION																																		
TIME - ROCK UNIT	BIOSTRATIGRAPHIC ZONE	FORAMINIFERS	DIATOMS																																							
early Pliocene	NN15-14 (N)	AG		0.5				<p>Greenish gray (5GY 6/1) foram-nannofossil ooze bioturbated throughout and with disseminated pyrite throughout. Rare shell fragments seen.</p> <p>SMEAR SLIDE SUMMARY (%):</p> <table border="1"> <tr><td>1, 51</td><td>4, 42</td></tr> <tr><td>D</td><td>D</td></tr> </table> <p>Texture:</p> <table border="1"> <tr><td>Sand</td><td>10</td><td>20</td></tr> <tr><td>Silt</td><td>20</td><td>30</td></tr> <tr><td>Clay</td><td>70</td><td>50</td></tr> </table> <p>Composition:</p> <table border="1"> <tr><td>Quartz</td><td>5</td><td>10</td></tr> <tr><td>Foraminifers</td><td>15</td><td>20</td></tr> <tr><td>Calc. nannofossils</td><td>70</td><td>60</td></tr> <tr><td>Diatoms</td><td><5</td><td>5</td></tr> <tr><td>Sponge spicules</td><td><5</td><td>5</td></tr> </table> <p>ORGANIC CARBON AND CARBONATE (%):</p> <table border="1"> <tr><td>Organic carbon</td><td>2, 36</td></tr> <tr><td>Carbonate</td><td>0, 26</td></tr> <tr><td></td><td>58</td></tr> </table>	1, 51	4, 42	D	D	Sand	10	20	Silt	20	30	Clay	70	50	Quartz	5	10	Foraminifers	15	20	Calc. nannofossils	70	60	Diatoms	<5	5	Sponge spicules	<5	5	Organic carbon	2, 36	Carbonate	0, 26		58
		1, 51	4, 42																																							
	D	D																																								
	Sand	10	20																																							
Silt	20	30																																								
Clay	70	50																																								
Quartz	5	10																																								
Foraminifers	15	20																																								
Calc. nannofossils	70	60																																								
Diatoms	<5	5																																								
Sponge spicules	<5	5																																								
Organic carbon	2, 36																																									
Carbonate	0, 26																																									
	58																																									
AG		1.0																																								
AG		2																																								
AG		3																																								
AG		4																																								
		CC																																								

SITE 548 HOLE CORE 29 CORED INTERVAL 181.0-186.0 m		FOSSIL CHARACTER		SECTION METERS	GRAPHIC LITHOLOGY	DRELLING DISTURBANCE STRUCTURES	SAMPLES	LITHOLOGIC DESCRIPTION																																																												
TIME - ROCK UNIT	BIOSTRATIGRAPHIC ZONE	FORAMINIFERS	DIATOMS																																																																	
early Pliocene	NN15-14 (N)	AG		0.5				<p>Light olive to greenish gray (5Y 6/1-5GY 6/1) nannofossil and foram-nannofossil ooze, with a marly unit in Section 2. Bioturbated and with disseminated pyrite throughout. Rare shell fragments. A large pebble (1-5 cm) at 40 cm in Section 2. Concentration of coarse pyrite between 40 and 52 cm in Section 2.</p> <p>SMEAR SLIDE SUMMARY (%):</p> <table border="1"> <tr><td>1, 124</td><td>2, 47</td><td>3, 145</td><td>4, 3</td></tr> <tr><td>D</td><td>D</td><td>D</td><td>D</td></tr> </table> <p>Texture:</p> <table border="1"> <tr><td>Sand</td><td>5</td><td>40</td><td>30</td></tr> <tr><td>Silt</td><td>25</td><td>30</td><td>30</td></tr> <tr><td>Clay</td><td>70</td><td>30</td><td>70</td></tr> </table> <p>Composition:</p> <table border="1"> <tr><td>Quartz</td><td><5</td><td>20</td><td>10</td></tr> <tr><td>Mica</td><td>10</td><td>10</td><td>10</td></tr> <tr><td>Carbonate unsp.</td><td>10</td><td>10</td><td>15</td></tr> <tr><td>Foraminifers</td><td>5</td><td>10</td><td>5</td></tr> <tr><td>Calc. nannofossils</td><td>80</td><td>30</td><td>70</td></tr> <tr><td>Diatoms</td><td>10</td><td>10</td><td>50</td></tr> <tr><td>Sponge spicules</td><td>-</td><td>-</td><td>5</td></tr> </table> <p>ORGANIC CARBON AND CARBONATE (%):</p> <table border="1"> <tr><td>Organic carbon</td><td>1, 82</td><td>2, 82</td><td>3, 82</td></tr> <tr><td>Carbonate</td><td>-</td><td>0, 20</td><td>0, 08</td></tr> <tr><td></td><td>81</td><td>62</td><td>70</td></tr> </table>	1, 124	2, 47	3, 145	4, 3	D	D	D	D	Sand	5	40	30	Silt	25	30	30	Clay	70	30	70	Quartz	<5	20	10	Mica	10	10	10	Carbonate unsp.	10	10	15	Foraminifers	5	10	5	Calc. nannofossils	80	30	70	Diatoms	10	10	50	Sponge spicules	-	-	5	Organic carbon	1, 82	2, 82	3, 82	Carbonate	-	0, 20	0, 08		81	62	70
		1, 124	2, 47	3, 145					4, 3																																																											
	D	D	D	D																																																																
	Sand	5	40	30																																																																
Silt	25	30	30																																																																	
Clay	70	30	70																																																																	
Quartz	<5	20	10																																																																	
Mica	10	10	10																																																																	
Carbonate unsp.	10	10	15																																																																	
Foraminifers	5	10	5																																																																	
Calc. nannofossils	80	30	70																																																																	
Diatoms	10	10	50																																																																	
Sponge spicules	-	-	5																																																																	
Organic carbon	1, 82	2, 82	3, 82																																																																	
Carbonate	-	0, 20	0, 08																																																																	
	81	62	70																																																																	
AG		1.0																																																																		
AG		2																																																																		
AG		3																																																																		
AG		4																																																																		
		CC																																																																		

SITE 548 HOLE CORE 28 CORED INTERVAL 176.0-181.0 m		FOSSIL CHARACTER		SECTION METERS	GRAPHIC LITHOLOGY	DRELLING DISTURBANCE STRUCTURES	SAMPLES	LITHOLOGIC DESCRIPTION																																								
TIME - ROCK UNIT	BIOSTRATIGRAPHIC ZONE	FORAMINIFERS	DIATOMS																																													
early Pliocene	NN15-14 (N)	AG		0.5				<p>Greenish gray (5GY 6/1) to light bluish gray (5B 7/1) nannofossil or foram-nannofossil ooze burrowed and with disseminated pyrite throughout. Occasional shell fragments.</p> <p>SMEAR SLIDE SUMMARY (%):</p> <table border="1"> <tr><td>1, 120</td><td>3, 20</td></tr> <tr><td>D</td><td>D</td></tr> </table> <p>Texture:</p> <table border="1"> <tr><td>Sand</td><td>10</td><td>10</td></tr> <tr><td>Silt</td><td>30</td><td>20</td></tr> <tr><td>Clay</td><td>60</td><td>70</td></tr> </table> <p>Composition:</p> <table border="1"> <tr><td>Quartz</td><td>10</td><td>10</td></tr> <tr><td>Mica</td><td>-</td><td>10</td></tr> <tr><td>Carbonate unsp.</td><td>10</td><td>20</td></tr> <tr><td>Foraminifers</td><td>10</td><td>5</td></tr> <tr><td>Calc. nannofossils</td><td>70</td><td>50</td></tr> <tr><td>Sponge spicules</td><td>-</td><td>5</td></tr> </table> <p>ORGANIC CARBON AND CARBONATE (%):</p> <table border="1"> <tr><td>Organic carbon</td><td>2, 84</td><td>3, 84</td></tr> <tr><td>Carbonate</td><td>0, 13</td><td>0, 18</td></tr> <tr><td></td><td>53</td><td>54</td></tr> </table>	1, 120	3, 20	D	D	Sand	10	10	Silt	30	20	Clay	60	70	Quartz	10	10	Mica	-	10	Carbonate unsp.	10	20	Foraminifers	10	5	Calc. nannofossils	70	50	Sponge spicules	-	5	Organic carbon	2, 84	3, 84	Carbonate	0, 13	0, 18		53	54
		1, 120	3, 20																																													
	D	D																																														
	Sand	10	10																																													
Silt	30	20																																														
Clay	60	70																																														
Quartz	10	10																																														
Mica	-	10																																														
Carbonate unsp.	10	20																																														
Foraminifers	10	5																																														
Calc. nannofossils	70	50																																														
Sponge spicules	-	5																																														
Organic carbon	2, 84	3, 84																																														
Carbonate	0, 13	0, 18																																														
	53	54																																														
AG		1.0																																														
AG		2																																														
AG		3																																														
AG		4																																														
		CC																																														

SITE 548 HOLE CORE 30 CORED INTERVAL 186.0-191.0 m		FOSSIL CHARACTER		SECTION METERS	GRAPHIC LITHOLOGY	DRELLING DISTURBANCE STRUCTURES	SAMPLES	LITHOLOGIC DESCRIPTION																									
TIME - ROCK UNIT	BIOSTRATIGRAPHIC ZONE	FORAMINIFERS	DIATOMS																														
early Pliocene	NN15-14 (N)	AG		0.5				<p>Greenish gray (5GY 6/1) to light olive gray (5Y 6/1) foraminiferal-nannofossil ooze. Intensely bioturbated and with disseminated pyrite throughout. Section 1, 15-30 cm rich in pyrite (~30%).</p> <p>SMEAR SLIDE SUMMARY (%):</p> <table border="1"> <tr><td>4, 8</td></tr> <tr><td>D</td></tr> </table> <p>Texture:</p> <table border="1"> <tr><td>Sand</td><td>20</td></tr> <tr><td>Silt</td><td>20</td></tr> <tr><td>Clay</td><td>60</td></tr> </table> <p>Composition:</p> <table border="1"> <tr><td>Quartz</td><td>10</td></tr> <tr><td>Foraminifers</td><td>20</td></tr> <tr><td>Calc. nannofossils</td><td>60</td></tr> <tr><td>Diatoms</td><td>10</td></tr> </table> <p>ORGANIC CARBON AND CARBONATE (%):</p> <table border="1"> <tr><td>Organic carbon</td><td>2, 82</td><td>3, 82</td></tr> <tr><td>Carbonate</td><td>0, 17</td><td>0, 12</td></tr> <tr><td></td><td>62</td><td>67</td></tr> </table>	4, 8	D	Sand	20	Silt	20	Clay	60	Quartz	10	Foraminifers	20	Calc. nannofossils	60	Diatoms	10	Organic carbon	2, 82	3, 82	Carbonate	0, 17	0, 12		62	67
		4, 8																															
	D																																
	Sand	20																															
Silt	20																																
Clay	60																																
Quartz	10																																
Foraminifers	20																																
Calc. nannofossils	60																																
Diatoms	10																																
Organic carbon	2, 82	3, 82																															
Carbonate	0, 17	0, 12																															
	62	67																															
AG		1.0																															
AG		2																															
AG		3																															
AG		4																															
		CC																															

SITE 548		HOLE		CORE 31		CORED INTERVAL		191.0–196.0 m		
TIME – ROCK UNIT	BIOSTRATIGRAPHIC ZONE	FOSSIL CHARACTER			SECTION METERS	GRAPHIC LITHOLOGY	DRILLING DISTURBANCE STRUCTURES	SAMPLES	LITHOLOGIC DESCRIPTION	
		FORAMINIFERS	NAINFOSSILS	RADIOLARIANS						DIATOMS
early Pliocene	N13–12 (N)	AG			0.5			5GY 6/1	Interbedded layers of greenish gray (5GY 6/1) and light bluish gray (5B 7/1) nanofossil ooze. Bioturbated and with scattered pyrite throughout. Large burrows seen at contacts between layers of different colors.	
		AG			1.0					5B 7/1
		AG			1.5					5GY 6/1
		AG			2.0					5B 7/1
		AG			2.5					5GY 6/1
		AG			3.0					5B 7/1
	N18 (F)	AG			3.5			5GY 6/1	SMEAR SLIDE SUMMARY (%): 1, 99 D Texture: Sand 20 Silt 30 Clay 50 Composition: Quartz 5 Carbonate unspec. 15 Foraminifers 10 Calc. nanofossils 70 ORGANIC CARBON AND CARBONATE (%): Organic carbon 0.15 3.82 Carbonate 61 56	
		AG			4.0					5B 7/1
		AG			4.5					5GY 6/1
		AG			5.0					5B 7/1
		AG			5.5					5GY 6/1
		AG			6.0					5B 7/1
CC										

SITE 548		HOLE		CORE 32		CORED INTERVAL		196.0–201.0 m		
TIME – ROCK UNIT	BIOSTRATIGRAPHIC ZONE	FOSSIL CHARACTER			SECTION METERS	GRAPHIC LITHOLOGY	DRILLING DISTURBANCE STRUCTURES	SAMPLES	LITHOLOGIC DESCRIPTION	
		FORAMINIFERS	NAINFOSSILS	RADIOLARIANS						DIATOMS
early Pliocene	N12–13 (N)	AG			0.5			5GY 6/1	Unit 1: marly nanofossil ooze, greenish gray (5GY 6/1), firm, homogeneous, silty, scattered dark flecks.	
		AG			1.0					5B 7/1
		AG			1.5					5GY 6/1
		AG			2.0					5B 7/1
		AG			2.5					5GY 6/1
		AG			3.0					5B 7/1
	N18 (F)	AG			3.5			5B 7/1	Unit 2: nanofossil ooze, light bluish gray (5B 7/1), firm, mottled, varying quantities of silt. Note: all contacts are gradational. Lens of silt.	
		AG			4.0					5GY 6/1
		AG			4.5					5B 7/1
		AG			5.0					5GY 6/1
		AG			5.5					5B 7/1
		AG			6.0					5GY 6/1
CC										

— Greenish silty mud layer
— Lens of silt

SITE 548		HOLE		CORE 33		CORED INTERVAL		201.0–206.0 m		
TIME – ROCK UNIT	BIOSTRATIGRAPHIC ZONE	FOSSIL CHARACTER			SECTION METERS	GRAPHIC LITHOLOGY	DRILLING DISTURBANCE STRUCTURES	SAMPLES	LITHOLOGIC DESCRIPTION	
		FORAMINIFERS	NAINFOSSILS	RADIOLARIANS						DIATOMS
early Pliocene	N17 (F)	AG			0.5			5Y 7/1	Unit 1: nanofossil ooze, blue gray (5Y 7/1–5B 7/1) firm, mottled scattered small black flecks.	
		AG			1.0					5B 7/1
		AG			1.5					5Y 7/1
		AG			2.0					5B 7/1
		AG			2.5					5Y 7/1
		AG			3.0					5B 7/1
	N18 (F)	AG			3.5			5GY 6/1	Unit 2: marly nanofossil ooze, greenish gray (5GY 6/1) firm, variable amount of silt, moderately bioturbated, scattered small (<mm) shell fragments and black flecks.	
		AG			4.0					5B 7/1
		AG			4.5					5GY 6/1
		AG			5.0					5B 7/1
		AG			5.5					5GY 6/1
		AG			6.0					5B 7/1
CC										

Note: all contacts are gradational.

SMEAR SLIDE SUMMARY (%):

	2, 75	3, 40	3, 82	3, 98
D				

Texture:

	7	25	10	20
Sand				
Silt	25	35	18	30
Clay	63	40	75	50

Composition:

	15	5	10	25
Quartz				
Mica	–	–	5	–
Clay	5	5	5	<5
Glauconite	Tr	–	–	–
Pyrite	–	35	–	–
Carbonate unspec.	10	15	5	15
Foraminifers	15	10	10	10
Calc. nanofossils	50	30	60	35
Sponge spicules	5	–	5	5

ORGANIC CARBON AND CARBONATE (%):

	2, 58
Organic carbon	0.15
Carbonate	61

SITE 548 HOLE CORE 34 CORED INTERVAL 206.0-209.0 m

TIME - ROCK UNIT	BIOSTRATIGRAPHIC ZONE	FOSSIL CHARACTER			SECTION METERS	GRAPHIC LITHOLOGY	DRILLING DISTURBANCE STRUCTURES	SAMPLES	LITHOLOGIC DESCRIPTION
		FORAMINIFERS	NANNOFOSSILS	RADIOLARIANS					
early Pliocene	NN13-12 (N)	AG	CG		0.5				<p>VOID</p> <p>Unit 1: silty sand, greenish gray (SGY 8/1), soft, homogeneous, some darker mottling.</p> <p>Unit 2: marly nannofossil ooze, greenish gray (SGY 6/1), firm, mottled, varying amounts of silt, scattered small (< mm) shell fragments and black flecks.</p> <p>Unit 3: nannofossil ooze, blue gray (SB 7/1), firm, mottled, scattered black flecks.</p> <p>SMEAR SLIDE SUMMARY (%):</p> <p>1, 59 D</p> <p>Texture:</p> <p>Sand 25 Silt 35 Clay 40</p> <p>Composition:</p> <p>Quartz 30 Clay 5 Glauconite 5 Carbonate unsp. 15 Foraminifers 5 Calc. nannofossils 35 Sponge spicules 5</p> <p>ORGANIC CARBON AND CARBONATE (%):</p> <p>2, 41 Organic carbon 0.27 Carbonate 53</p>
		AG			1.0				
		AG			2				
	N18 (F)	AG	CM		3				

SITE 548 HOLE CORE 35 CORED INTERVAL 209.0-211.0 m

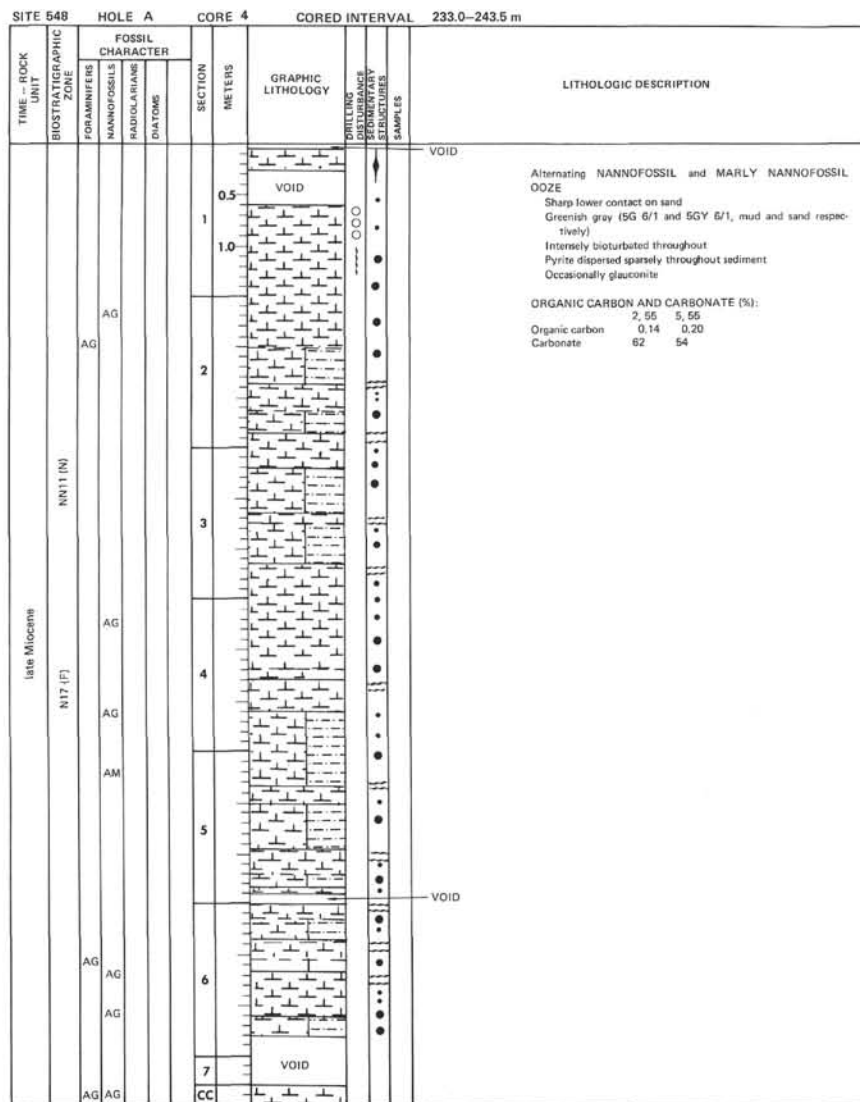
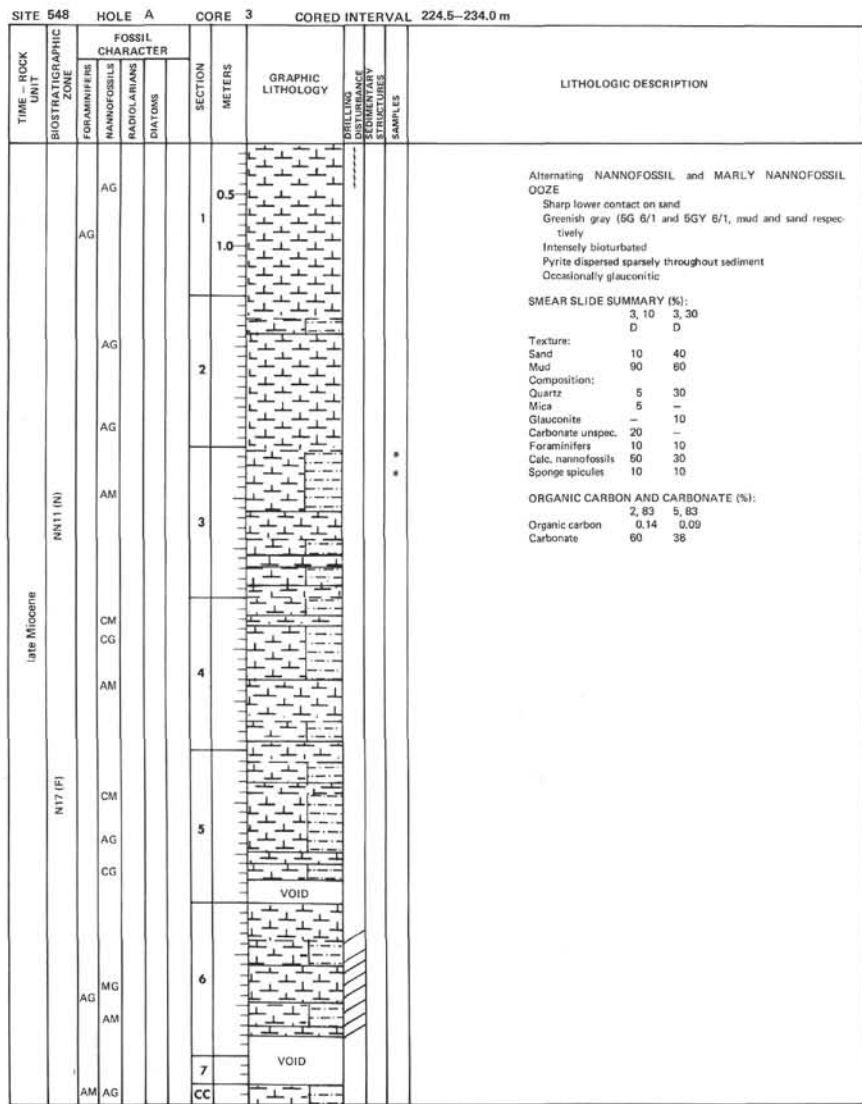
TIME - ROCK UNIT	BIOSTRATIGRAPHIC ZONE	FOSSIL CHARACTER			SECTION METERS	GRAPHIC LITHOLOGY	DRILLING DISTURBANCE STRUCTURES	SAMPLES	LITHOLOGIC DESCRIPTION
		FORAMINIFERS	NANNOFOSSILS	RADIOLARIANS					
early Pliocene	NN13-12 (N)	AG	AM		0.5				<p>Unit 1: nannofossil ooze, blue gray (SB 7/1-5GY 7/1), firm, bioturbated in shades of blue gray, scattered black flecks.</p> <p>ORGANIC CARBON AND CARBONATE (%):</p> <p>1, 51 Organic carbon 0.18 Carbonate 53</p>
		AG	CM		1.0			Laminations	
	N18 (F)	AG	CM		2				
					CC				

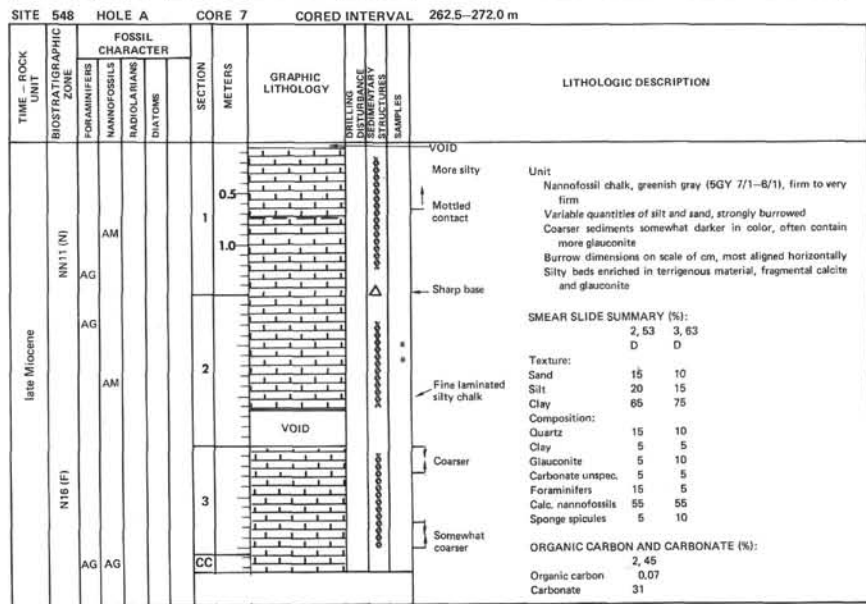
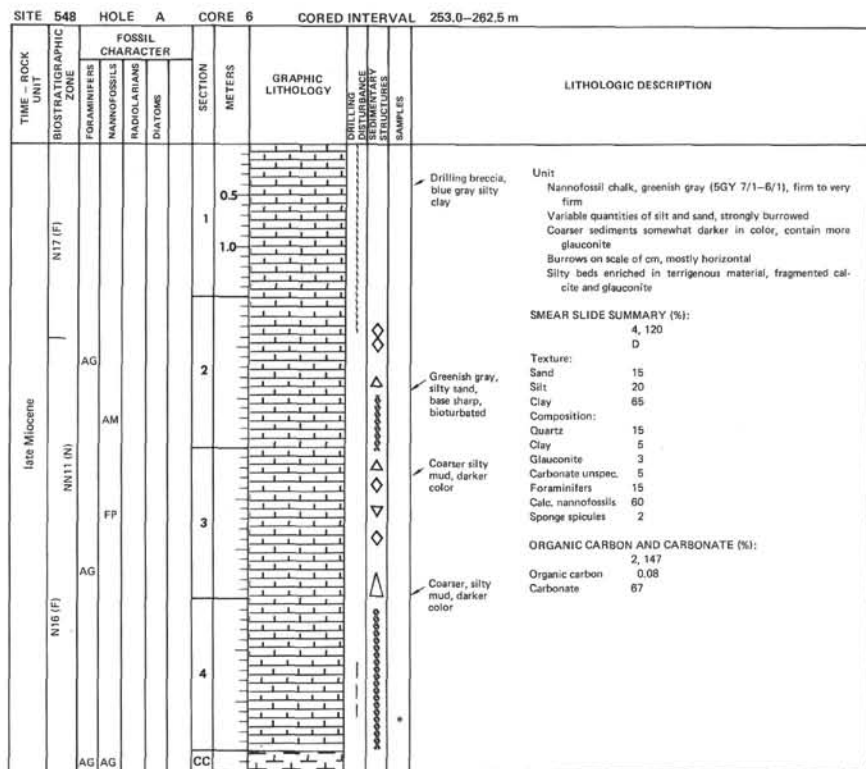
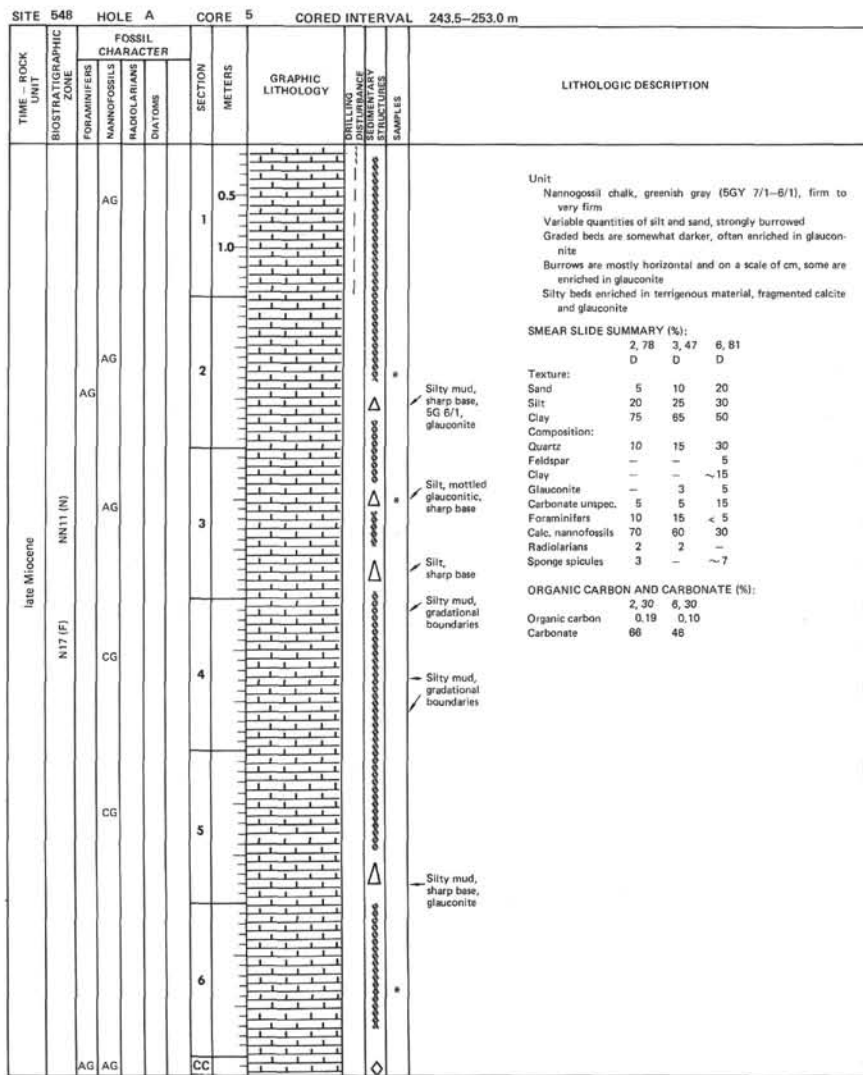
SITE 548 HOLE A CORE 1 CORED INTERVAL 205.5-215.0 m

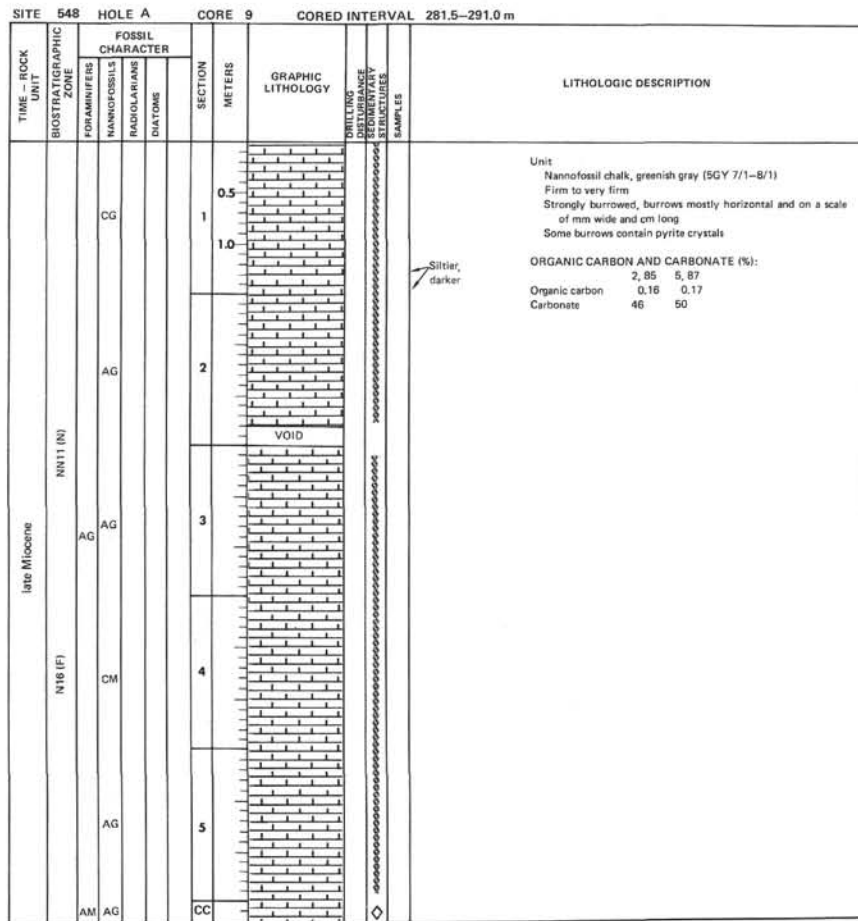
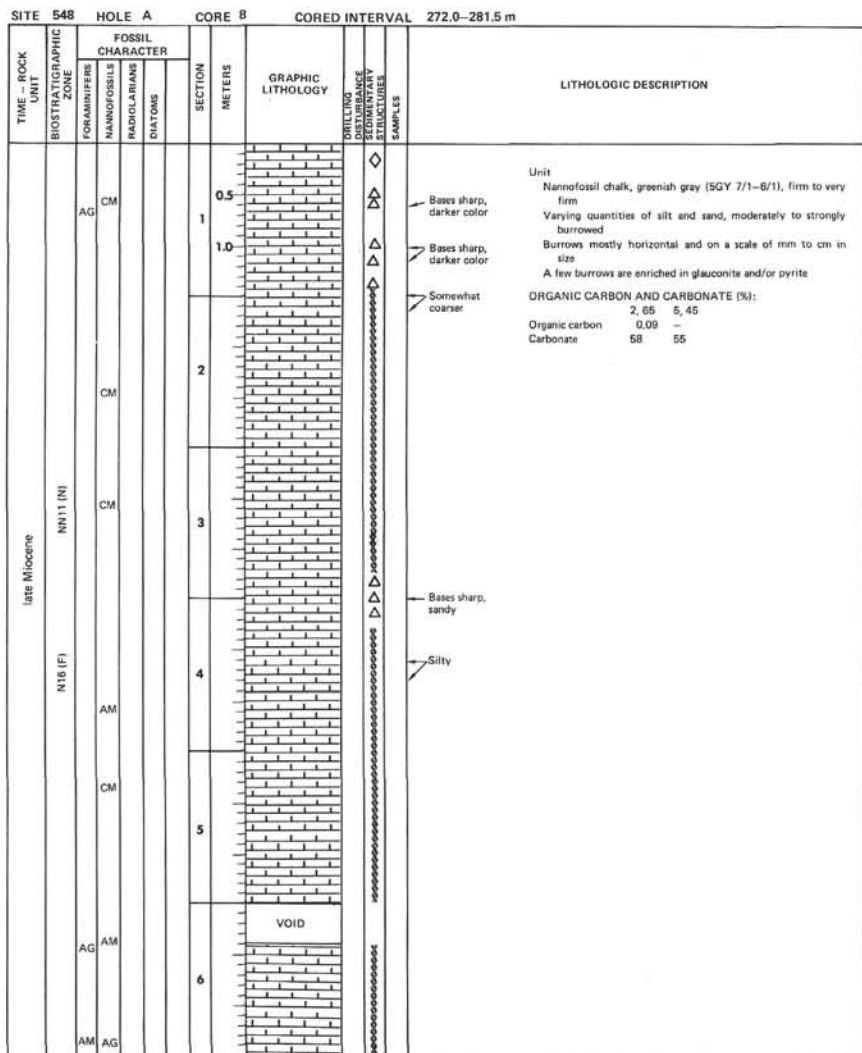
TIME - ROCK UNIT	BIOSTRATIGRAPHIC ZONE	FOSSIL CHARACTER			SECTION METERS	GRAPHIC LITHOLOGY	DRILLING DISTURBANCE STRUCTURES	SAMPLES	LITHOLOGIC DESCRIPTION
		FORAMINIFERS	NANNOFOSSILS	RADIOLARIANS					
	N17 (F)								<p>Nannofossil ooze mud in Core-Catcher only; nothing retrieved from remainder of core.</p>
	NN11 (N)	AG							

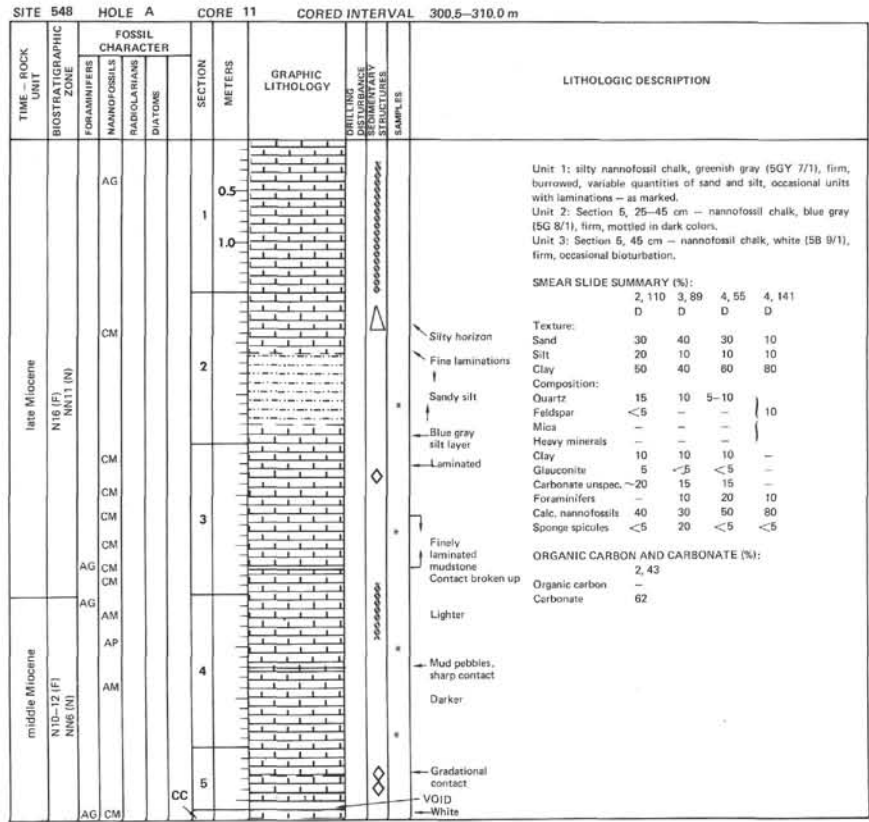
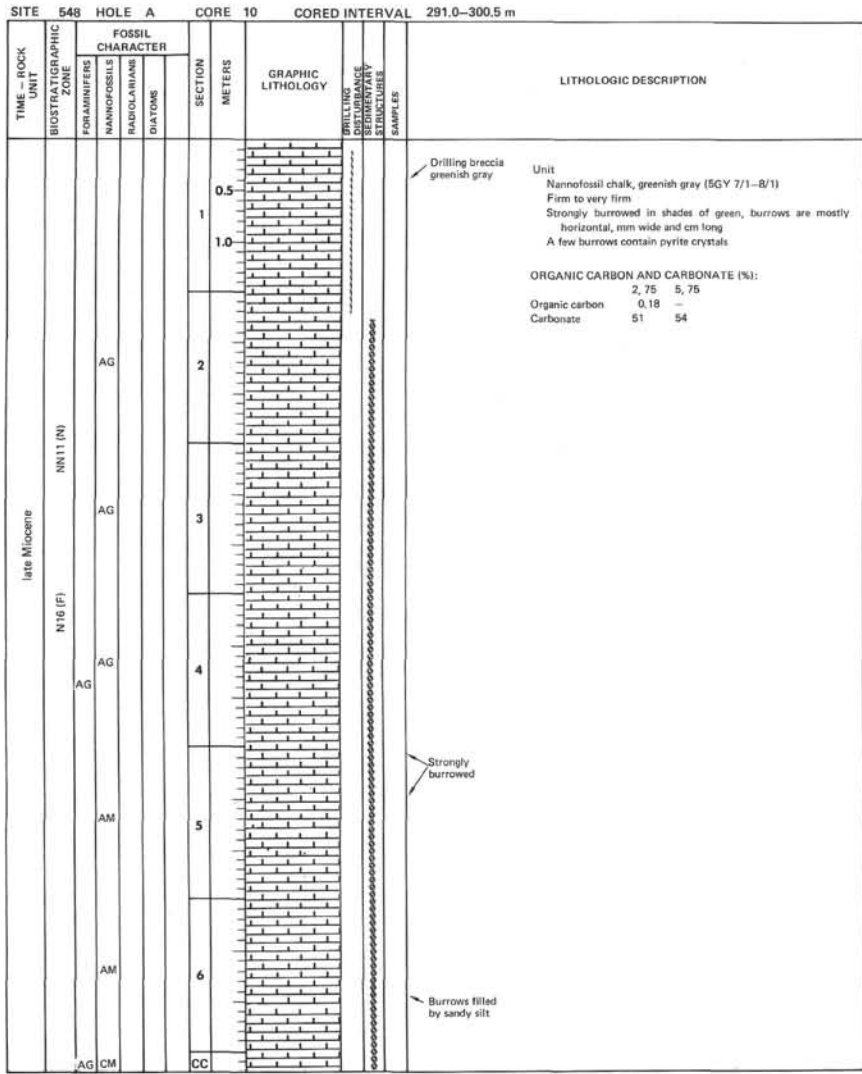
SITE 548 HOLE A CORE 2 CORED INTERVAL 215.0-224.5 m

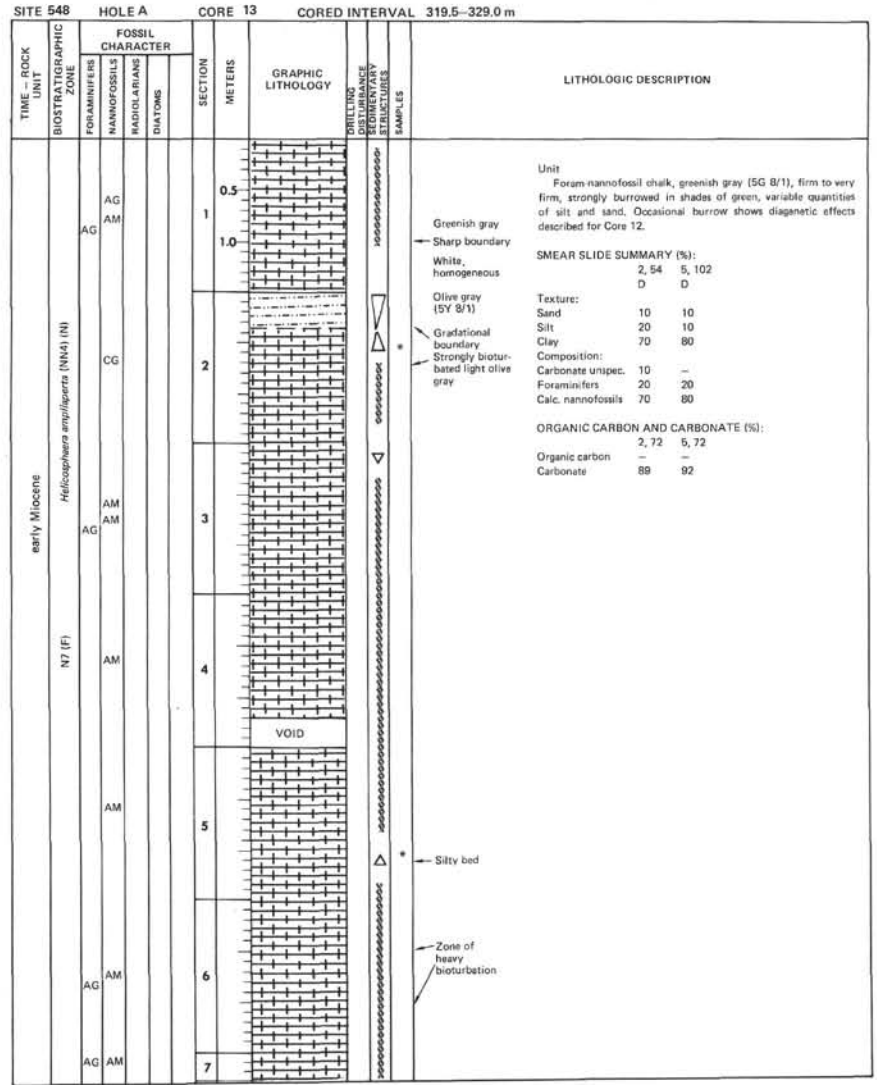
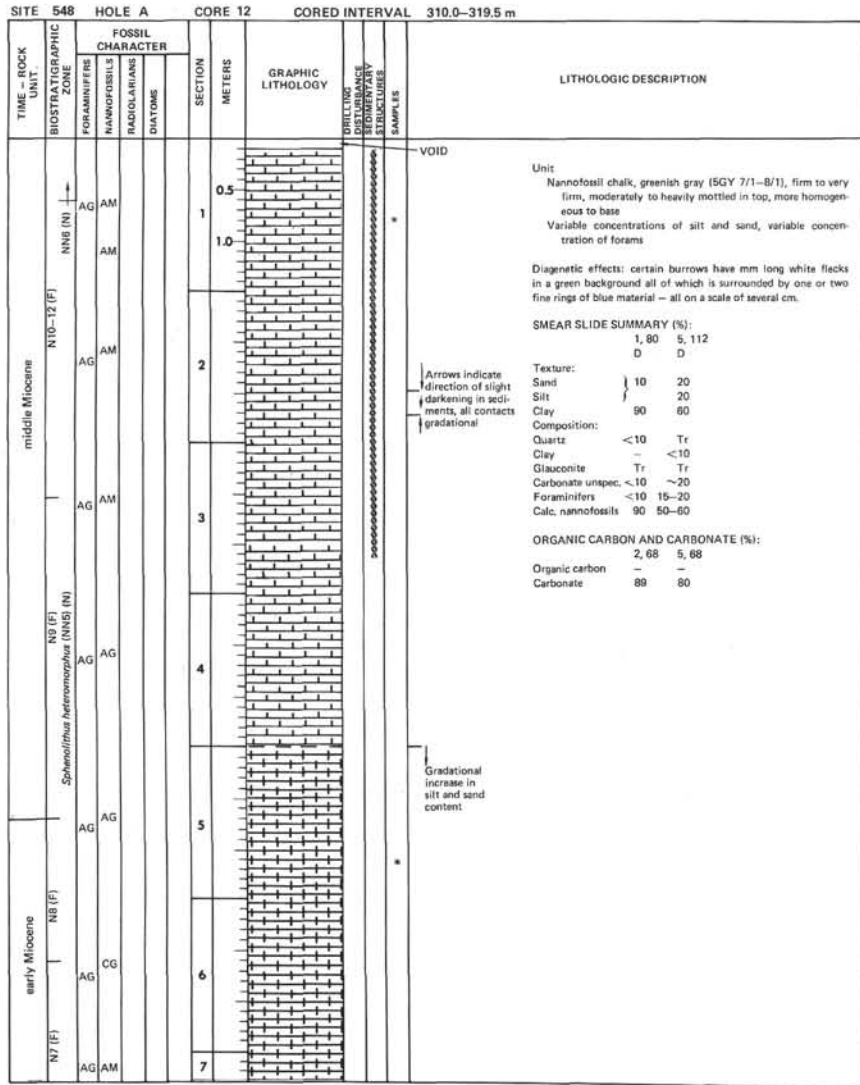
TIME - ROCK UNIT	BIOSTRATIGRAPHIC ZONE	FOSSIL CHARACTER			SECTION METERS	GRAPHIC LITHOLOGY	DRILLING DISTURBANCE STRUCTURES	SAMPLES	LITHOLOGIC DESCRIPTION
		FORAMINIFERS	NANNOFOSSILS	RADIOLARIANS					
late Miocene	Discosaster polyoperculus (NN11) (N)	AM			0.5				<p>NANNOFOSSIL OOZE</p> <p>Greenish gray (SGY 6/1 and 5G 6/1)</p> <p>Firm, massive, burrow-mottled and pyritized throughout</p> <p>Any bedding destroyed by burrowing</p> <p>VOID</p> <p>VOID</p>
		AG			1.0				
		AG			2				
		CM			3				
	N17 (F)	AG	CM		4			<p>NANNOFOSSIL OOZE and MARLY NANNOFOSSIL OOZE</p> <p>In a series of upward-fining sequences</p> <p>Greenish gray (SGY 6/1 and 5G 6/1)</p> <p>Firm</p> <p>Abrupt contact above mud, gradual above sand</p> <p>Pyritized and intensely burrowed</p>	
					CC			<p>SMEAR SLIDE SUMMARY (%):</p> <p>4, 10 4, 30 D D</p> <p>Texture:</p> <p>Sand 30 10 Mud 70 90</p> <p>Composition:</p> <p>Quartz 15 5 Glauconite 15 - Carbonate unsp. - 10 Foraminifers 10 5 Calc. nannofossils 50 80 Diatoms 5 - Sponge spicules 5 Tr</p> <p>ORGANIC CARBON AND CARBONATE (%):</p> <p>2, 100 Organic carbon 0.18 Carbonate 54</p>	

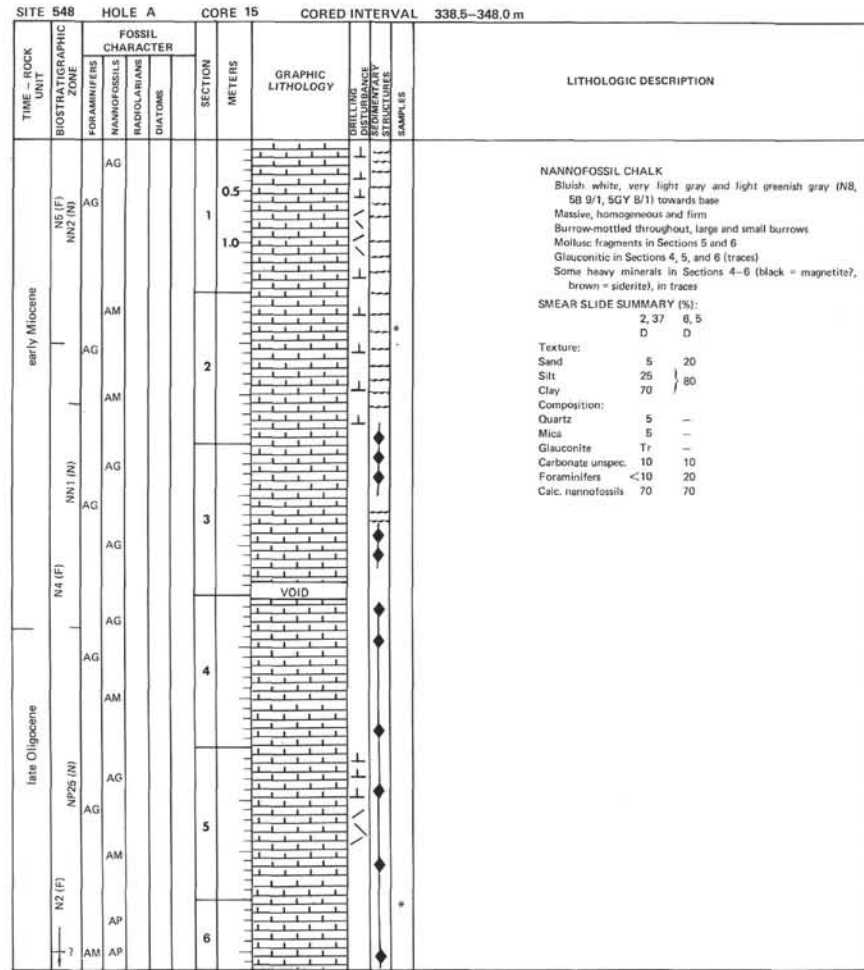
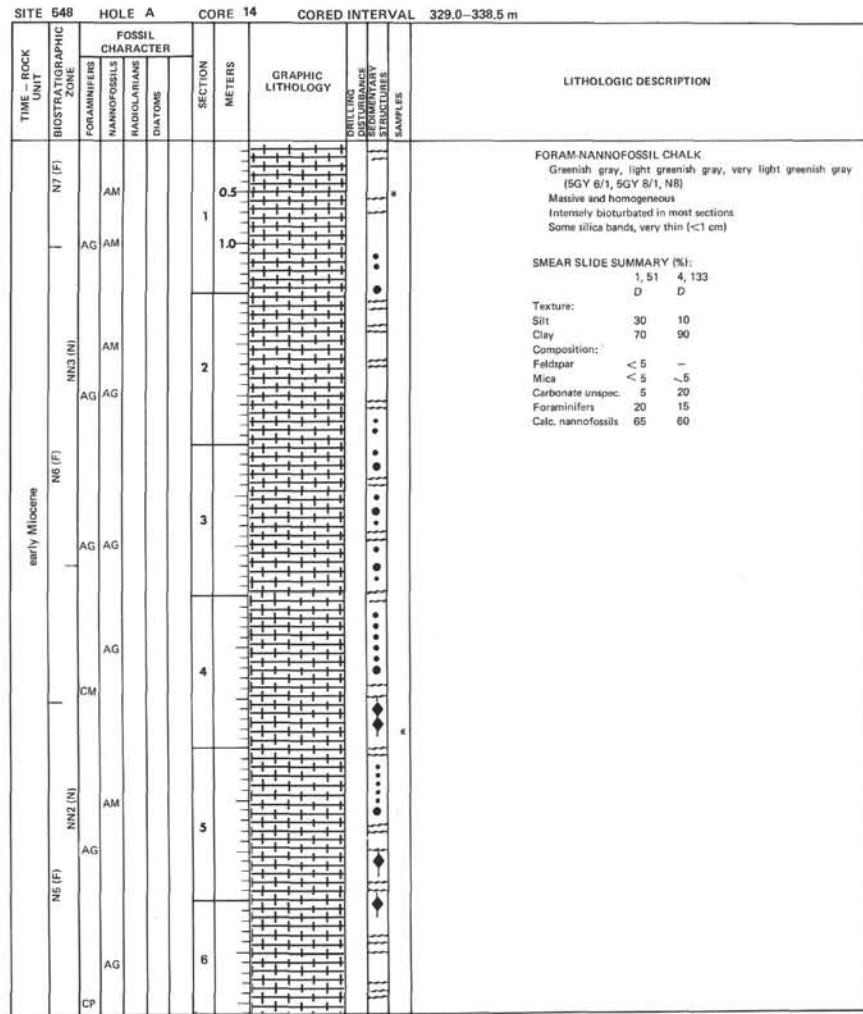


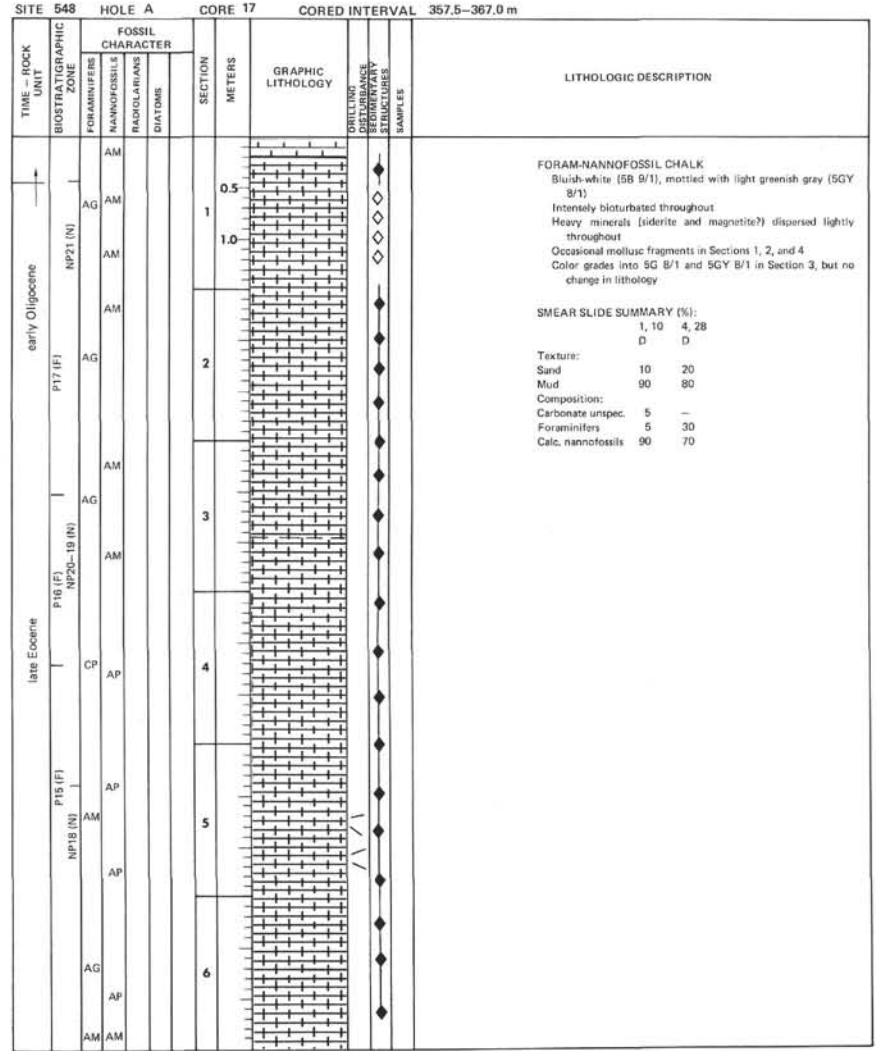
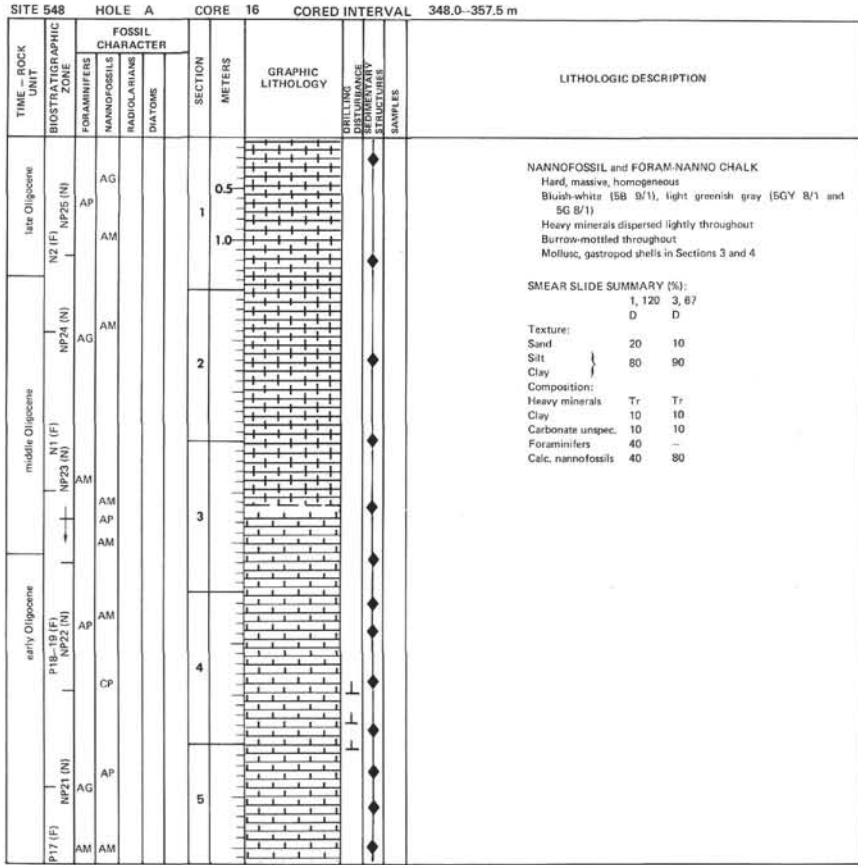


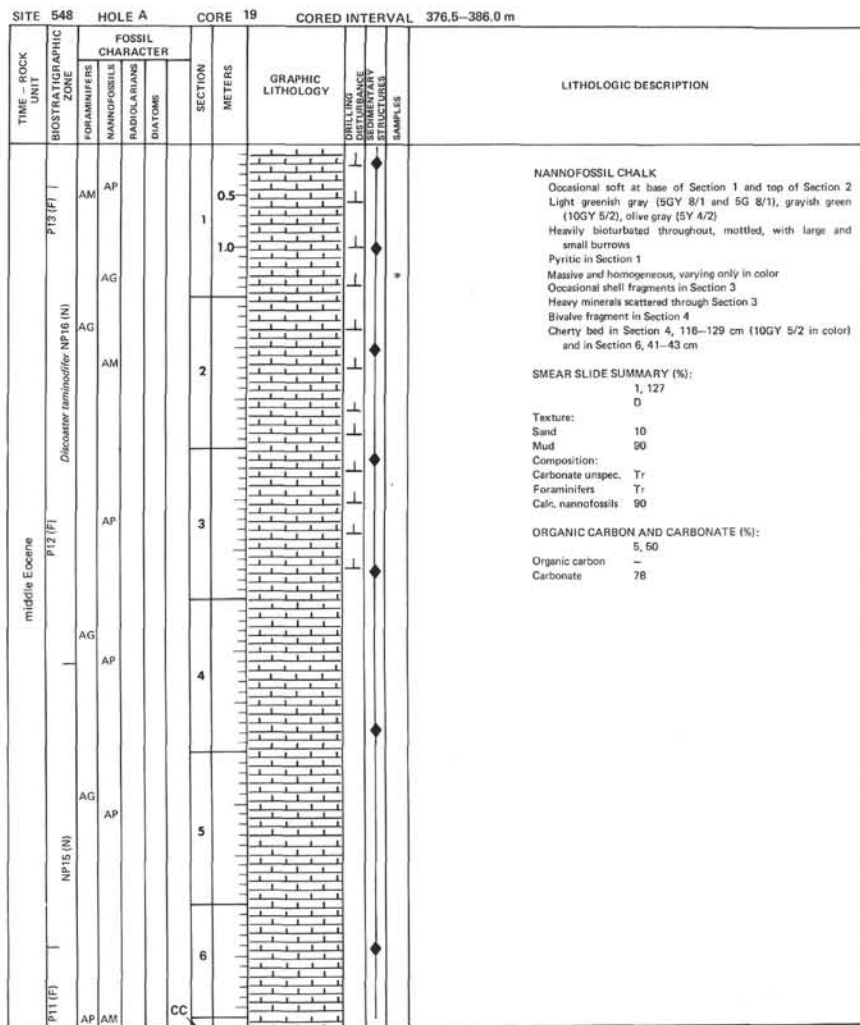
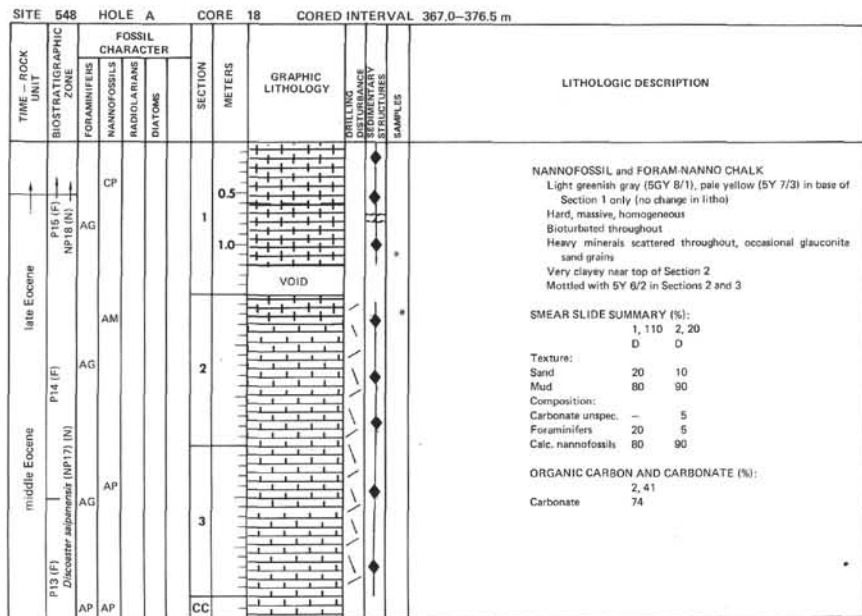










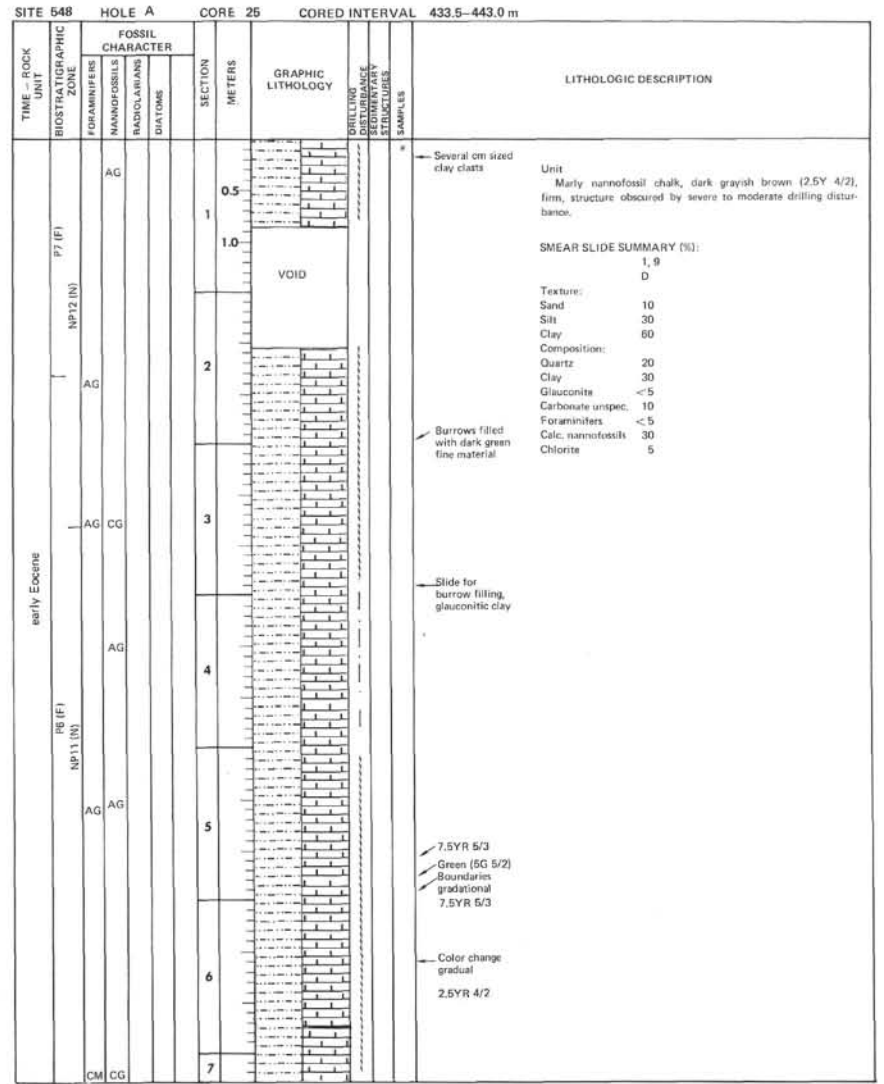
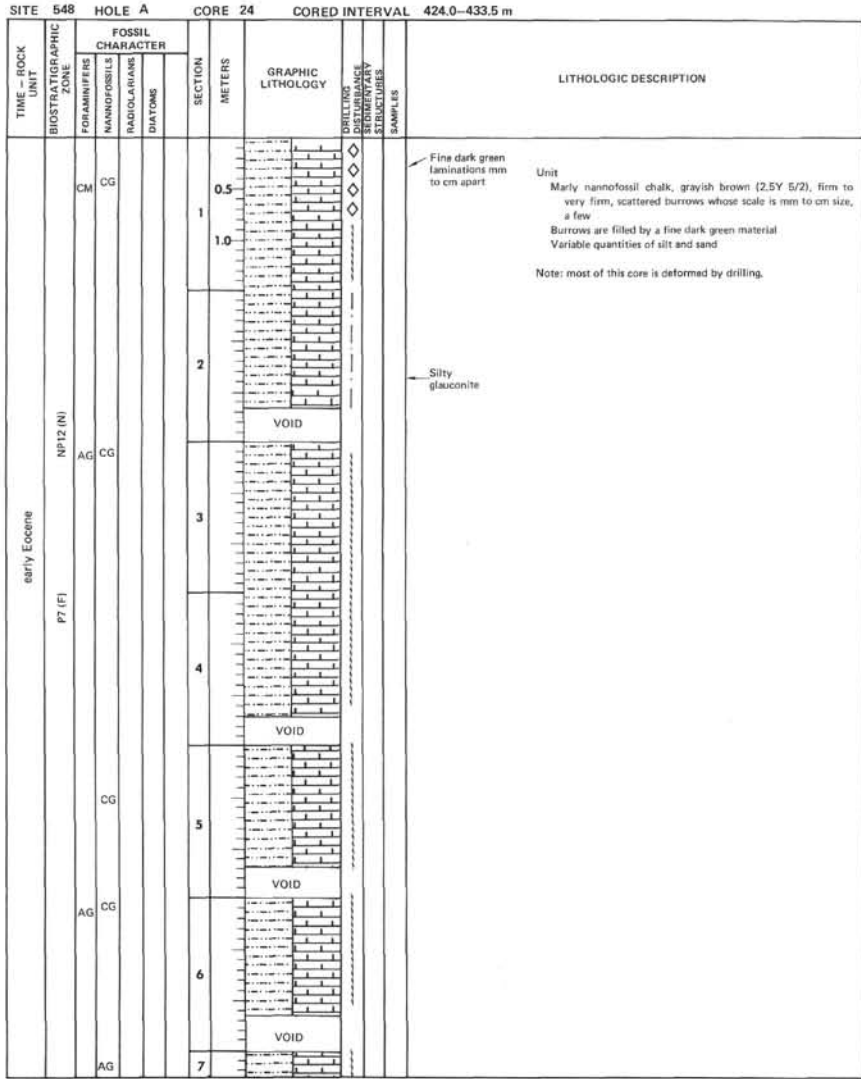


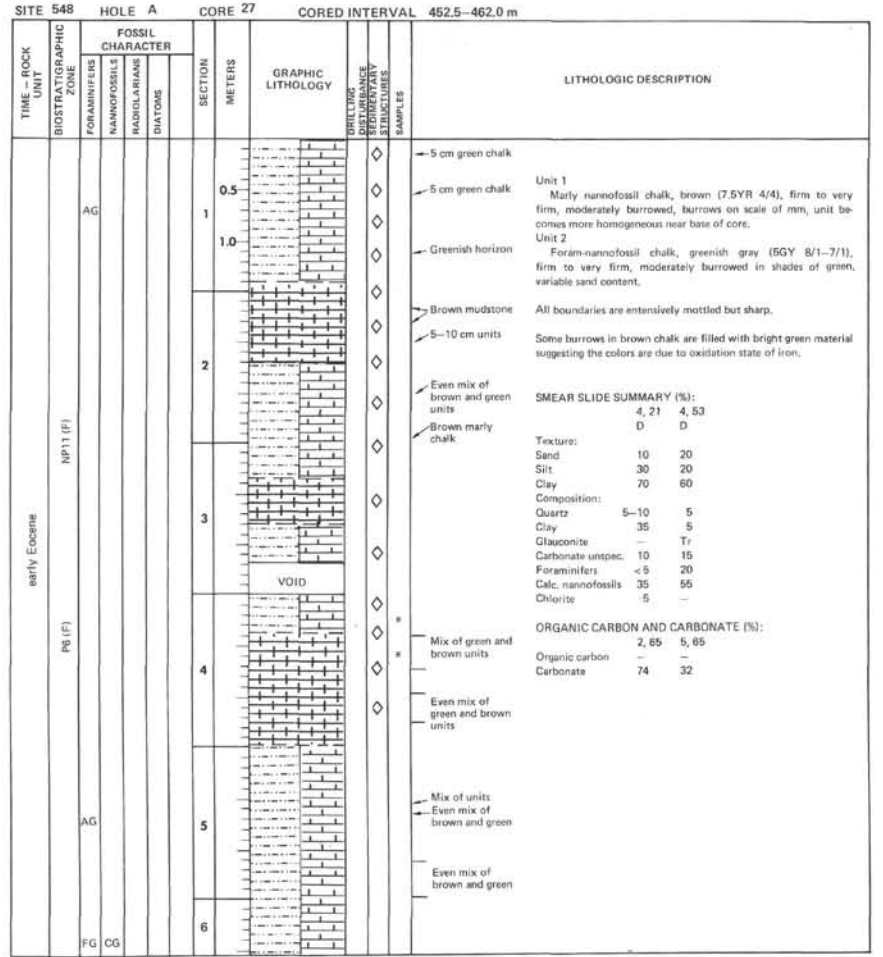
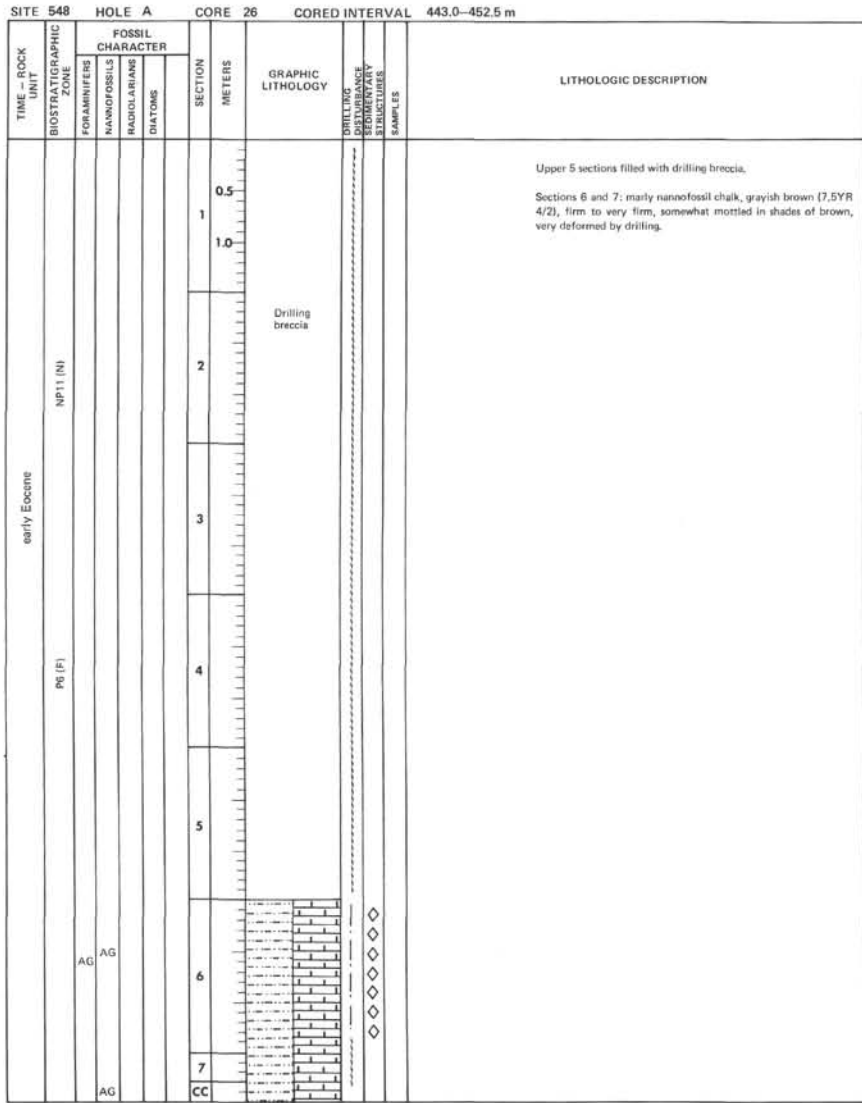
SITE 548		HOLE A		CORE 20		CORED INTERVAL 386.0-395.5 m		
TIME - ROCK UNIT	BIOSTRATIGRAPHIC ZONE	FOSSIL CHARACTER			SECTION METERS	GRAPHIC LITHOLOGY	CORRELATION DISTURBANCE SEDIMENTARY STRUCTURES SAMPLES	LITHOLOGIC DESCRIPTION
		FORAMINIFERS	NANNOFOSSILS	RADIOLARIANS				
middle Eocene	P11 (F) <i>Chilogrammitis alatus</i> (NP15) (N)	AG	AP			0.5		<p>FORAM-NANNOFOSSIL OOZE</p> <p>Intensely bioturbated</p> <p>Firm, massive and homogeneous throughout</p> <p>Mottled, with thin beds of 5GY B/1 chalk in Section 2</p> <p>Tiny shell fragments dispersed sparsely throughout</p> <p>Animal tracks ϕ in Core-Catcher</p> <p>Chert nodules in Section 3, 6-8 cm</p> <p>SMEAR SLIDE SUMMARY (%):</p> <p>Sand 3, 5</p> <p>D</p> <p>Texture:</p> <p>Sand 10</p> <p>Mud 90</p> <p>Composition:</p> <p>Foraminifers 15</p> <p>Calc. nannofossils 80</p>
		AP			1			
		AG			2			
		AP			3			
				4	CC			

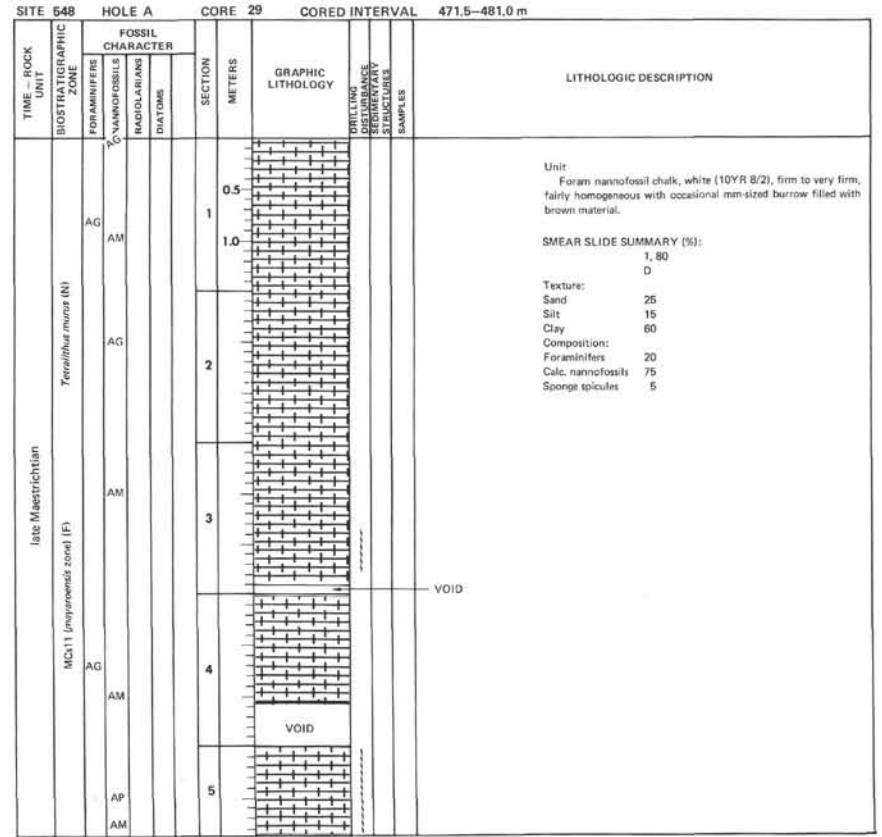
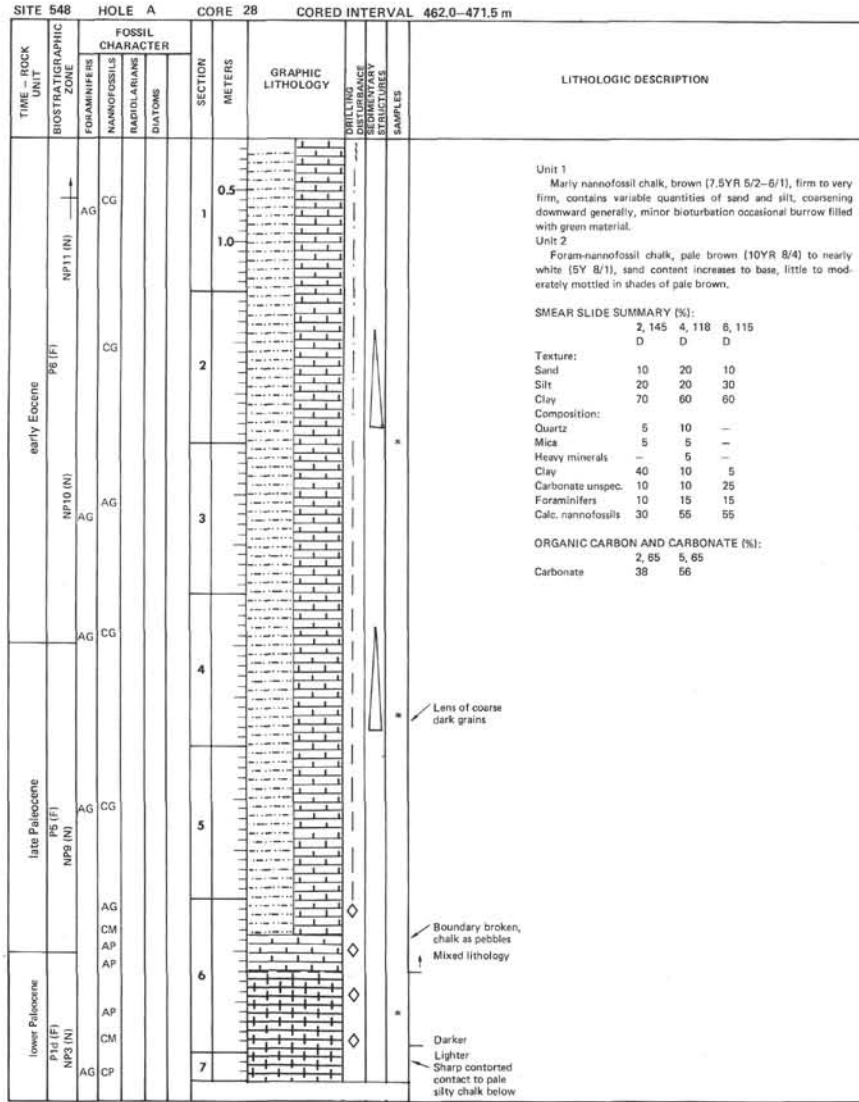
SITE 548		HOLE A		CORE 21		CORED INTERVAL 395.5-405.0 m		
TIME - ROCK UNIT	BIOSTRATIGRAPHIC ZONE	FOSSIL CHARACTER			SECTION METERS	GRAPHIC LITHOLOGY	CORRELATION DISTURBANCE SEDIMENTARY STRUCTURES SAMPLES	LITHOLOGIC DESCRIPTION
		FORAMINIFERS	NANNOFOSSILS	RADIOLARIANS				
middle Eocene	P10 (F) <i>Chilogrammitis alatus</i> (NP15) (N)	AP	AM			0.5		<p>FORAM-NANNO CHALK</p> <p>Light greenish gray (5G B/1 and 5GY B/1)</p> <p>Firm, massive</p> <p>Intensely burrow-mottled throughout</p> <p>More pyritic in burrows</p> <p>Chert nodules in Section 1, 58-59 cm; Section 2, 130-135 cm; Section 3, 70-71 cm; and Section 4, 132-136 cm</p> <p>Some chert pebbles in a mud matrix filling in burrows</p> <p>SMEAR SLIDE SUMMARY (%):</p> <p>Sand 3, 60</p> <p>D</p> <p>Texture:</p> <p>Sand 10</p> <p>Mud 90</p> <p>Composition:</p> <p>Carbonate unsp. 10</p> <p>Calc. nannofossils 80</p> <p>ORGANIC CARBON AND CARBONATE (%):</p> <p>Organic carbon 2, 74</p> <p>Carbonate 70</p>
		AP			1			
		AG			2			
		AP			3			
				4	CC			

SITE 548		HOLE A		CORE 22		CORED INTERVAL 405.0-414.5 m		
TIME - ROCK UNIT	BIOSTRATIGRAPHIC ZONE	FOSSIL CHARACTER			SECTION METERS	GRAPHIC LITHOLOGY	LITHOLOGIC DESCRIPTION	
		FORAMINIFERS	NANNOFOSSILS	RADIOLARIANS				DIAATOMS
middle Eocene	P10 (F)	NP15 (N)	AP			0.5	Unit 1 Nannofossil chalk, greenish gray (5GY 7/1), firm to very firm, moderately burrowed in shades of green, variable quantities of sand and silt. Unit 2 Marly nannofossil chalk, olive gray (5Y 4/2) firm, moderately burrowed.	
			AG			1.0		
middle Eocene	NP14 (N)	AM	CG			2	SMEAR SLIDE SUMMARY (%): 3, 80 6, 10 6, 28 D D D Texture: Sand 15 20 10 Silt 35 20 20 Clay 50 60 70 Composition: Quartz 2 10 Feldspar - < 5 15 Mica - - Clay 20 10 20 Glauconite 5 < 5 5 Carbonate unsp. 38 5 - Foraminifers 5 15 - Calc. nannofossils 30 50 50 Sponge spicules - - 10	
			AP			3		ORGANIC CARBON AND CARBONATE (%): Organic carbon 5, 91 Carbonate 63
			AM			4		
early Eocene	P7 (F)	NP12 (N)	AM			5	VOID	
			AG					
			AM					
early Eocene	P7 (F)	NP12 (N)	AM			6	Sharp contact Sediment clasts	
early Eocene	FG	CG				7	VOID	

SITE 548		HOLE A		CORE 23		CORED INTERVAL 414.5-424.0 m	
TIME - ROCK UNIT	BIOSTRATIGRAPHIC ZONE	FOSSIL CHARACTER			SECTION METERS	GRAPHIC LITHOLOGY	LITHOLOGIC DESCRIPTION
		FORAMINIFERS	NANNOFOSSILS	RADIOLARIANS			
early Eocene	NP12 (N)	CG	AG			0.5	Unit Very marly nannofossil chalk, dark gray brown (2.5Y 4/2), firm, moderately to infrequently burrowed with burrows on scale of mm. Occasional burrow filled with fine dark green mineral. SMEAR SLIDE SUMMARY (%): 1, 60 D Texture: Sand 20 Silt 20 Clay 60 Composition: Quartz 15 Clay 30 Glauconite < 5 Carbonate unsp. 10 Foraminifers 5-10 Calc. nannofossils 30 Sponge spicules 5
			CG			1.0	
early Eocene	P7 (F)	CG	CM			3	ORGANIC CARBON AND CARBONATE (%): Organic carbon 2, 64 Carbonate 17
			CG			4	
early Eocene	CC					VOID	VOID



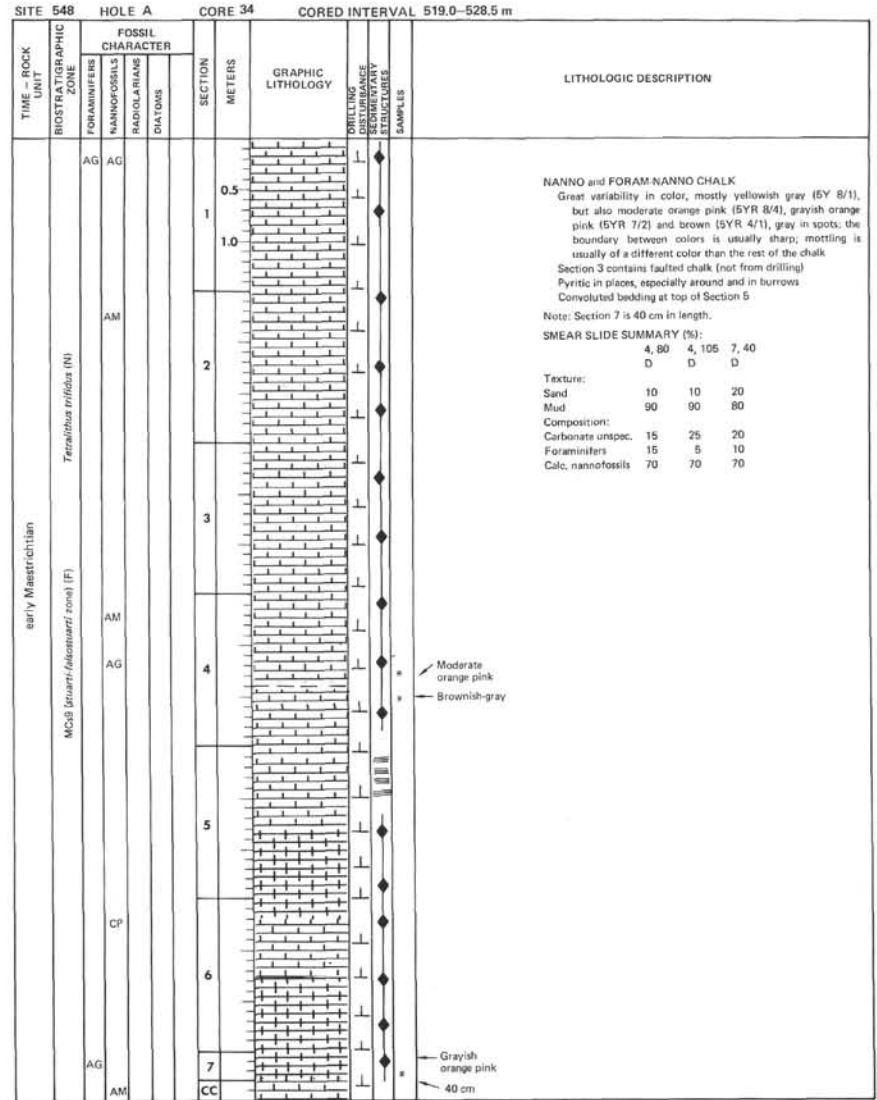
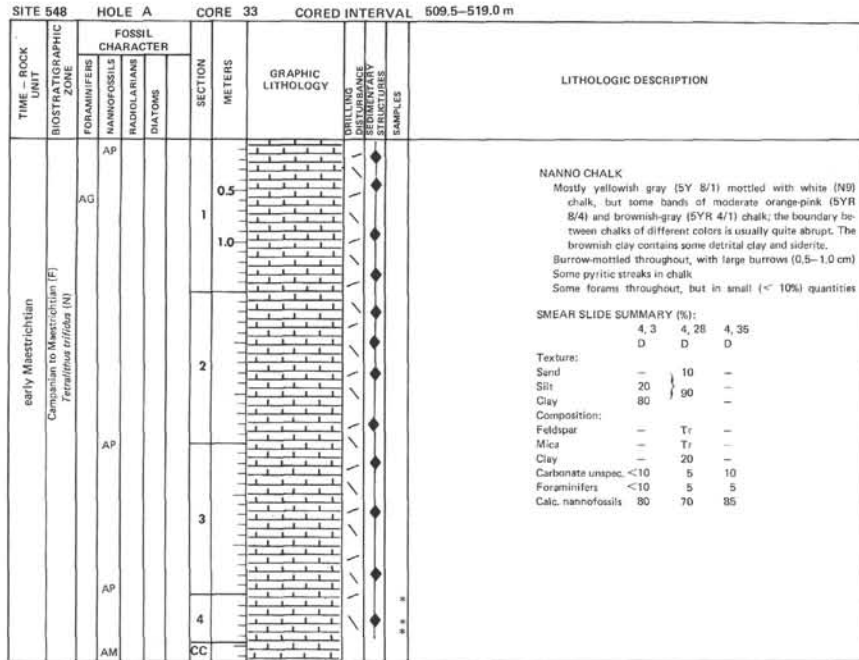




SITE 548		HOLE A		CORE 30		CORED INTERVAL 481.0–490.5 m							
TIME - ROCK UNIT	BIOSTRATIGRAPHIC ZONE	FOSSIL CHARACTER			SECTION METERS	GRAPHIC LITHOLOGY	DRILLING DISTURBANCE STRUCTURES	SAMPLES	LITHOLOGIC DESCRIPTION				
		FORAMINIFERS	NANNOFOSSILS	RADIOLARIANS						DIATOMS			
late Maestrichtian	MCx11 (<i>Myarconis</i> zone) (F)	AG	AM						<p>NANNOFOSSIL CHALK White (N9) Firm, massive and homogeneous chalk</p> <p>SMEAR SLIDE SUMMARY (%): 3, 70 D</p> <p>Texture: Mud 100 Composition: Calc. nannofossils 100</p>				
		AG	AM										
		AG	AM										

SITE 548		HOLE A		CORE 32		CORED INTERVAL 500.0–509.5 m								
TIME - ROCK UNIT	BIOSTRATIGRAPHIC ZONE	FOSSIL CHARACTER			SECTION METERS	GRAPHIC LITHOLOGY	DRILLING DISTURBANCE STRUCTURES	SAMPLES	LITHOLOGIC DESCRIPTION					
		FORAMINIFERS	NANNOFOSSILS	RADIOLARIANS						DIATOMS				
middle to early Maestrichtian	± lower MCx10 to MCx9 (<i>Uxert-/Abouzi</i> zone) (F)	AG	AM						<p>NANNOFOSSIL CHALK Yellowish-gray (5Y 8/1) mottled by burrows filled with white (N9) chalk, slightly pyritized; pyrite also around burrows and disseminated lightly throughout core Brownish streaks (Fe7Mn7) in Section 1, 2–3 and 146–148 cm; Section 2, 2–4 cm; and Section 4, 65–67 cm Section 2–Section 3, 44 cm have large chunks of calcite and some mollusc shells dispersed throughout</p> <p>SMEAR SLIDE SUMMARY (%): 1, 100 D</p> <p>Texture: Sand 5 Mud 95 Composition: Carbonate unspec. 10 Foraminifers 5 Calc. nannofossils 80</p>					
		AG	AM											
		AG	AM											
		AG	AP											

SITE 548		HOLE A		CORE 31		CORED INTERVAL 490.5–500.0 m							
TIME - ROCK UNIT	BIOSTRATIGRAPHIC ZONE	FOSSIL CHARACTER			SECTION METERS	GRAPHIC LITHOLOGY	DRILLING DISTURBANCE STRUCTURES	SAMPLES	LITHOLOGIC DESCRIPTION				
		FORAMINIFERS	NANNOFOSSILS	RADIOLARIANS						DIATOMS			
middle Maestrichtian	± lower MCx10 (<i>gasperi</i> zone) (F)	AG	AM						<p>NANNOFOSSIL CHALK (30% unspecified calcareous) Firm massive and homogeneous White (N9), moderate orange pink (5YR 8/4), and yellowish green (5Y 8/1) Sections 2 and 3 burrow-mottled, yellowish gray with white burrow-filling with black pyritic streaks Mud unspecified calcareous sediment, silt-sized</p> <p>SMEAR SLIDE SUMMARY (%): 1, 135 2, 60 D D</p> <p>Texture: Sand 10 – Mud 90 100 Composition: Carbonate unspec. 5 30 Foraminifers 5 – Calc. nannofossils 90 70</p>				
		AG	AM										
		AG	AP										

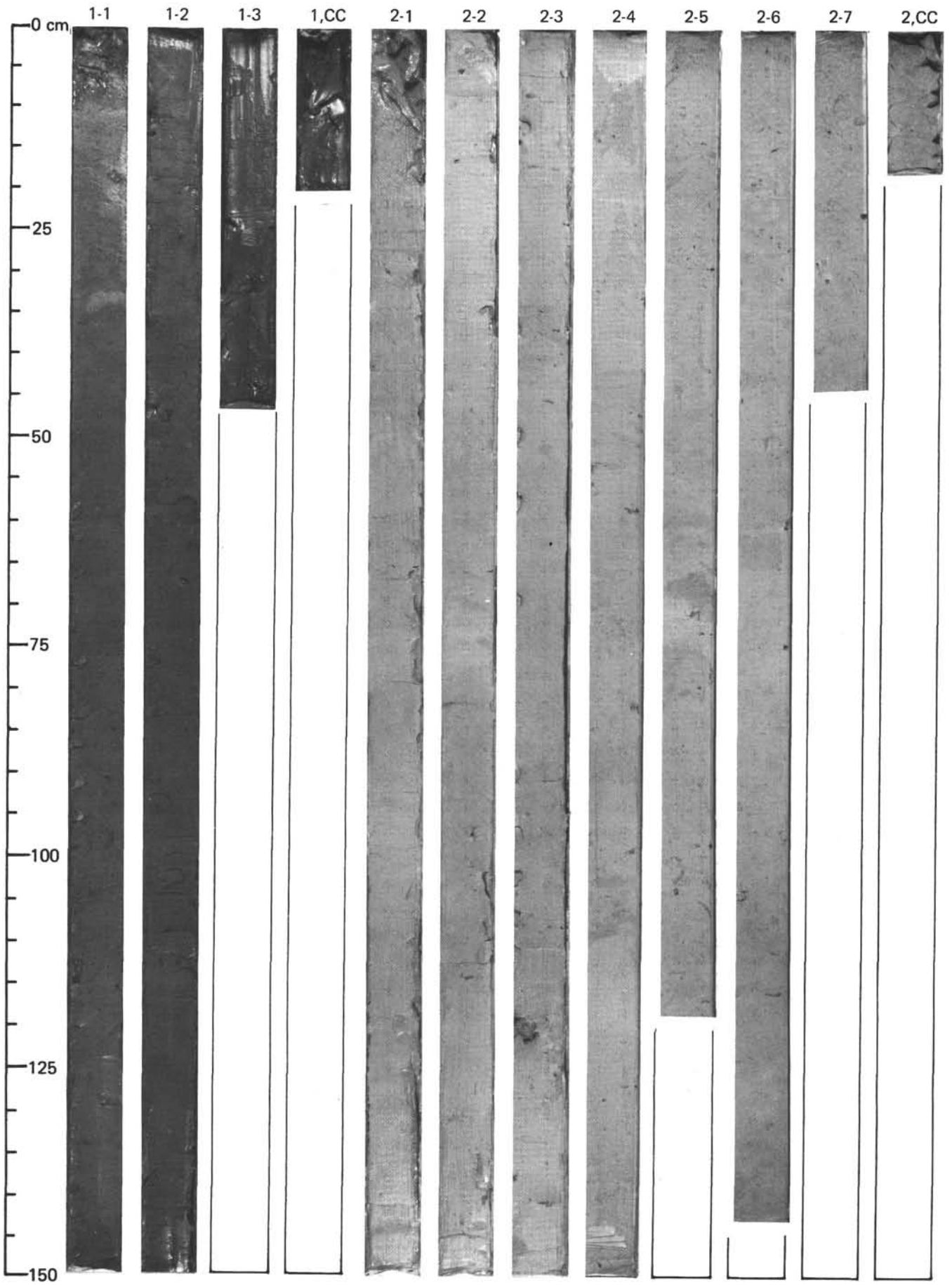


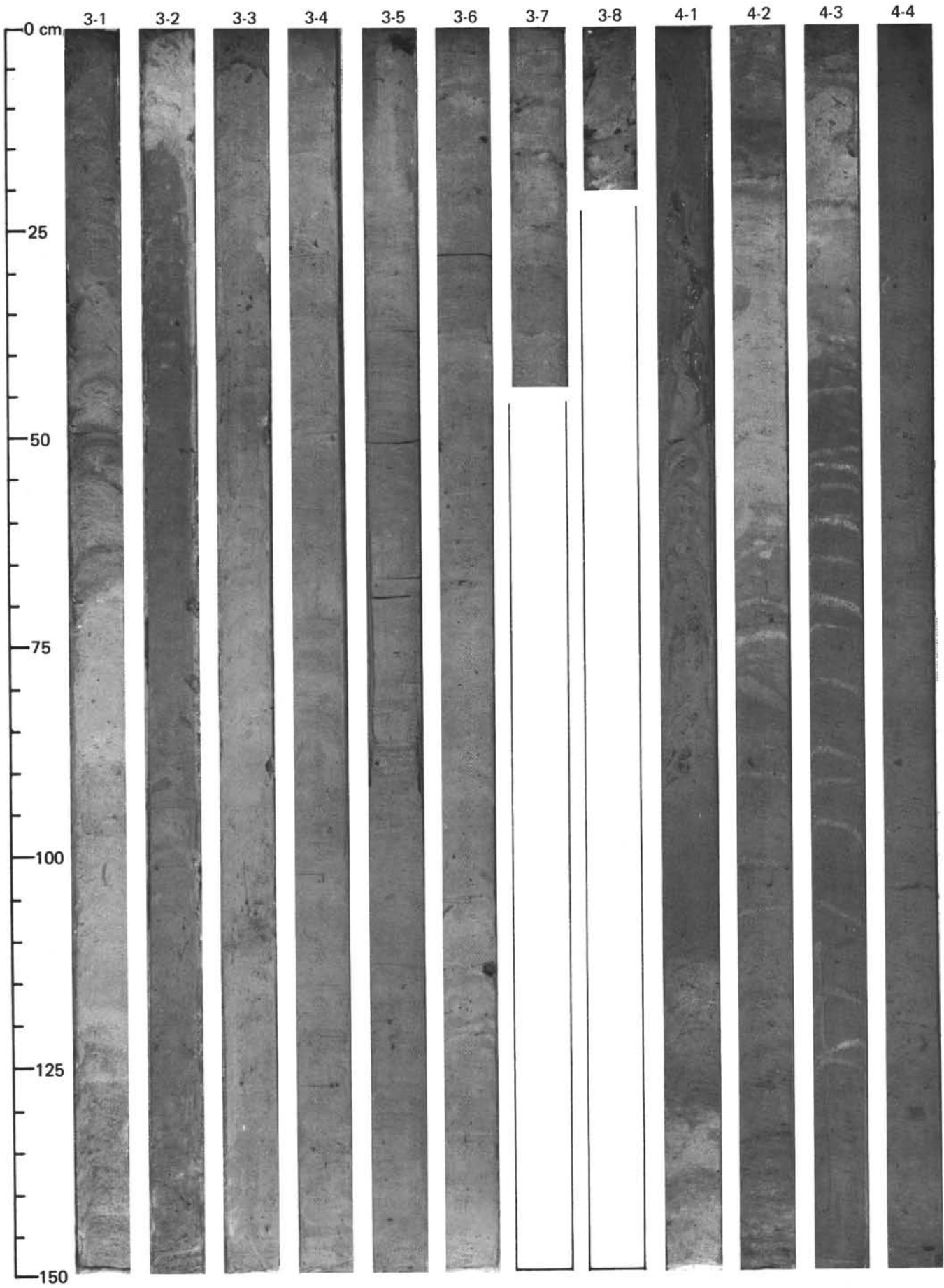
SITE 548		HOLE A		CORE 35		CORED INTERVAL		528.5–535.5 m	
TIME – ROCK UNIT	BIOSTRATIGRAPHIC ZONE	FOSSIL CHARACTER			SECTION METERS	GRAPHIC LITHOLOGY	DRILLING DISTURBANCE STRUCTURES	SAMPLES	LITHOLOGIC DESCRIPTION
		FORAMINIFERS	NANNOFOSSILS	RADIOLARIANS					
late Campanian	MC7-8 <i>Inflavastartus</i> / <i>ovata</i> and <i>calcarata</i> zones (F) late Campanian (N) <i>Terratibius trifidus</i> (N)	AG	AM		0.5 1 1.0 2			*	<p>FORAM-NANNOFOSSIL CHALK Mottled very pale orange (10YR 8/2) and very light gray (N8) chalk; large burrows, 1–2 cm</p> <p>SMEAR SLIDE SUMMARY (%): 1, 30 D</p> <p>Texture: Sand 10 Mud 90</p> <p>Composition: Carbonate unsp. Tr Foraminifera 20 Calc. nannofossils 80</p>

SITE 548		HOLE A		CORE 38		CORED INTERVAL		347.0–551.0 m	
TIME – ROCK UNIT	BIOSTRATIGRAPHIC ZONE	FOSSIL CHARACTER			SECTION METERS	GRAPHIC LITHOLOGY	DRILLING DISTURBANCE STRUCTURES	SAMPLES	LITHOLOGIC DESCRIPTION
		FORAMINIFERS	NANNOFOSSILS	RADIOLARIANS					
					0.5 1 1.0 2				<p>BASEMENT ROCK Metaquartzite(?) Black (N1)</p> <p>← Contains scattered fragments of black shale</p>

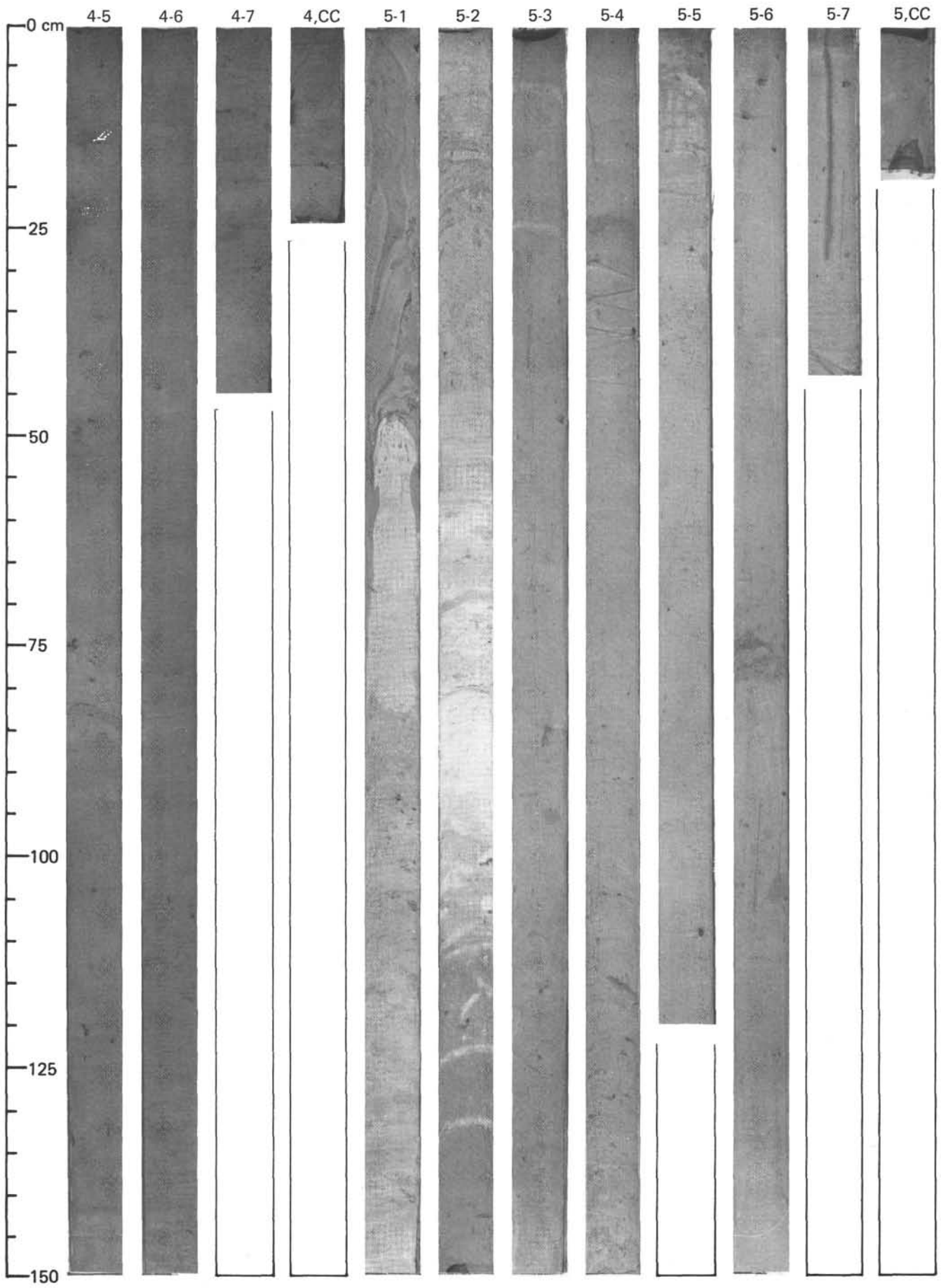
SITE 548		HOLE A		CORE 36		CORED INTERVAL		535.5–538.0 m	
TIME – ROCK UNIT	BIOSTRATIGRAPHIC ZONE	FOSSIL CHARACTER			SECTION METERS	GRAPHIC LITHOLOGY	DRILLING DISTURBANCE STRUCTURES	SAMPLES	LITHOLOGIC DESCRIPTION
		FORAMINIFERS	NANNOFOSSILS	RADIOLARIANS					
					1				<p>BASEMENT ROCK Metaquartzite(?) Black (N1)</p>

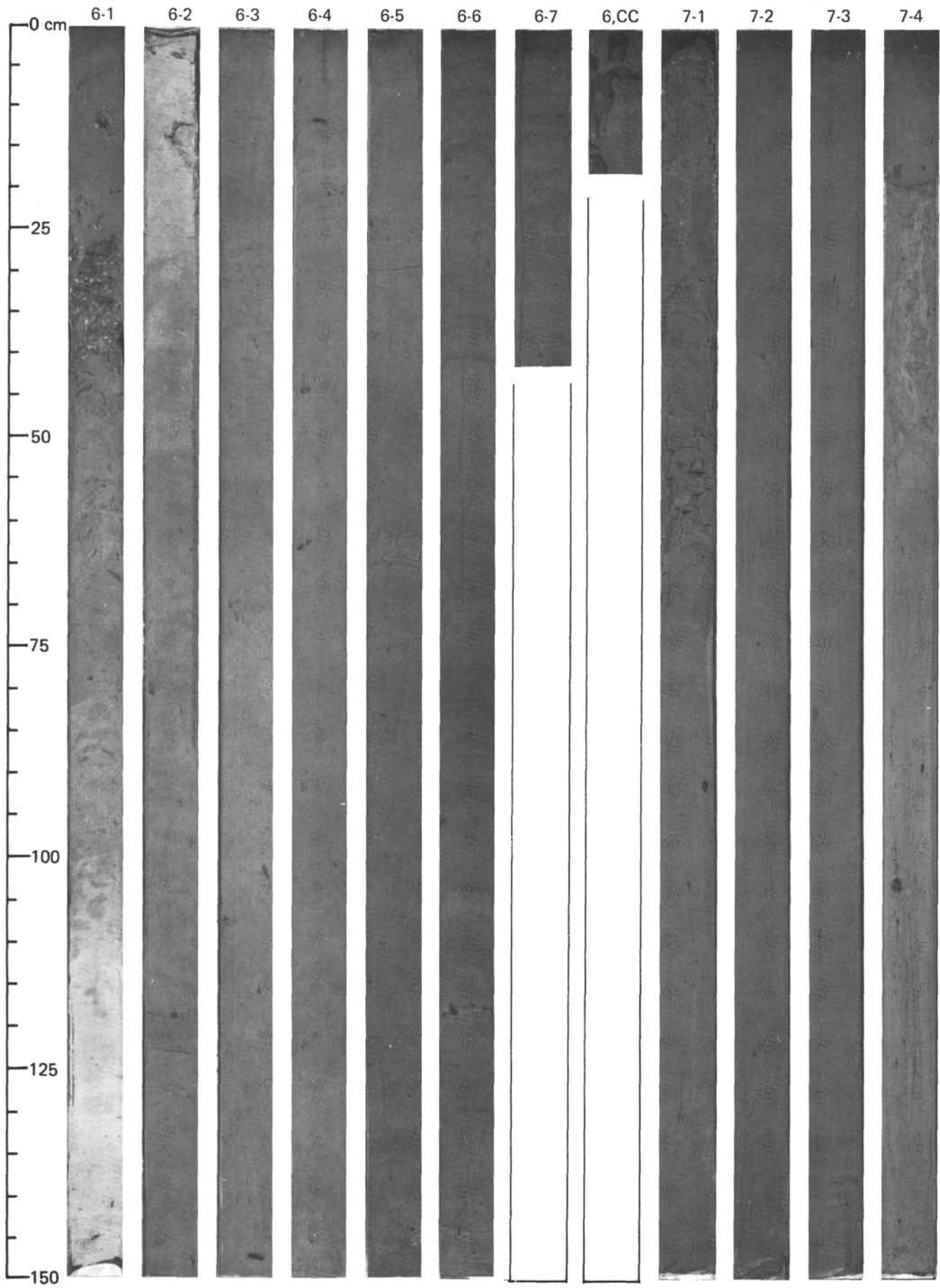
SITE 548		HOLE A		CORE 37		CORED INTERVAL		538.0–547.0 m	
TIME – ROCK UNIT	BIOSTRATIGRAPHIC ZONE	FOSSIL CHARACTER			SECTION METERS	GRAPHIC LITHOLOGY	DRILLING DISTURBANCE STRUCTURES	SAMPLES	LITHOLOGIC DESCRIPTION
		FORAMINIFERS	NANNOFOSSILS	RADIOLARIANS					
					1				<p>BASEMENT ROCK Metaquartzite(?) Black (N1)</p>



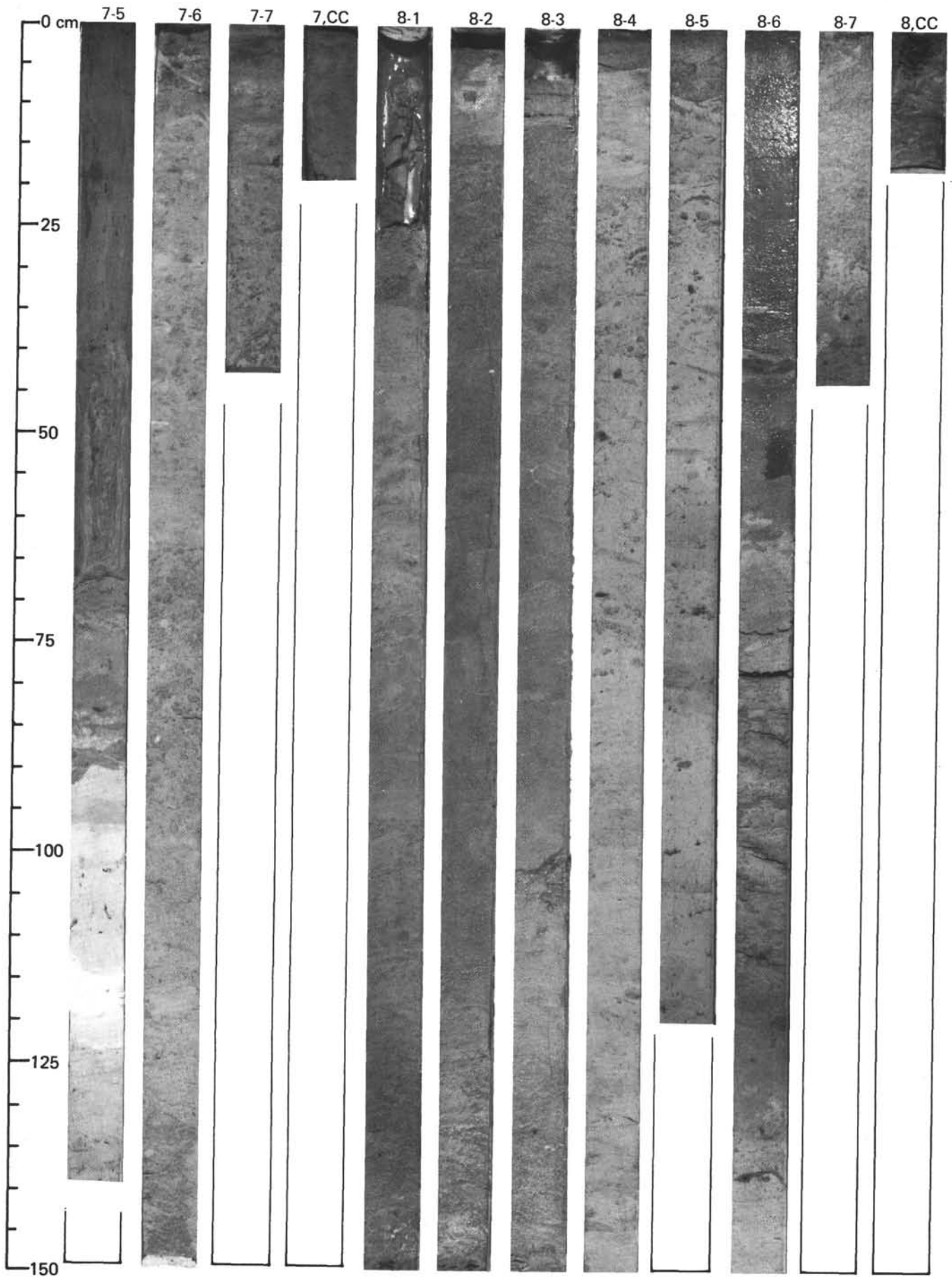


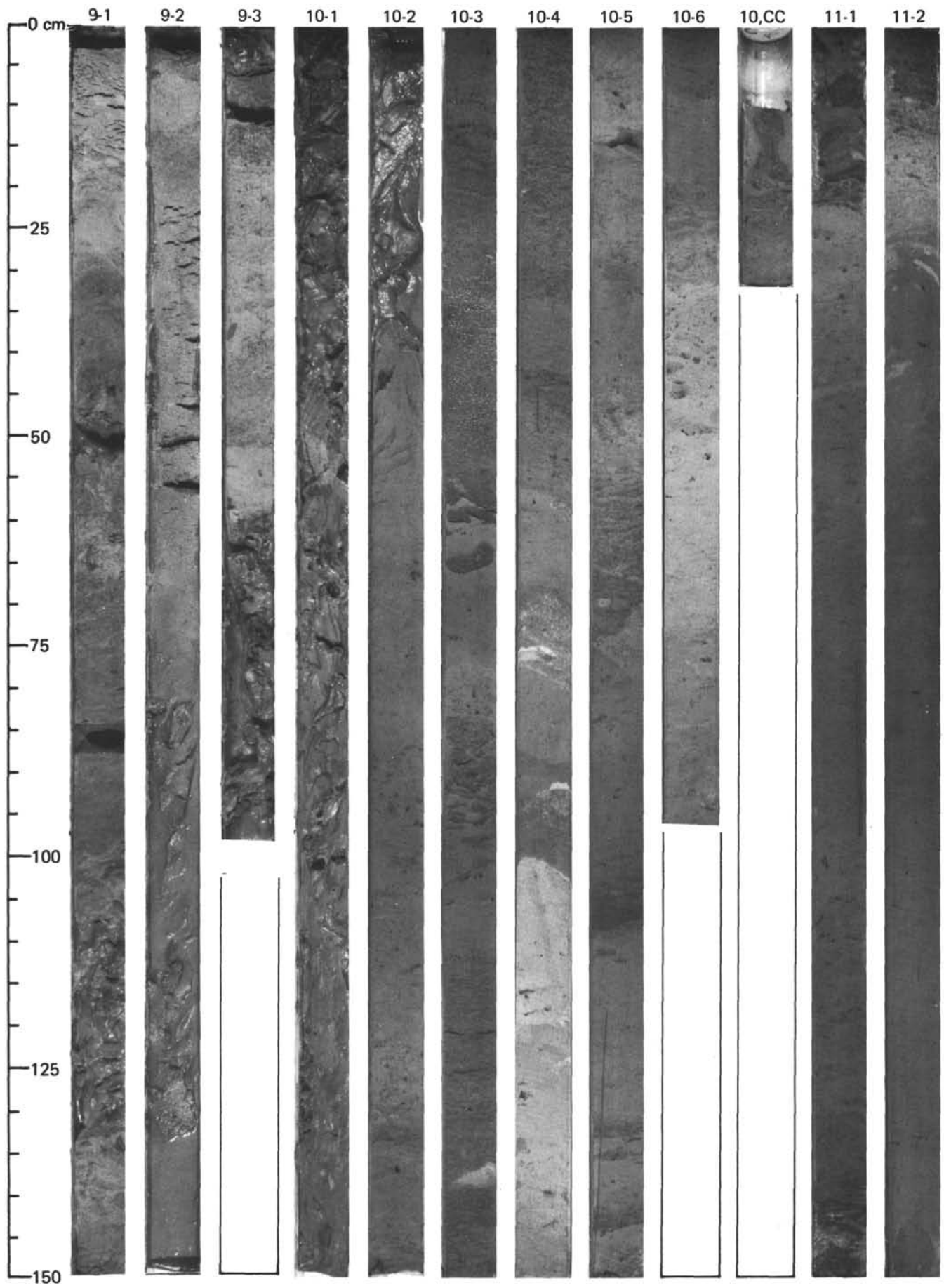
SITE 548 (HOLE 548)

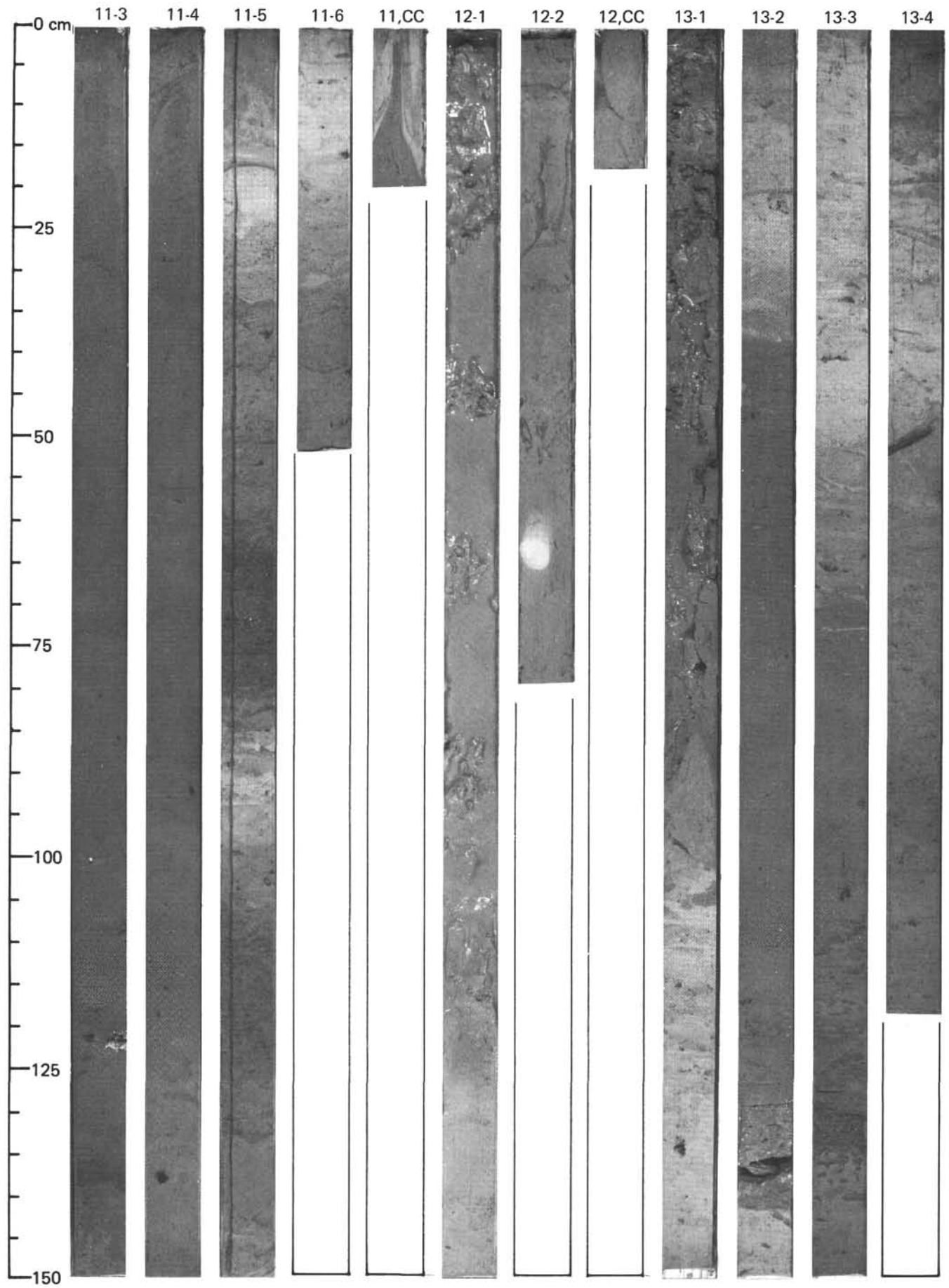


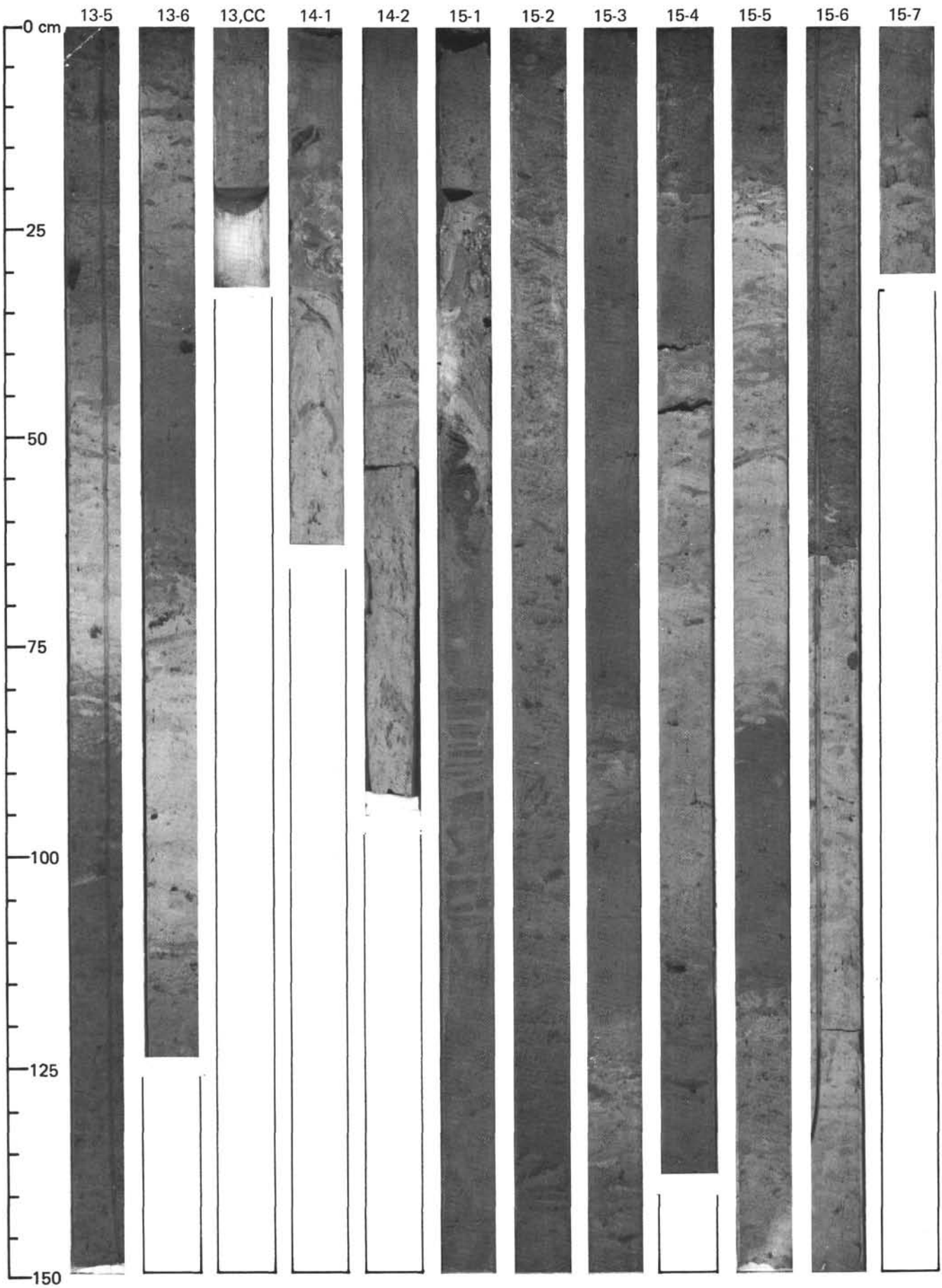


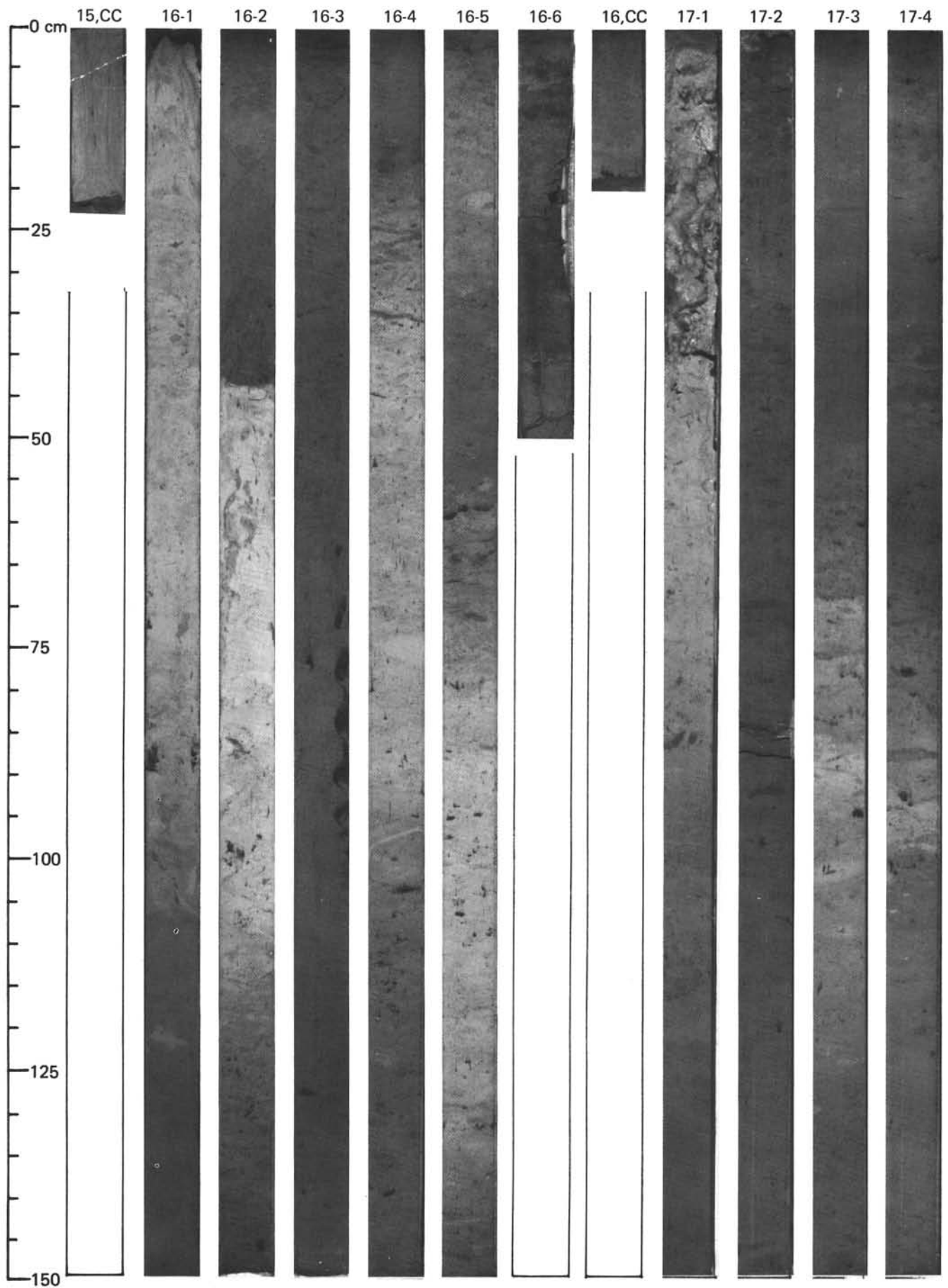
SITE 548 (HOLE 548)

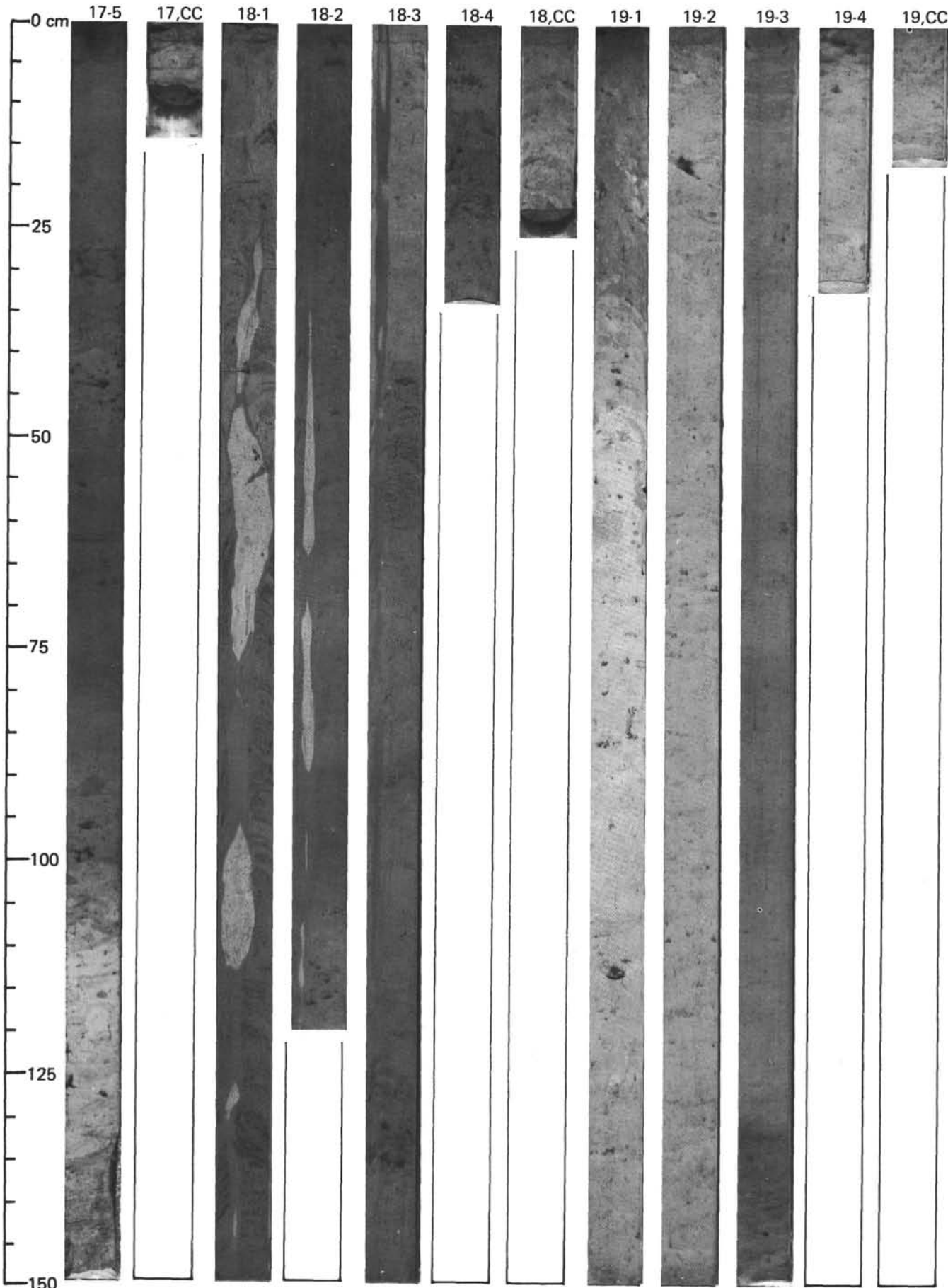




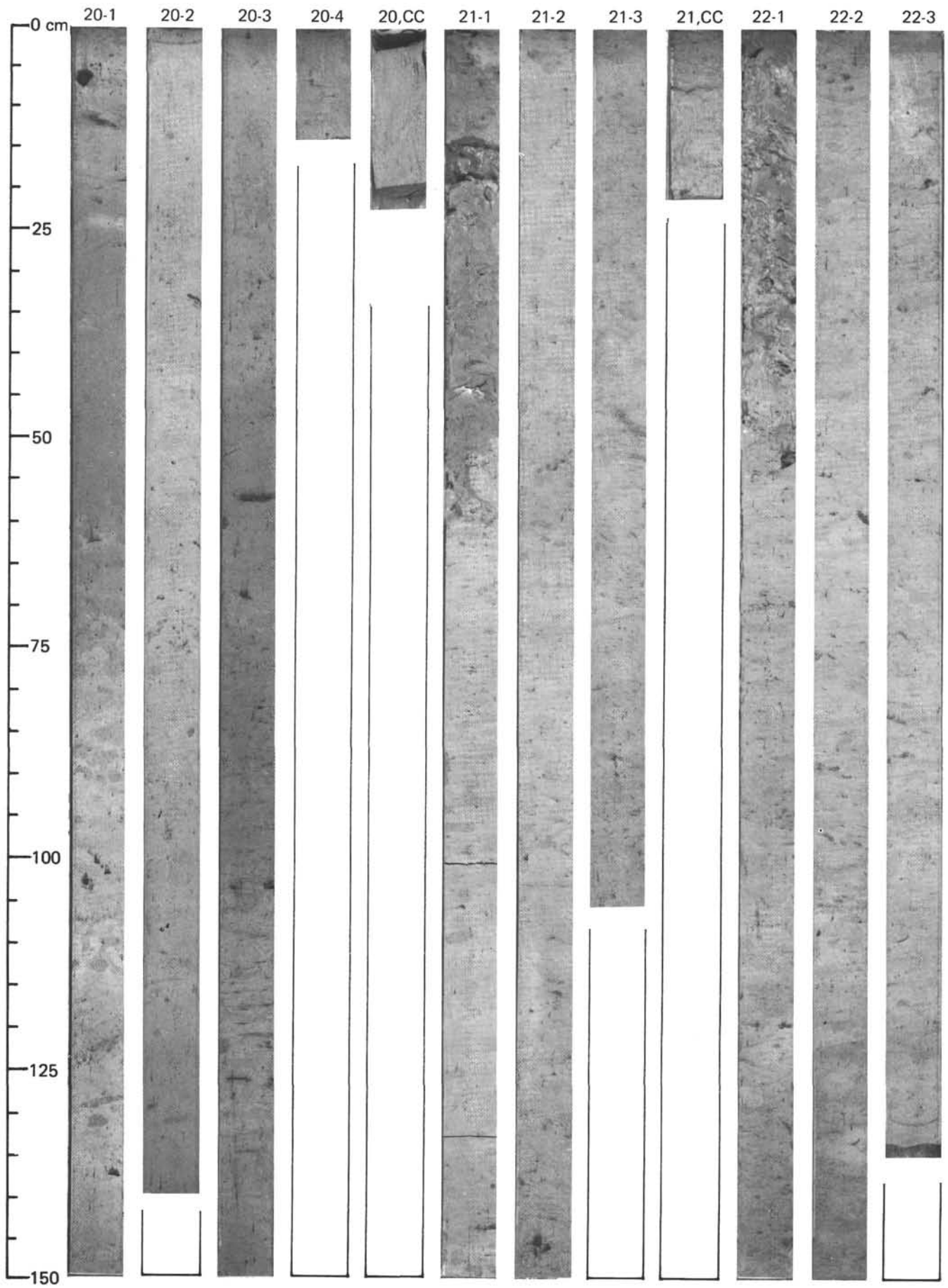


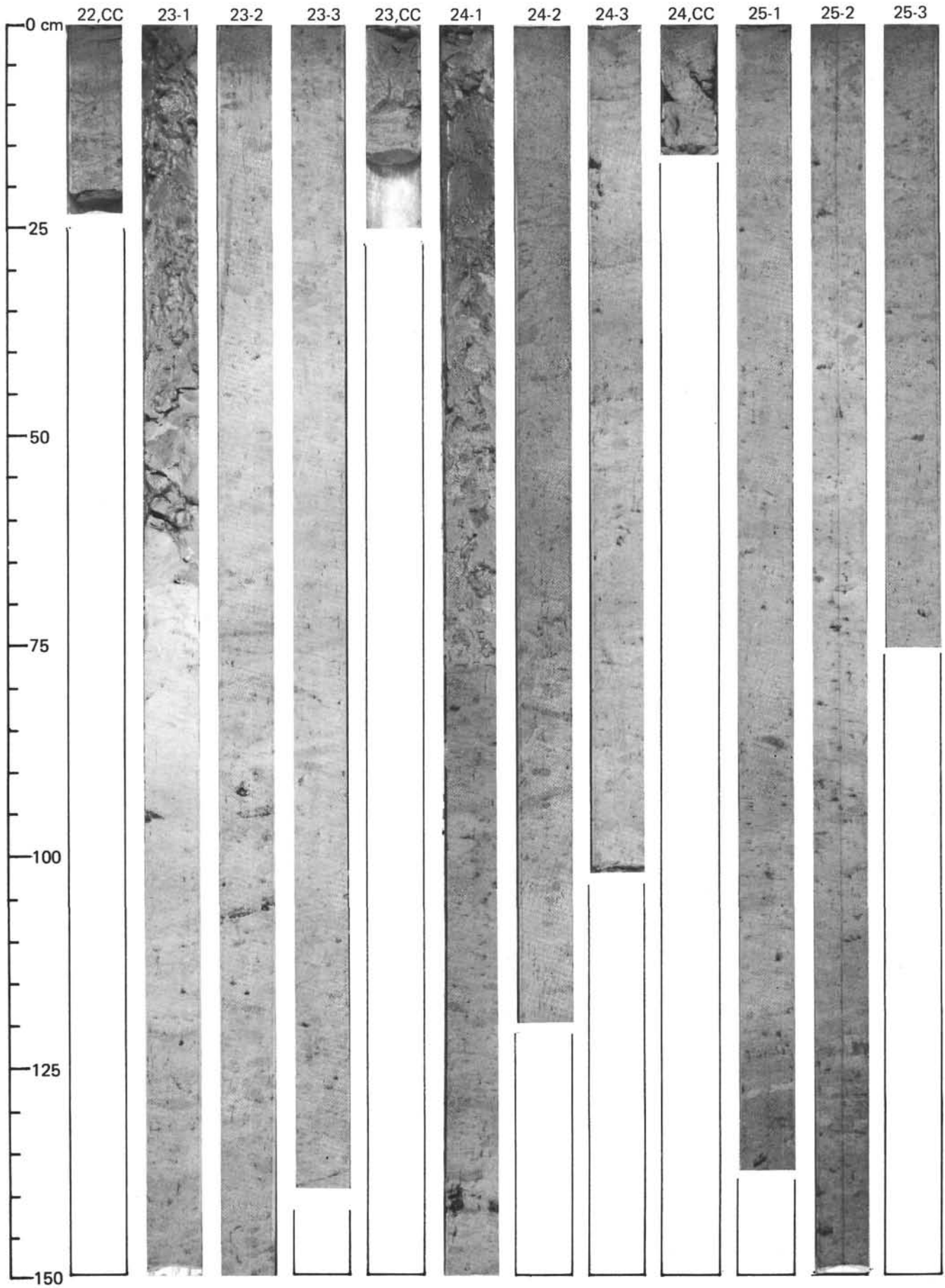




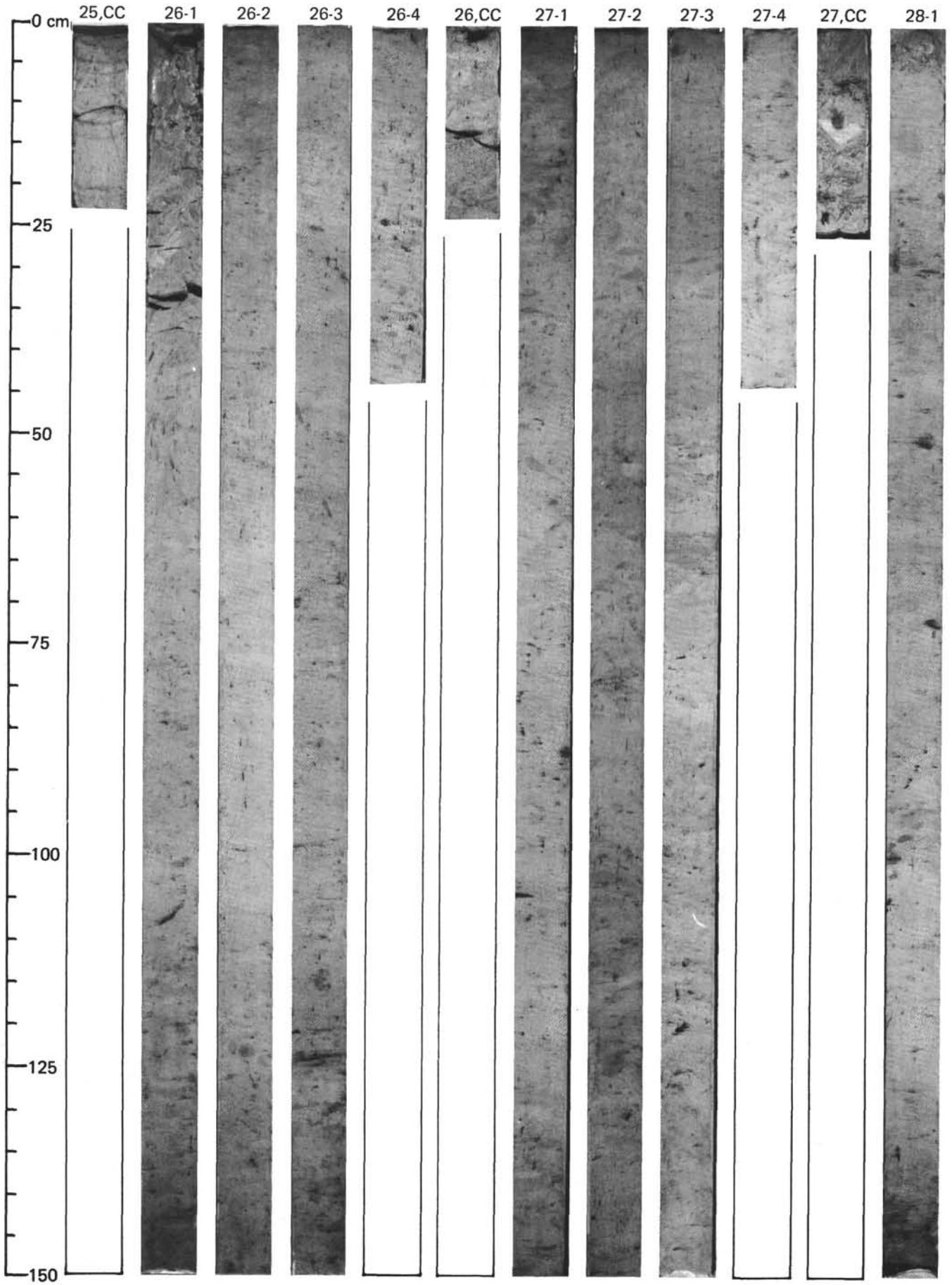


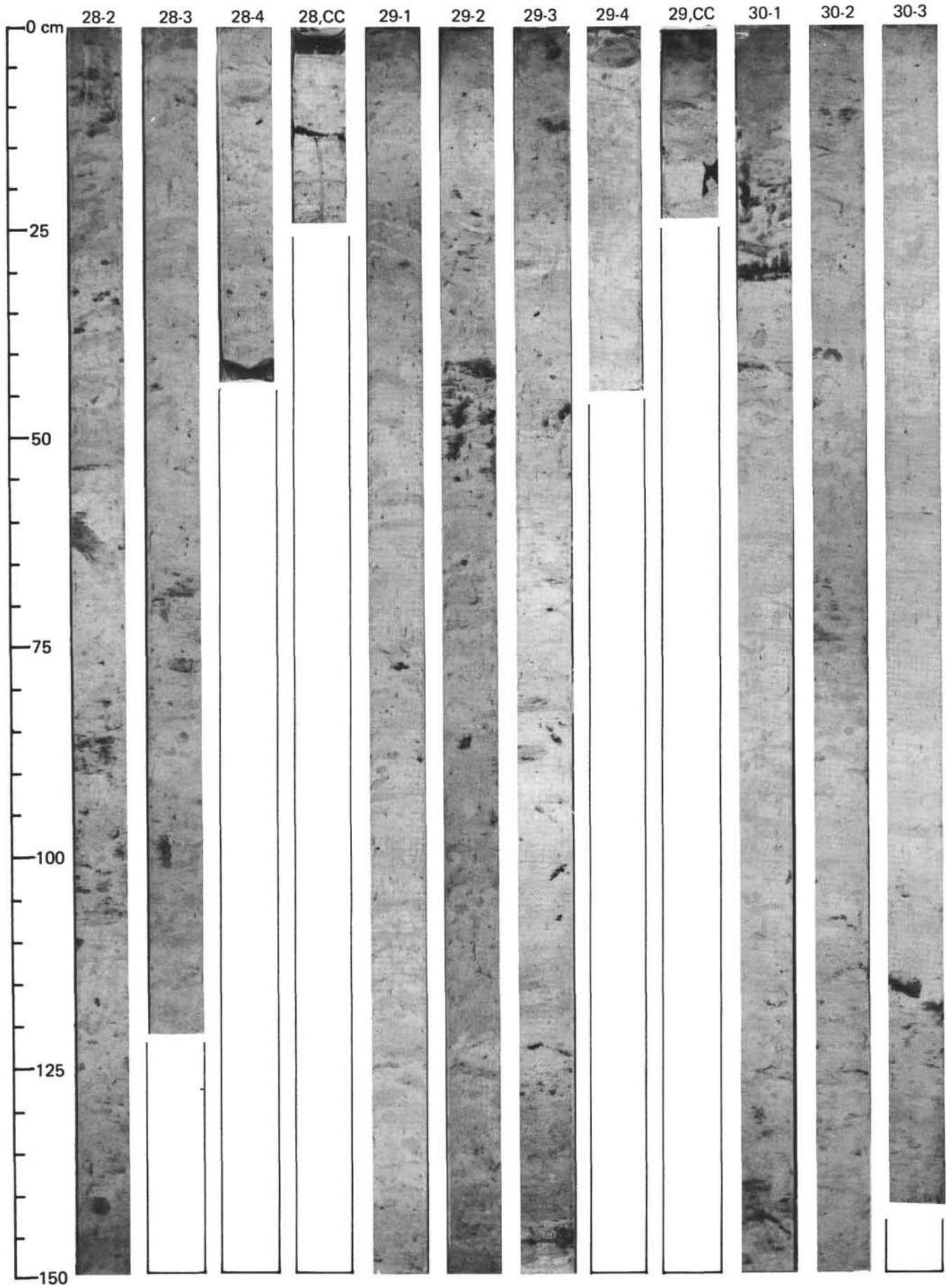
SITE 548 (HOLE 548)

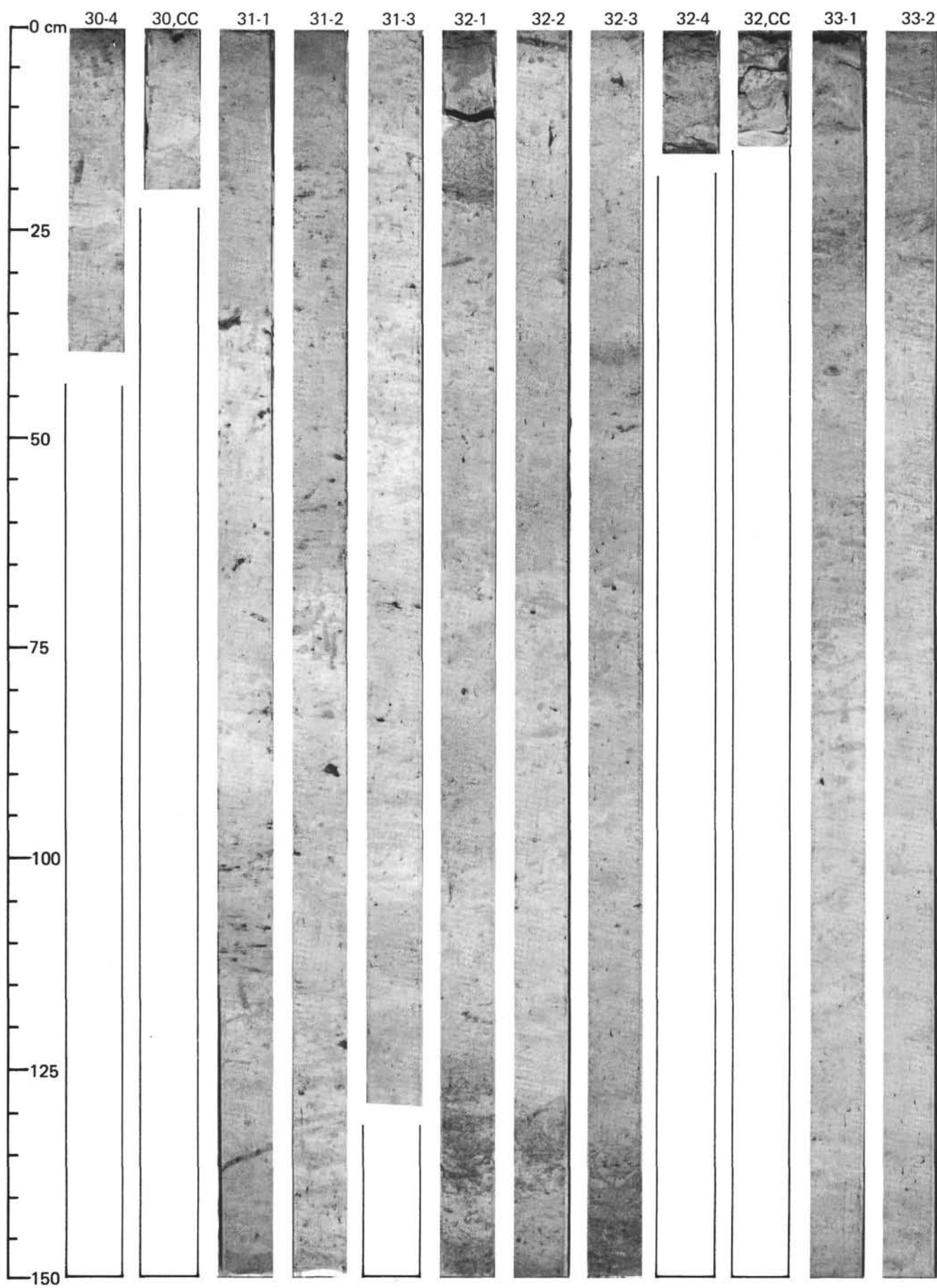


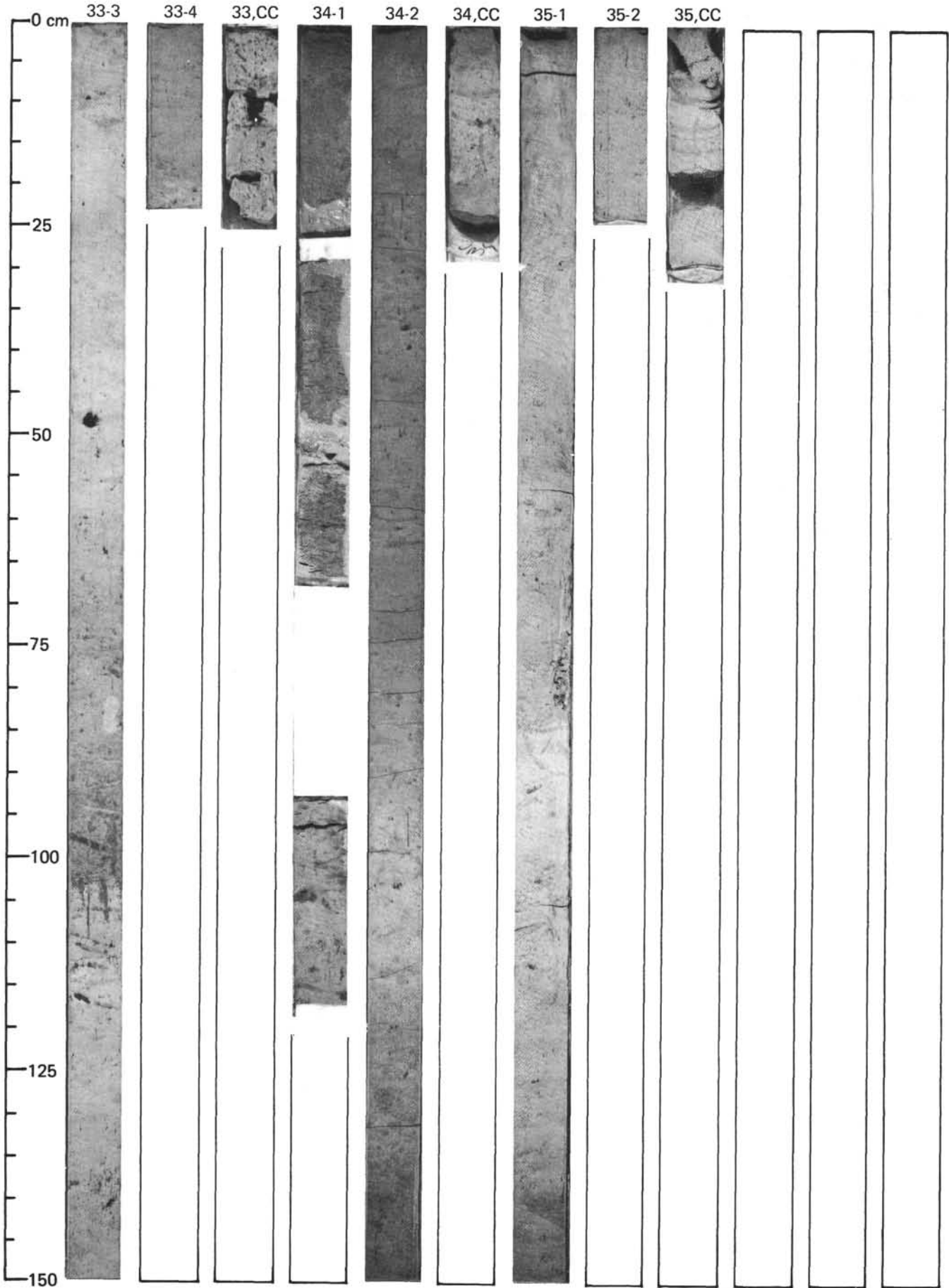


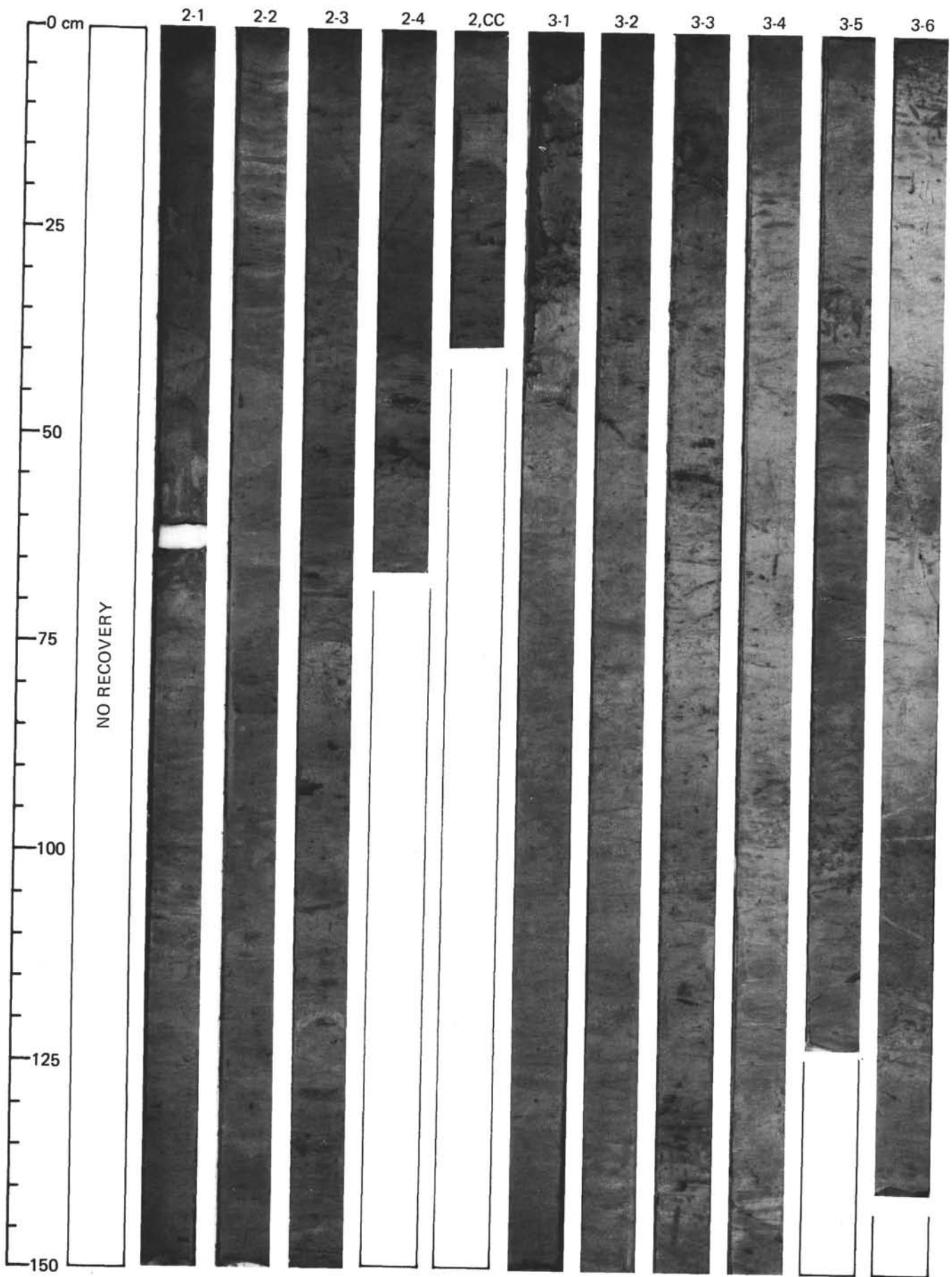
SITE 548 (HOLE 548)

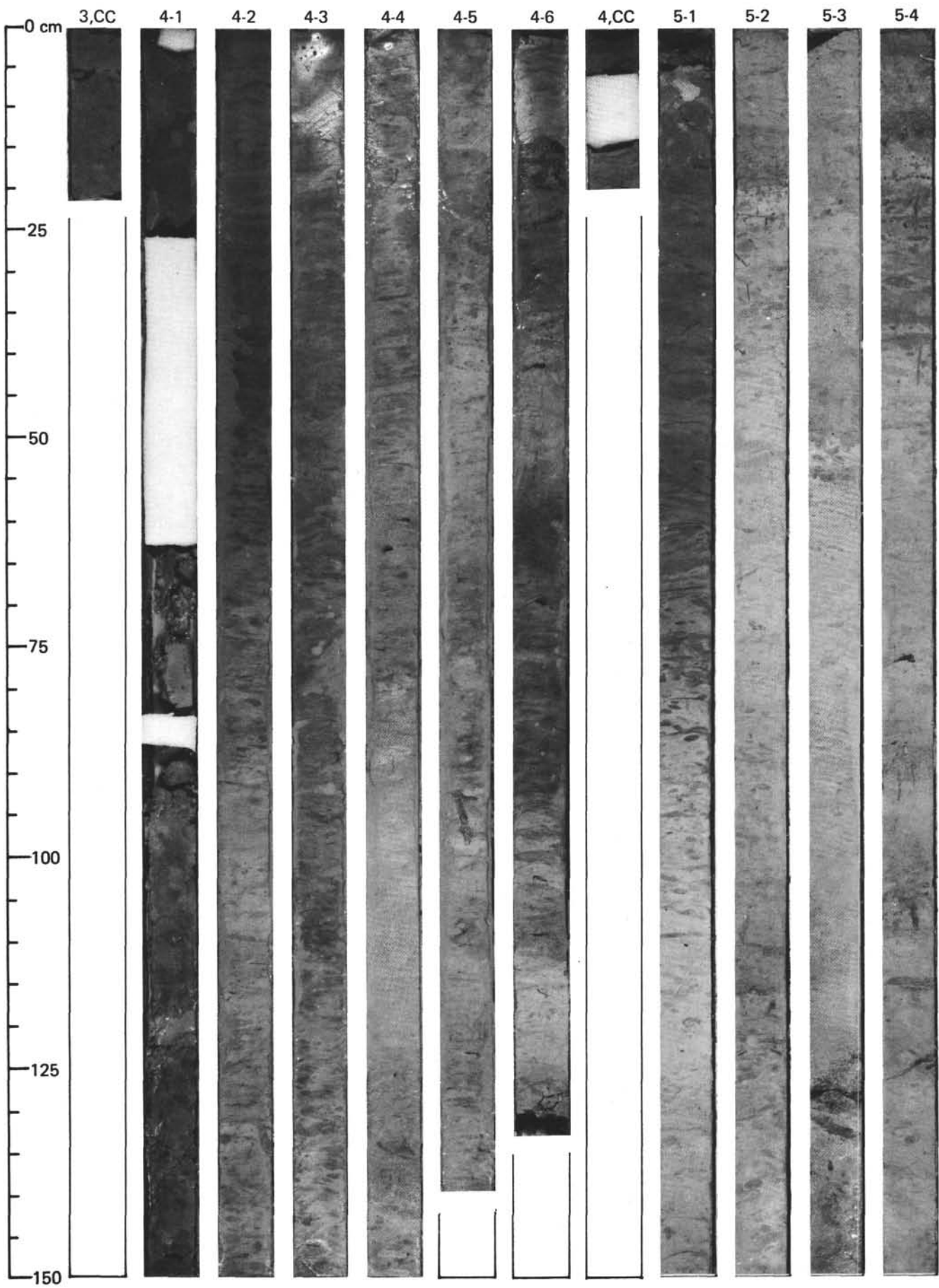




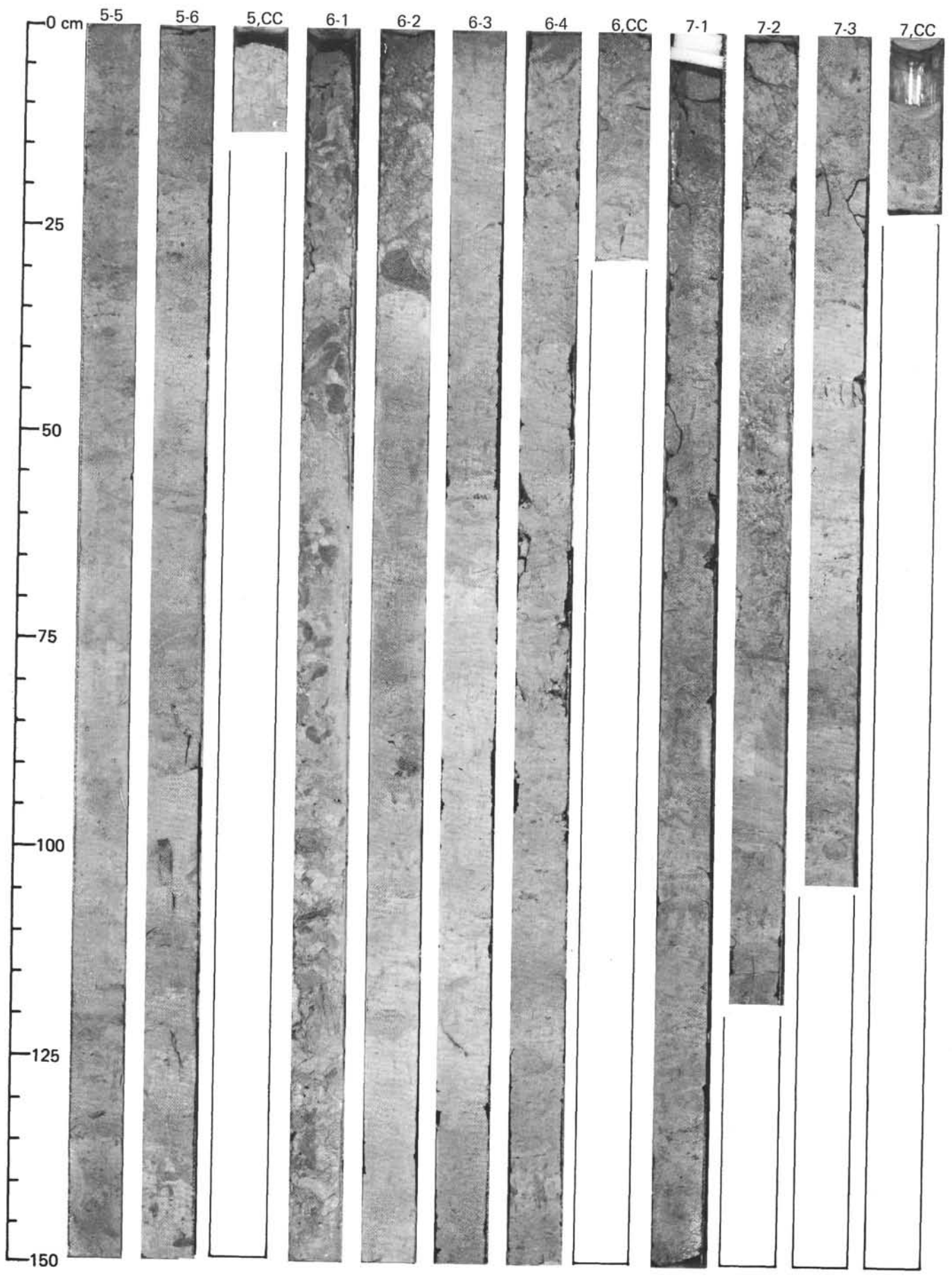


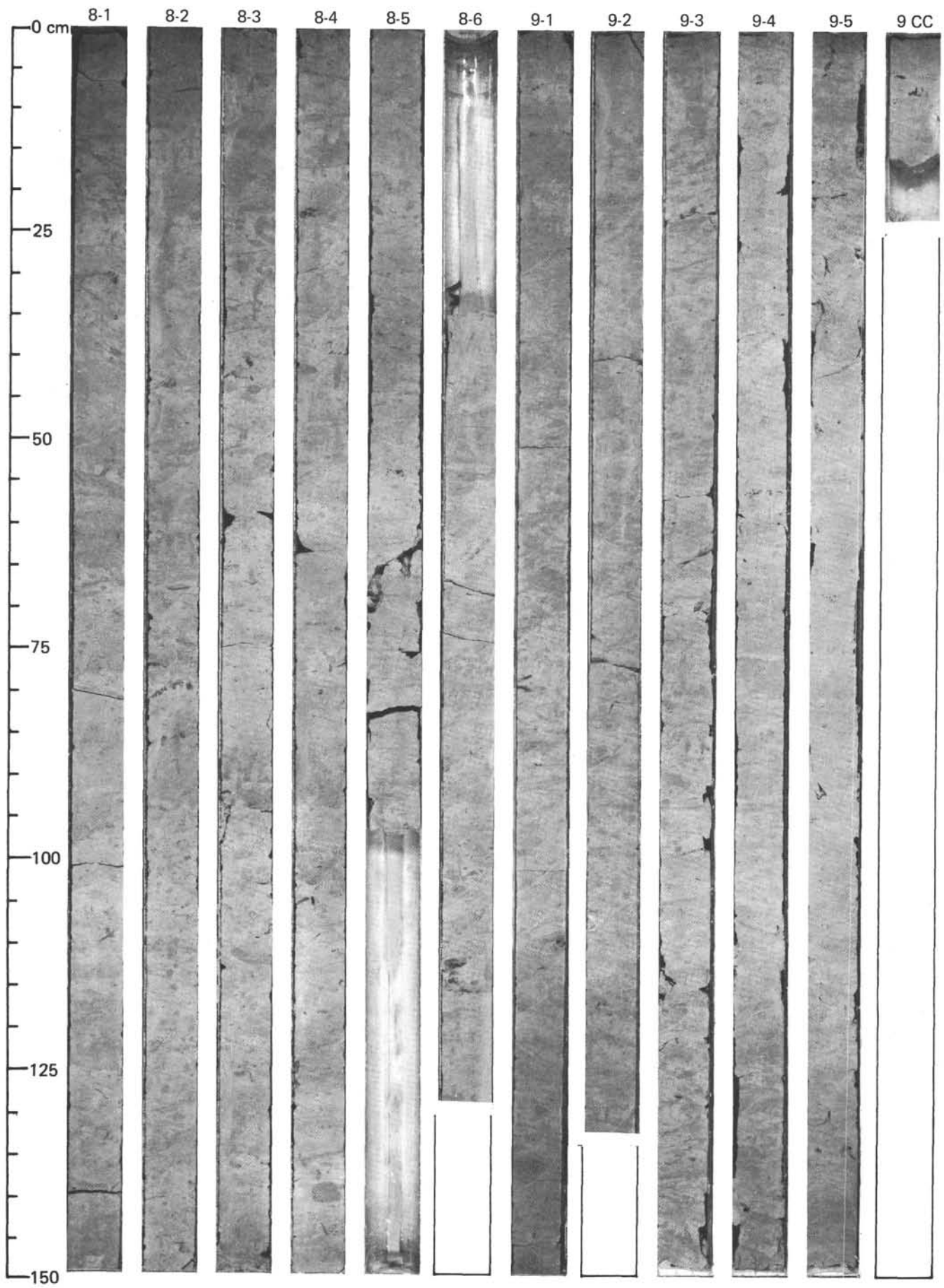


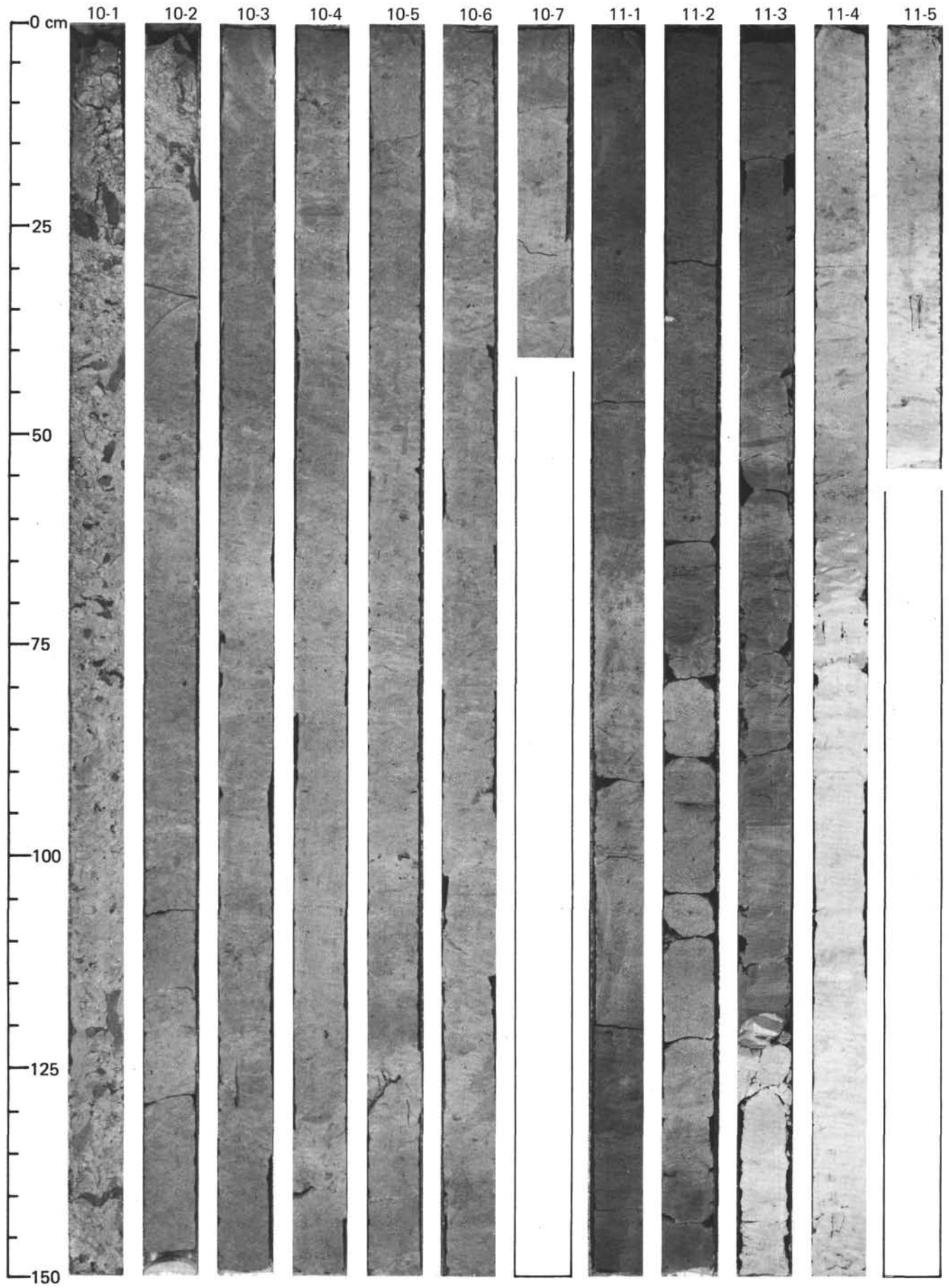


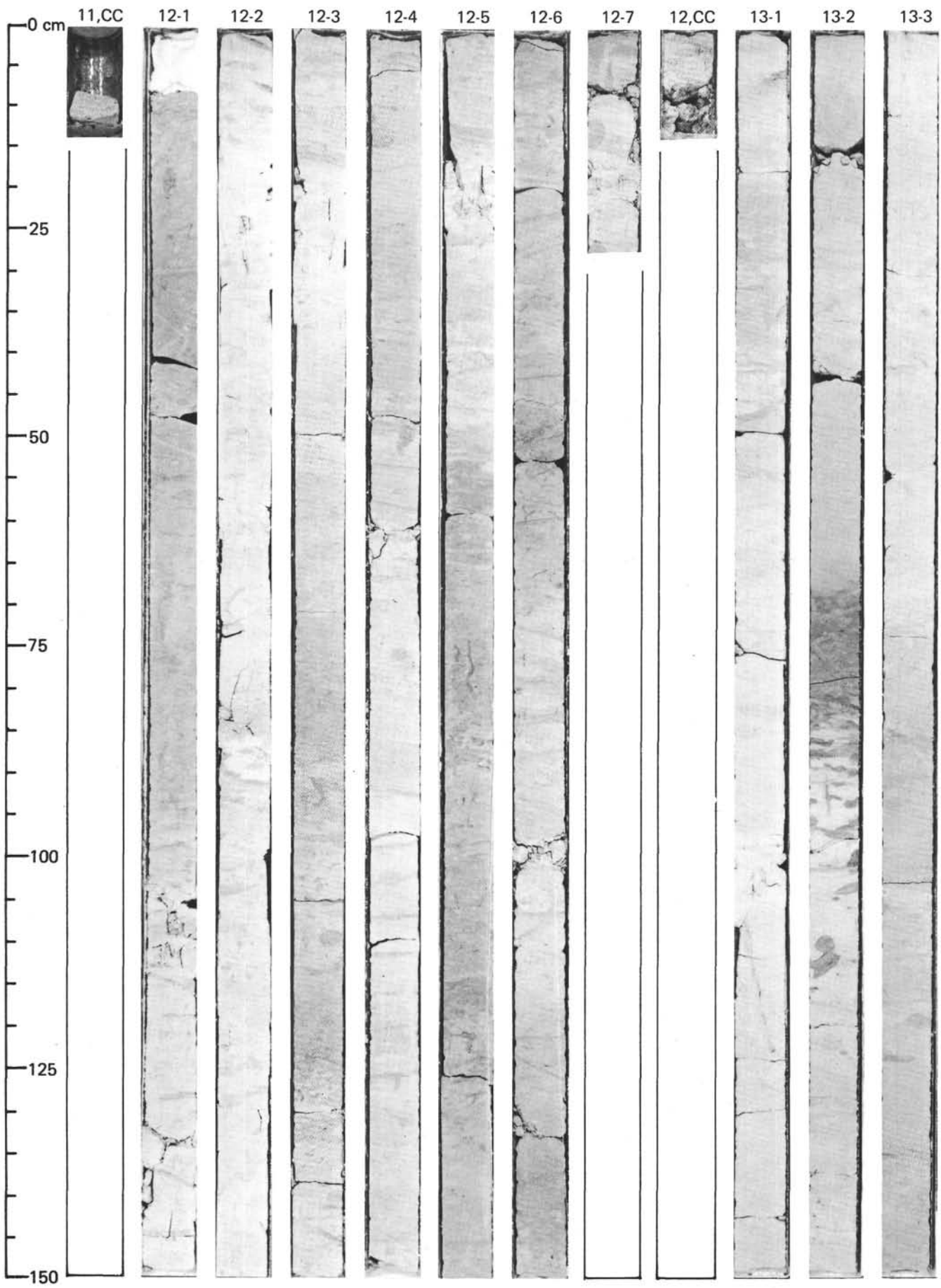


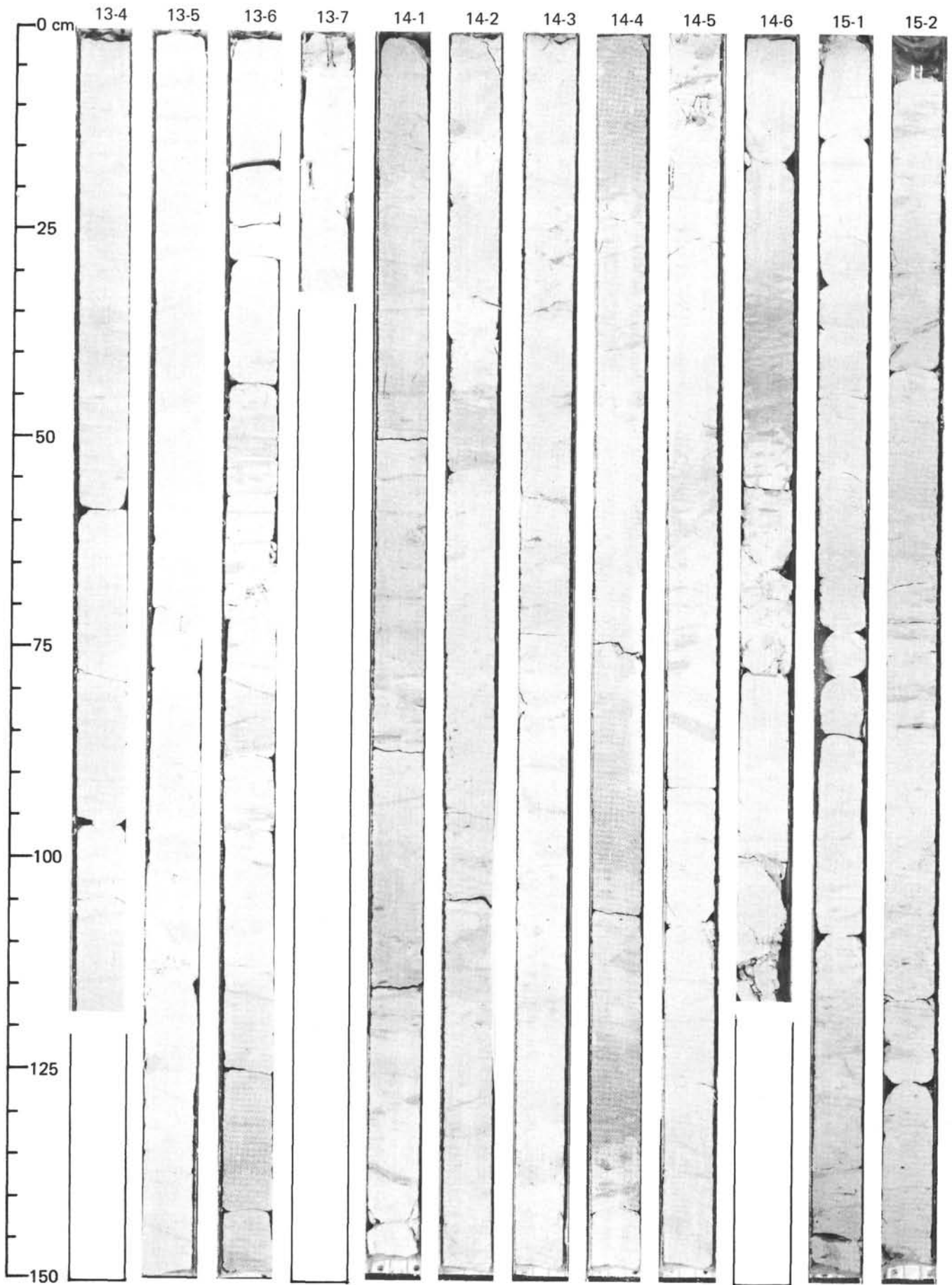
SITE 548 (HOLE 548A)

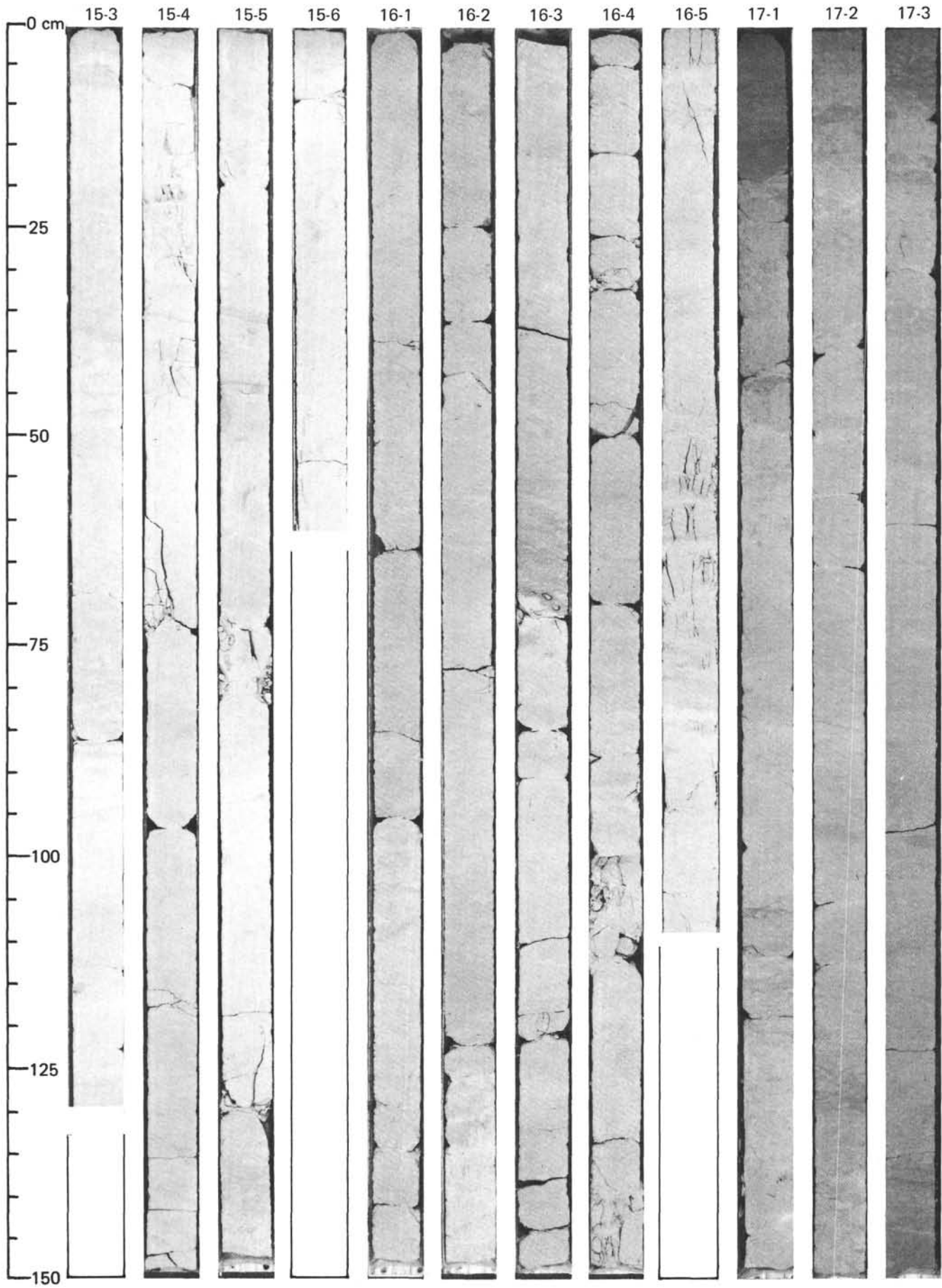


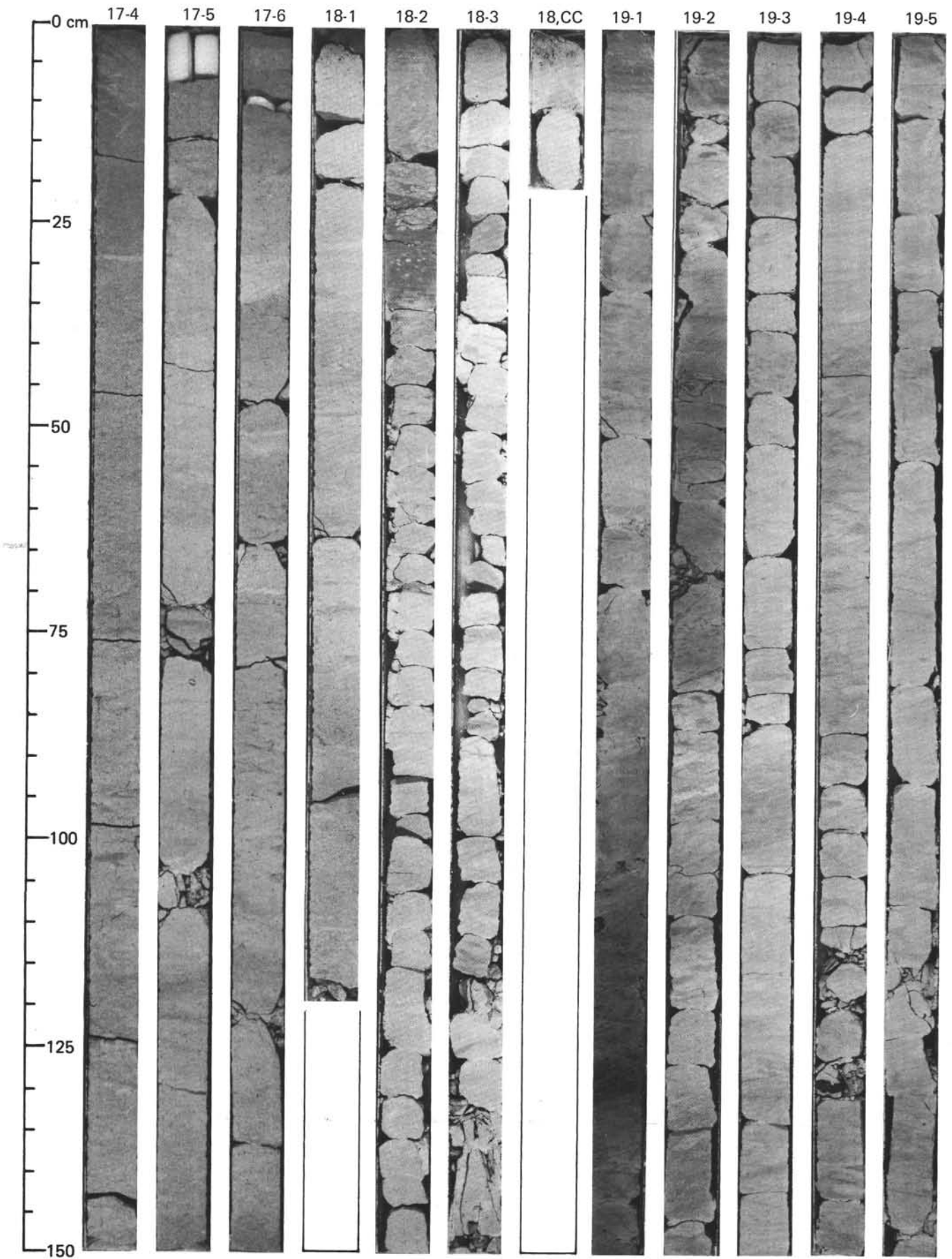


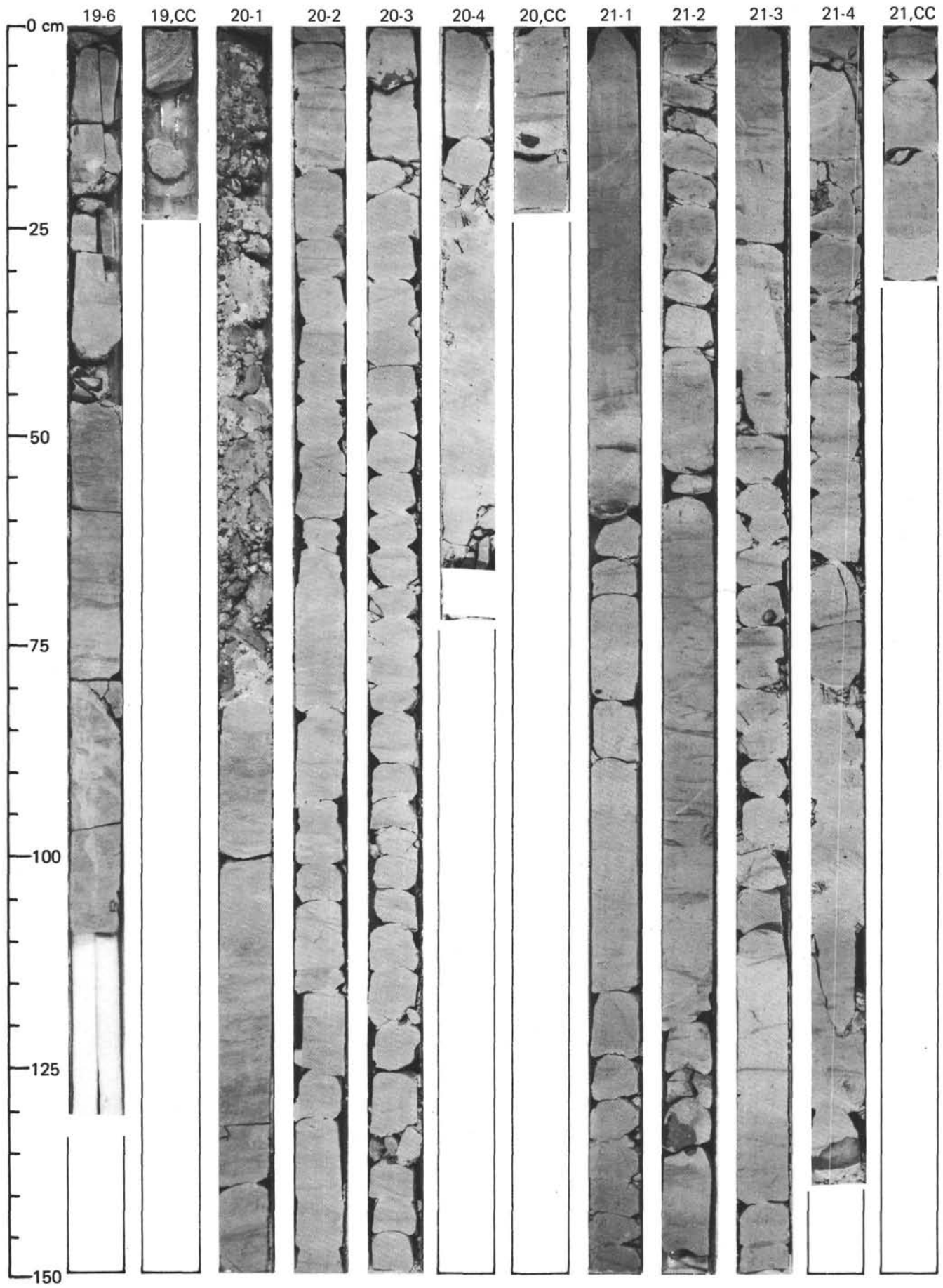




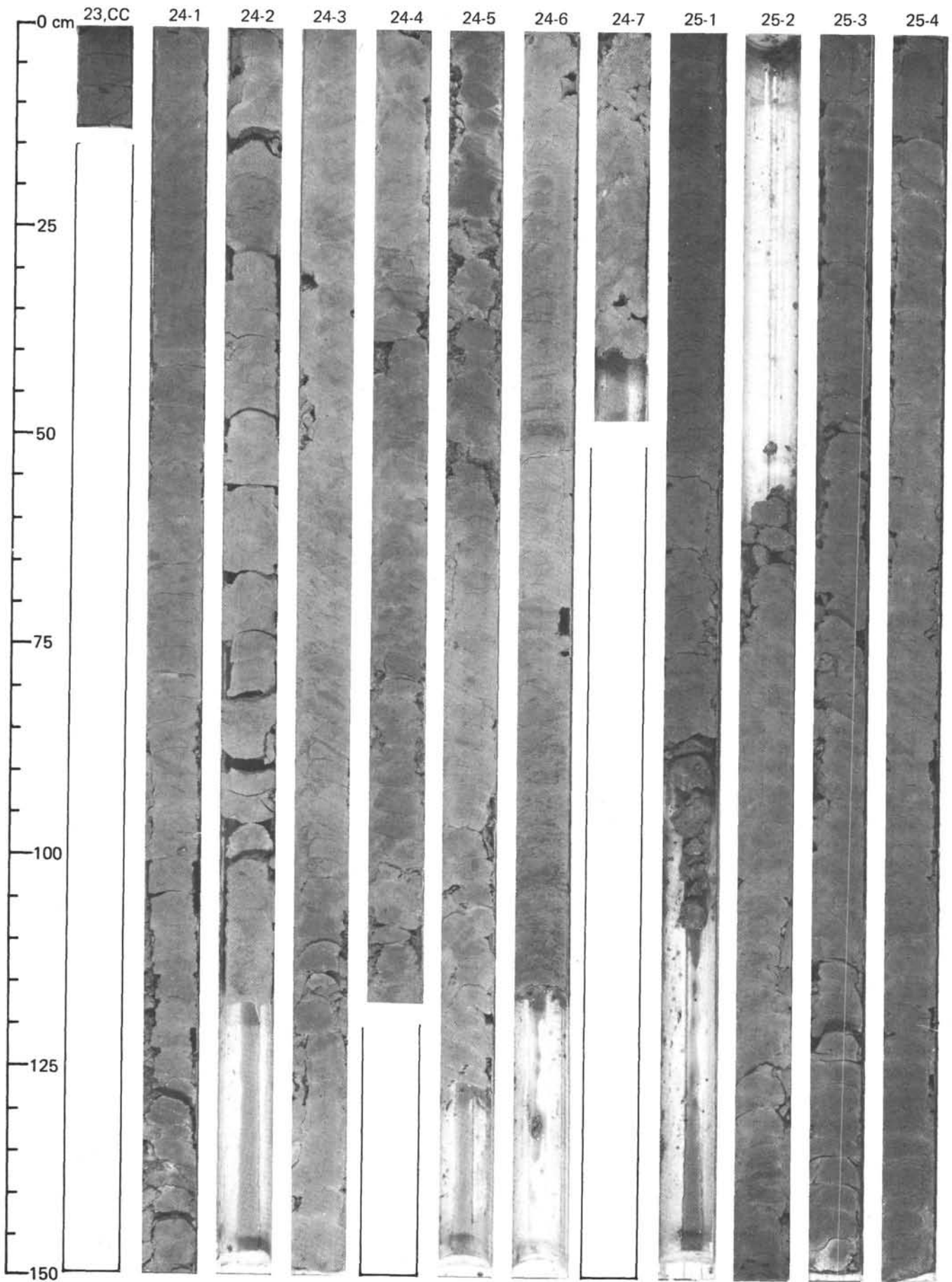




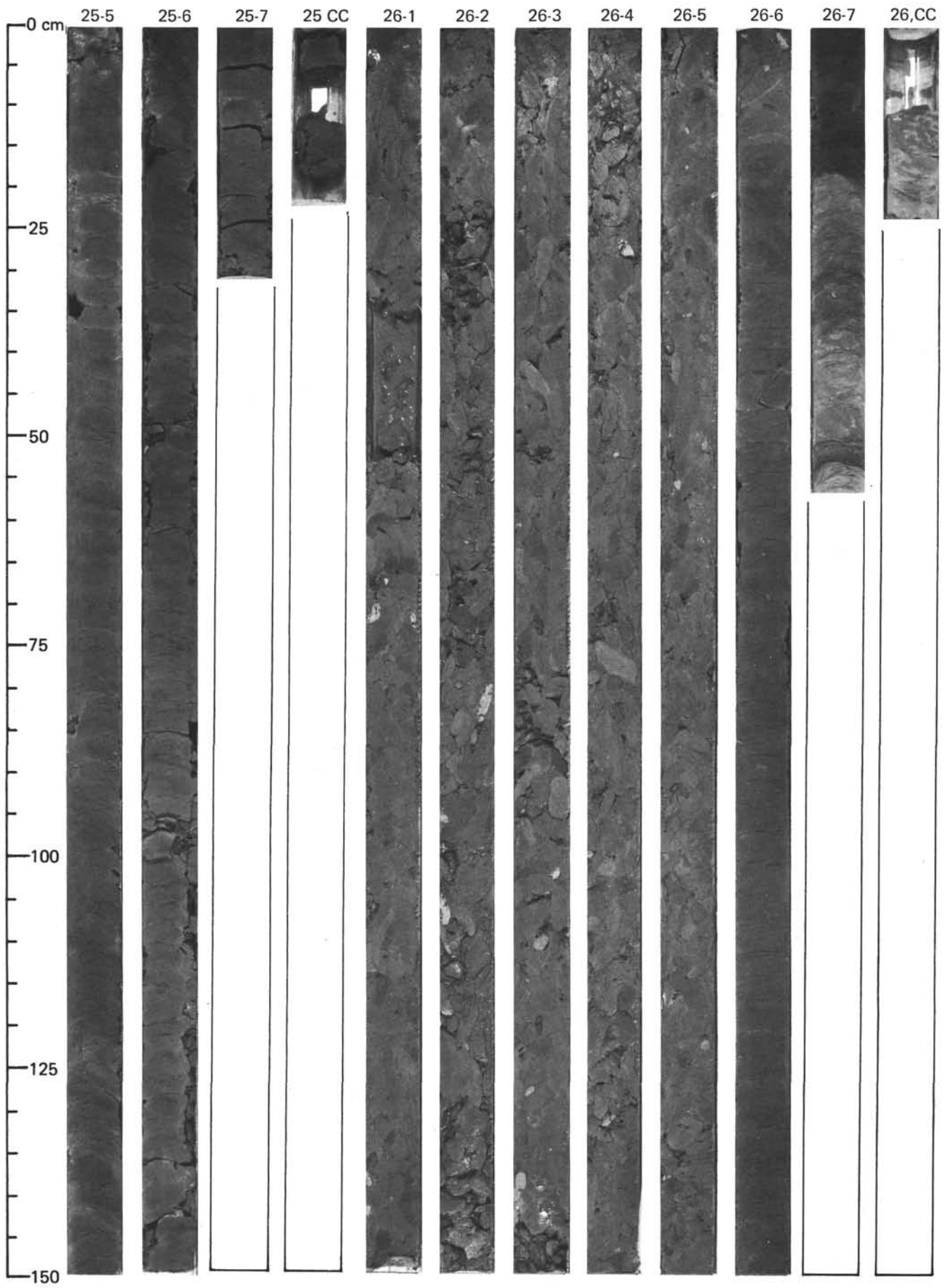


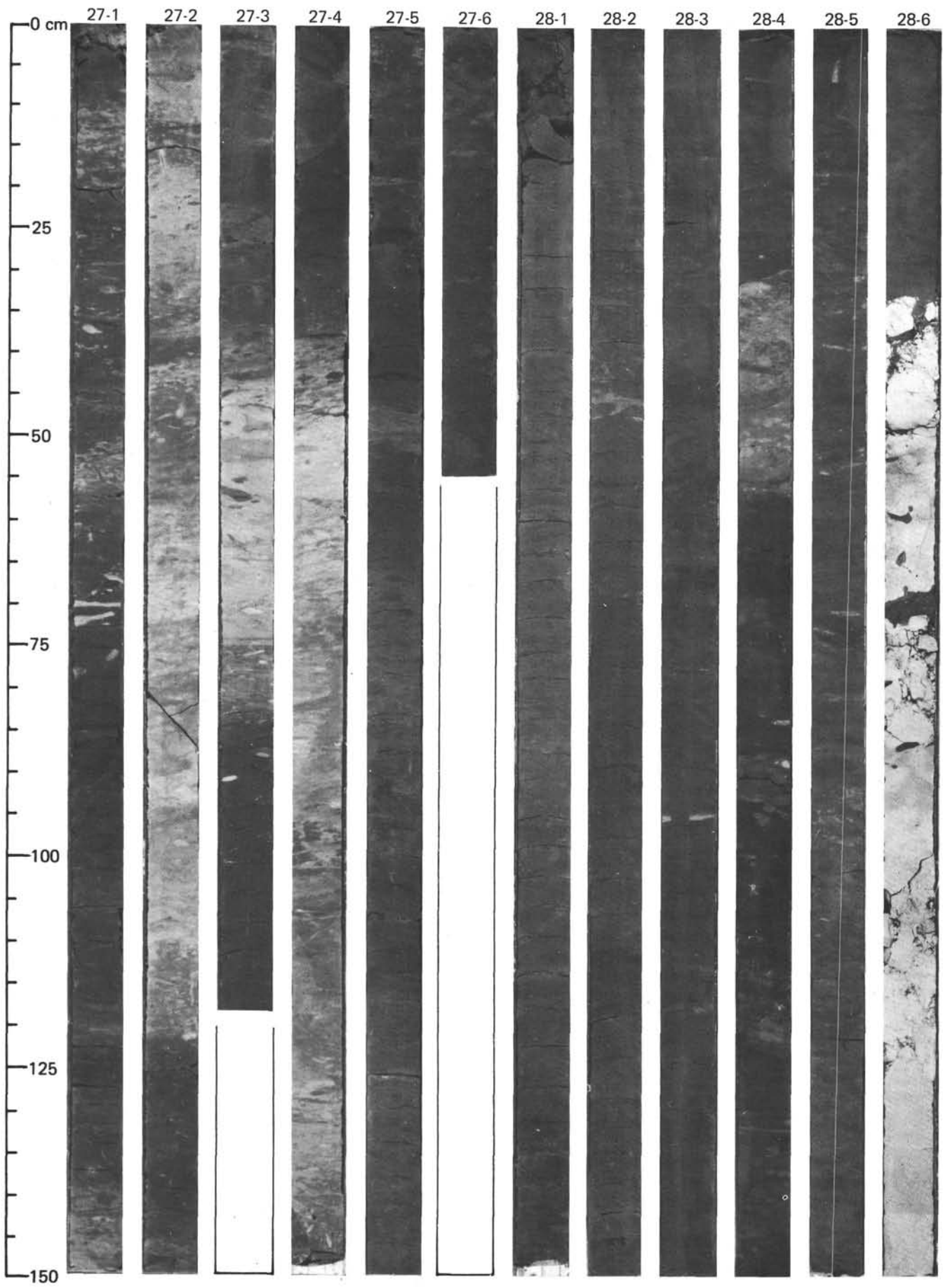


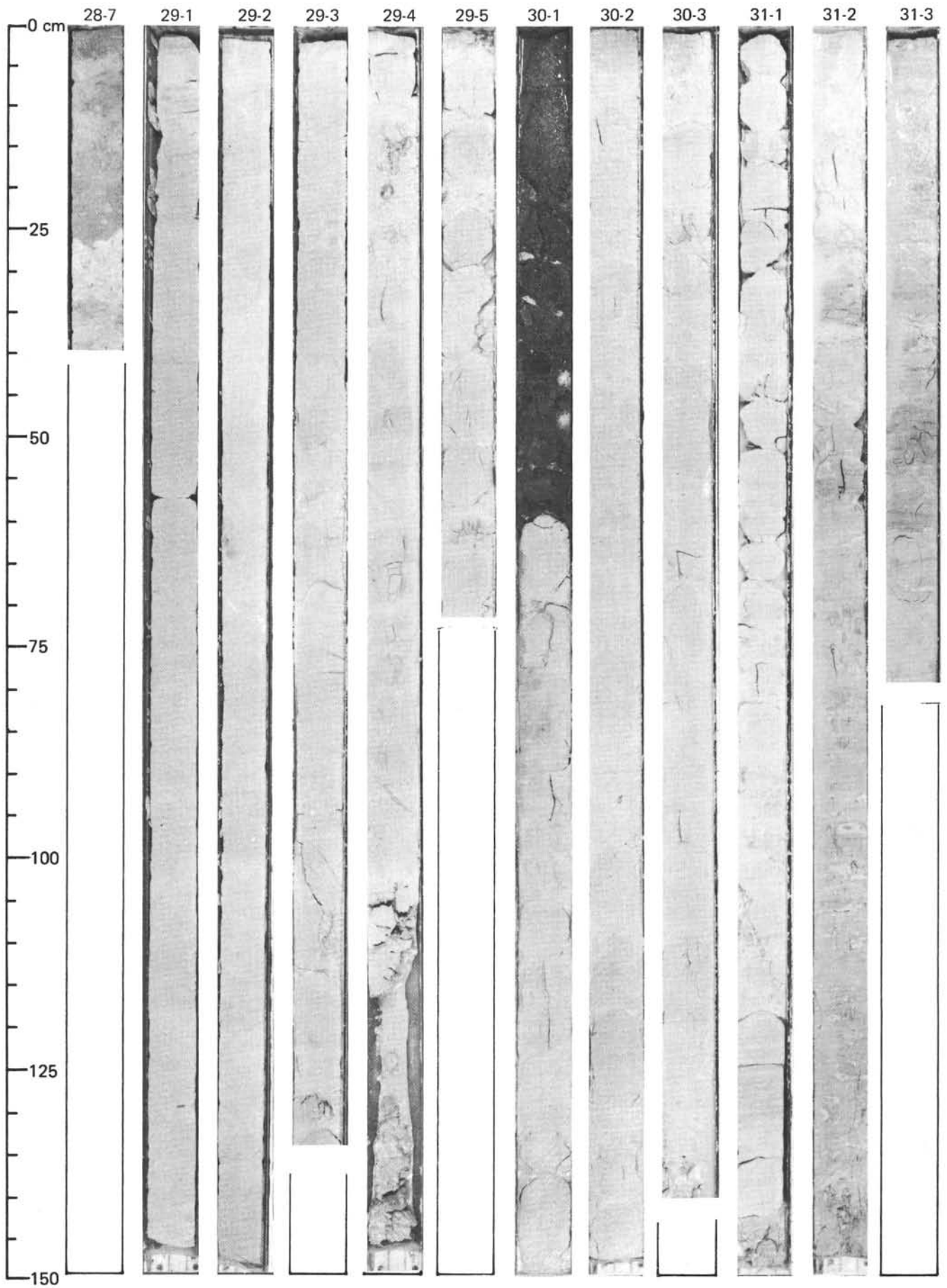


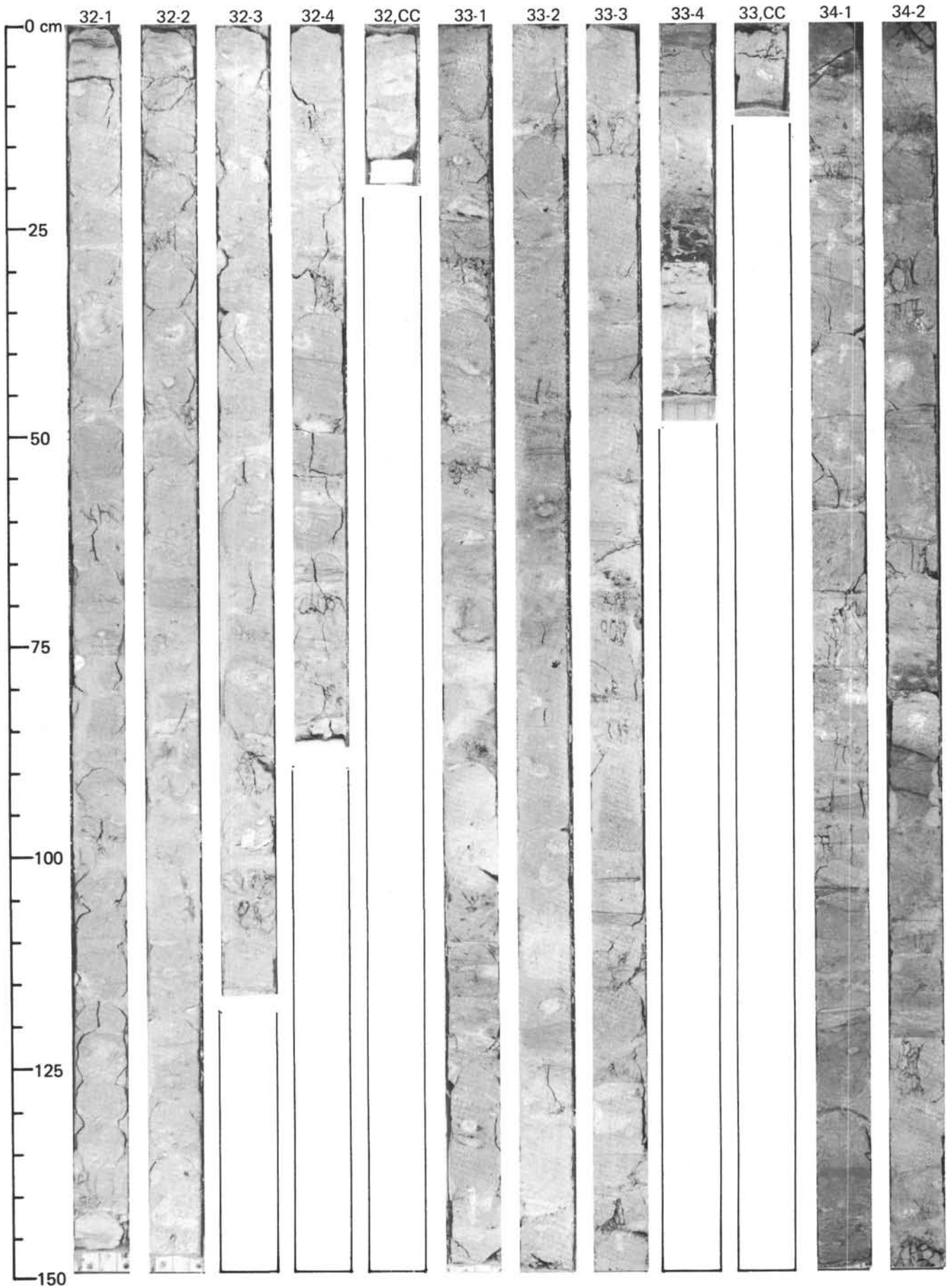


SITE 548 (HOLE 548A)









SITE 548 (HOLE 548A)

